EPILEPSY MUTATIONS IN DIFFERENT REGIONS OF THE NAV1.2 CHANNEL CAUSE

DISTINCT BIOPHYSICAL EFFECTS

Emily R. Mason

Submitted to the faculty of the University Graduate School
in partial fulfillment of the requirements
for the degree
Doctor of Philosophy
in the Department of Pharmacology and Toxicology,
Indiana University
June 2020

Accepted by the Graduate Faculty of Indiana University, in partial
fulfillment of the requirements for the degree of Doctor of Philosophy.

Doctoral Committee

_____

Theodore Cummins, Ph.D., Chair

_____

William Sullivan, Ph.D.

March 11, 2020

_____

Nickolay Brustovetsky, Ph.D.

_____

Patrick Sheets, Ph.D.

_____

Eri Hashino, Ph.D.

DEDICATION

This work is dedicated to patients and their families who struggle with

genetically-driven epilepsies.

ACKNOWLEDGEMENTS

I would like to express my deepest gratitude to everyone whose help and support saw me through my graduate work and made this dissertation possible. You are all amazing!

First, I want to thank God for His endless love and guidance, as well as for putting so many wholesome and supportive people in my life.

Secondly, I would like to thank my family for their love, encouragement, and guidance. My mother, Debra, has been especially important in my entire career path so far. She guided me into the world of biomedical research, recognized that it was a good fit for me, saw that I enjoyed it, encouraged me to stay on this career path, and has helped me navigate every step along the path. My maternal grandmother, Revenna, deserves credit for her work ethic and love of learning, which she has passed down to my mother and me. My dad, Barry, and my sister, Hannah, have been very empathetic and supportive of my research endeavors. Additionally, the love, acceptance, and support that I have always received from all my grandparents and other extended family members has helped to motivate me to always keep moving forward.

I would also like to thank all my wonderful friends for their loyalty, support, and encouragement.

I would like to acknowledge and thank my mentor, Dr. Cummins, for all of his guidance and support. Thank you for taking time out of your busy schedule to answer my questions and offer thoughtful and very helpful advice. Thank you, also, for giving me opportunities to attend conferences, present posters, present in lab meetings, and

mentor other students; these things helped me to develop my knowledge base, networking skills, and self-confidence.

I would also like to thank my other committee members, Dr. Bill Sullivan, Dr. Nick Brustovetsky, Dr. Patrick Sheets, and Dr. Eri Hashino. Thank you for your support and encouragement, which were much needed and greatly appreciated. Thank you for taking the time to lead me through the planning and completion of my research, papers, and presentations.

I would like to thank our collaborators at the University of California Los Angeles, David Geffen School of Medicine: Dr. Stephen Cannon and Dr. FenFen Wu. Thank you for providing valuable content for my first publication and for this dissertation by performing the oocyte electrophysiology experiments and helping me to analyze the resulting data.

Thanks to the past and present members of the Cummins lab, Reesha Patel, Cindy Barbosa, Zifan Pei, Yucheng Xiao, James Jackson, Adrienne Jackson, Claudia Pan, Agnes (Zybura) Wardrop, Ashley Frazee, and Patrick Milder for your mentorship, comraderie and encouragement. Thank you for making the lab environment warm and pleasant. I've enjoyed working with you!

I would like to thank the Pharmacology and Toxicology department for their support. Thanks to the administrative staff, including Lisa King, Amy Lawson, Joanna Plew, and Susan Gunter, for helping me navigate the processes and paperwork involved in my graduate studies and grant submissions. Thanks to all the students, post-docs,

and faculty from the department for your guidance, comraderie, and unique perspectives on both research and life in general.

Thanks to the IUSM Graduate Department, especially Tara Hobson and Brandy Woods. Thank you for working hard to ensure that other students and I were well-informed and had smooth and positive experiences throughout our IBMG experience and graduate work. Thank you also for your enthusiasm, encouragement, and for your invaluable assistance in preparing myself for the next steps in my career.

Emily R. Mason

EPILEPSY MUTATIONS IN DIFFERENT REGIONS OF THE NAV1.2 CHANNEL CAUSE

DISTINCT BIOPHYSICAL EFFECTS

While most cases of epilepsy respond well to common antiepileptic drugs, many genetically-driven epilepsies are refractory to conventional antiepileptic drugs. Over 250 mutations in the Nav1.2 gene (*SCN2A*) have been implicated in otherwise idiopathic cases of epilepsy, many of which are refractory to traditional antiepileptic drugs. Few of these mutations have been studied *in vitro* to determine their biophysical effects on the channels, which could reveal why the effects of some are refractory to traditional antiepileptic drugs. The goal of this dissertation was to characterize multiple epilepsy mutations in the *SCN2A* gene, which I hypothesized would have distinct biophysical effects on the channel's function. I used patch-clamp electrophysiology to determine the biophysical effects of three *SCN2A* epilepsy mutations (R1882Q, R853Q, and L835F). Wild-type (WT) or mutant human *SCN2A* cDNAs were expressed in human embryonic kidney (HEK) cells and subjected to a panel of electrophysiological assays. I predicted that the net effect of each of these mutations was enhancement of channel function; my results regarding the L835F and R1882Q mutations supported this hypothesis. Both mutations enhance persistent current, and R1882Q also impairs fast inactivation. However, examination of the same parameters for the R853Q mutation suggested a decrease of channel function. I hypothesized that the R853Q mutation creates a gating pore in the channel structure through which sodium leaks into the cell when the channel is in its resting conformation. This hypothesis was supported by

electrophysiological data from *Xenopus* oocytes, which showed a significant voltage-dependent leak current at negative potentials when they expressed the R853Q mutant channels. This was absent in oocytes expressing WT channels. Overall, these results suggest that individual mutations in the *SCN2A* gene generate epilepsy via distinct biophysical effects that may require novel and/or tailored pharmacotherapies for effective management.

Theodore Cummins, Ph.D., Chair

TABLE OF CONTENTS

LIST OF TABLES

LIST OF FIGURES

LIST OF ABBREVIATIONS

AED................Antiepileptic Drug

AIS................Axon initial segment

ANOVA................Analysis of Variance

DI-DIV................Voltage-gated sodium channel domains I-IV

DMEM................Dulbecco's Minimal Essential Medium

EGFP................Enhanced green fluorescent protein

F................Phenylalanine

FBS................Fetal Bovine Serum

HEK/HEK293................Human embryonic kidney [cells]

I/V................Current-voltage [relationship]

I_{NaT}................Transient sodium current

I_{NaP}................Persistent sodium current

I_{NaR}................Resurgent sodium current

L................Leucine

Nav................Voltage-gated sodium channel

Q................Glutamine

R................Arginine

SEM................Standard error of the mean

S1-S6................Segments 1-6, in a given Nav channel domain

TTX................Tetrodotoxin

WT................Wild-type

I. INTRODUCTION

<u>Overview</u>

Epilepsy is a set of devastating neurological disorders of the brain that cause seizures. The majority of epilepsy patients find that their seizures are effectively repressed by one or a combination of conventional antiepileptic drugs (AEDs). However, around 38% of epilepsy patients are refractory to these drugs and have great difficulty managing and repressing their seizures (French et al., 2007; Beleza et al., 2009; Loescher et al., 2013; Laxer et al., 2014; Moshe et al., 2015; Sirven et al., 2016). For such patients, when the root cause of their epilepsy is unknown despite imaging studies and neurological workups, genetic testing is often performed. There are many genes that are believed to be involved in the pathogenesis of epilepsy when they are mutated, including voltage-gated sodium channel (Nav) genes. One of the particular Nav genes that is often revealed to be mutated in cases of otherwise idiopathic epilepsy is Nav1.2, which is expressed in the membranes of neurons in the brain and is responsible, along with Nav1.6, for the generation and propagation of action potentials in excitatory neurons. Epilepsy is a result of an imbalance of excitatory and inhibitory neuron firing in the brain, so Nav1.2 mutations implicated in epilepsy pathogenesis are believed to enhance the activity of affected channels, leading the affected neurons to be hyperexcitable. This hyperexcitability causes the affected neurons to fire action potentials inappropriately, and the inappropriate neuronal activity is believed to play a key role in the generation of epileptic seizures.

As expected, many Nav1.2 mutations implicated in epilepsy have been shown, so far, to have effects on the channel that enhance the channel function. However, sodium channel blockers do not effectively suppress seizures in many of these patients, or in a majority of other patients with putatively epileptic Nav1.2 mutations. While some patients have found one or more sodium channel blockers to be helpful in reducing the severity or frequency of their seizures, few achieve seizure freedom with any antiepileptic drug (AED) or drug combination. In order to find pharmacotherapies that more effectively repress seizures in epileptic patients with Nav1.2 mutations, we must develop a better understanding of how the mutations are affecting the activity of the channels and why sodium channel blockers have limited efficacy for these patients. The primary aim of this study was to uncover the effects of three mutations on the biophysical activity of the Nav1.2 channel in order to identify aberrant channel functions that may represent novel AED targets.

Voltage-Gated Sodium (Nav) Channel Overview

The first evidence of voltage-gated sodium channels was discovered by Hodgkin and Katz in 1948, when these scientists observed that the sodium in the solution surrounding a giant axon from a squid was necessary for the axon to fire an action potential (Hodgkin & Katz, 1949). They and other scientists showed that action potentials, aka "nerve impulses," involve sodium flowing into the nerve and potassium flowing out (Rothenberg, 1950; Keynes & Lewis, 1951). Hodgkin and Huxley proposed that action potentials resulted from three ionic current components: sodium current (I_{Na}), potassium current (I_K), and a small leak current (I_l) comprised of chloride and other

ions (Hodgkin & Huxley, 1952). They observed that the sodium and potassium currents flowed through the membrane with different voltage dependent and kinetic properties, so they hypothesized that there were two separate conduction mechanisms, which are now known to be voltage-gated sodium and potassium channels, which allowed these ions to pass through the membrane (Hodgkin & Huxley, 1952). For sodium, they proposed that there were charged particles in the membrane which shifted when the membrane potential depolarized, into a conformation allowing the sodium ions to move through the membrane until a slow-moving particle, which is now known as the inactivation particle, shifts to block the flow of sodium ions (Hodgkin & Huxley, 1952). They proposed a similar mechanism for potassium, in which the charged particles shifted more slowly, so that the potassium conductance across the membrane peaked subsequently to the sodium conductance.

Voltage-gated sodium (Nav) channels were first isolated from animals in the early 1970s (Henderson & Wang, 1972; Levinson & Ellroy, 1973). In the early 1980s, saxitoxin, which was known to block sodium currents in nerves, was utilized to capture and isolate Nav channels from rat brains (Beneski & Catterall, 1980; Hartshorne & Catterall, 1981). Gel electrophoresis of the isolated proteins showed that the sodium channel consisted of one large (alpha) subunit and two smaller (beta) subunits (Hartshorne & Catterall, 1981; Hartshorne et al., 1982). In the mid-1980s, two Nav channel isoforms were isolated from rat brain and studied in order to deduce their DNA sequence, amino acid sequence, and approximate 2D structure (Noda et al. 1984, 1986a). The cDNA for these channels was then generated and injected into *Xenopus*

oocytes and found to produce functional rat brain sodium channels (Noda et al., 1986b), establishing the idea that the alpha subunits form fully functional channels without requiring any beta subunits.

Eventually, it was determined that there are 9 isoforms of the mammalian voltage-gated sodium channel (Nav) alpha subunit, termed Nav1.1-Nav1.9 and encoded by the genes *SCN1A-SCN5A* and *SCN8A-SCN11A* (Goldin et al., 2001). These voltage-gated sodium (Nav) channels are expressed in the plasma membranes of excitable cells, and they all share a common basic structure (shown in Fig. 1A-C), which consists of four structurally homologous domains, termed DI-DIV (Noda et al., 1984; Sato et al., 1998). Each domain consists of six transmembrane segments, termed S1-S6. The S4 segments are known as voltage-sensing segments, since each contains several positively-charged amino acid side chains that react to changes in the membrane potential by shifting and causing a conformational change in the channel protein (Noda et al., 1984; Stuehmer et al., 1989; indicated in Fig. 1A by shading and "+" symbols). The S5 and S6 segments of the four domains form the central pore, and the extracellular linkers between the S5 and S6 segments, known as pore loops, dip down slightly into the pore. A cluster of one residue from each of the four pore loops form the selectivity filter, which selectively interacts with sodium ions, allowing them, but not most other ions or molecules, to pass through into the central pore. When the membrane is at its resting potential (~-70 mV for neurons), the channel is in the closed conformation, in which the central pore is blocked and sodium cannot pass through into the cell, down its electrochemical gradient (Fig. 1C). When receptors on the postsynaptic neuron are activated by an

excitatory stimulus, the membrane depolarizes, due to either an intracellular buildup of

cations or the efflux of anions. In response to the membrane depolarization, the

voltage-sensing segments of Nav channels shift and cause the channels to enter the

activated conformation, in which the barrier within the pore is removed and sodium is

allowed to pass through into the cell. When the membrane potential is depolarized, the

inactivation particle, which is an amino acid motif in the linker between domains III and

IV, interacts with a site in or near the intracellular side of the central pore, occluding the

channel and cutting off the sodium current in a process known as fast inactivation.

Subsequently, Nav channels are believed to enter a slow-inactivated state, which is

independent of the inactivation particle and happens over a matter of seconds.

However, the mechanism and roles of slow inactivation in the contexts of neuronal

excitability and disease are poorly understood. At strongly depolarized membrane

potentials, voltage-gated potassium channels open, and potassium flows out of the cell,

down its concentration gradient, repolarizing the membrane potential. As the resting

membrane potential is restored, the channel shifts back into its resting (closed)

conformation and the inactivation particle dissociates from the central pore. In whole-

cell patch clamp electrophysiology experiments, under voltage clamp (see Sigworth

1980 for description of methodology), the inward current is represented by a downward

deflection of the current trace (Fig. 1D).

There are four β subunits, termed β1-β4, which associate with the α subunits

and modify their activity, thus modulating the excitability of the neurons (or other

excitable cells) in which they are expressed. These subunits, encoded by the genes

Scn1b-Scn4b, each contain an extracellular N-terminal V-type Ig domain, a single α-helical transmembrane segment, and an intracellular C-terminal domain. The β2 and β4 subunits covalently bond to α subunits via disulfide bridges, while β1 and β3 interact non-covalently with α subunits (Chen et al., 2012; Buffington & Rasband, 2013). The β subunit isoforms are differentially expressed in different excitable tissues and in different neuronal subpopulations. The effect of a β subunit on the α subunit activity depends on the β subunit isoform, the α subunit isoform, and the cell type in which they are studied; and these effects can include alterations of the voltage dependencies and/or gating kinetics of activation and inactivation. Additionally, the β subunits have been shown to function as cell adhesion molecules, via their Ig domain and independently of α subunits, (Srinivasan et al., 1998; Xiao et al., 1999) and to play roles in neurite outgrowth (Davis, Chen, & Isom, 2004; Miyazaki et al., 2007).

The nine isoforms of Nav1 channels differ in tissue distribution. Nav1.1, Nav1.2, Nav1.3, and Nav1.6 are found in the central nervous system, while Nav1.1, Nav1.6, Nav1.7, Nav1.8, and Nav1.9 are expressed in the peripheral nervous system. Nav1.4 and Nav1.5 are expressed in skeletal muscle and heart tissue, respectively. Therefore mutations in different Nav isoforms that alter their functions can result in different types of diseases. For instance, mutations in neuronal isoforms have been implicated in autism, epilepsy, schizophrenia, pain, and movement disorders; while mutations in the cardiac isoform (Nav1.5) are associated with cardiac diseases such as Brugada Syndrome, Long-QT Syndrome, and arrhythmias.
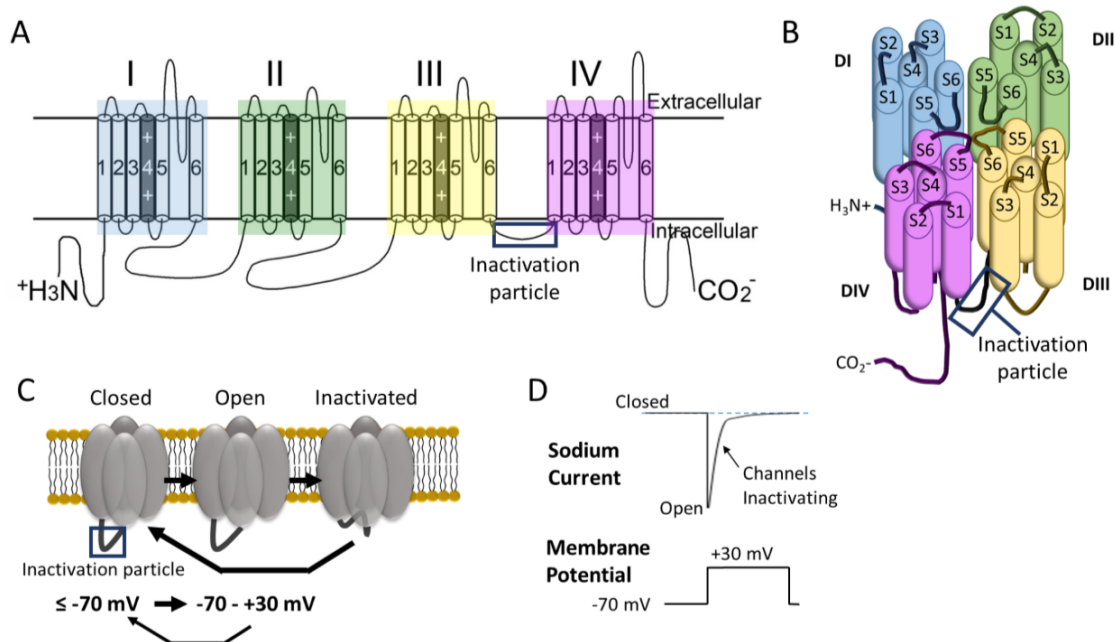
Figure 1. Voltage-gated sodium channel structure and function. (A) Secondary structure of a voltage-gated sodium (Nav) channel α subunit in a cell membrane. Domains I-IV are labeled "I – IV;" S1-S6 segments are labeled "1 – 6." Domains I – IV are color-coded to match (B), the tertiary structure of a voltage-gated sodium (Nav) channel α subunit, looking down at the channel from an extracellular perspective. (C) Nav channel conformational changes in response to changes in membrane potential. Upon depolarization, the channel shifts from the closed state to the open state; then the inactivation particle binds to occlude the central pore, which inactivates the current. Upon repolarization, the channel shifts from the inactivated state back to the closed state; and the inactivation particle dissociates from the central pore. (D) Representative sodium current trace (top) from whole-cell patch clamp recording in response to a single depolarization step (below). Image in (A) adapted with permission from figure 1A in "Gating Pore Currents Demonstrate Selective and Specific Modulation of Individual Sodium Channel Voltage-Sensors by Biological Toxins" by Y Xiao, K Blumenthal, and TR Cummins, 2014, *Molecular Pharmacology, 86*, p. 160. Copyright 2014 by the American Society for Pharmacology and Experimental Therapeutics .

Nav Channels of the Brain

Voltage-gated sodium channels were first observed in mammalian brains, through stains of voltage gated sodium channels in rodent brains, in the early 1980's; and these have since been identified as the Nav1.1, Nav1.2, and Nav1.6 isoforms (Westenbroek, Merrick, & Catterall, 1989; Westenbroek, Noebels, & Catterall, 1992;

Gong et al., 1999; Caldwell et al., 2000). Subsequent studies have confirmed the presence of those same three isoforms, along with Nav1.3, in human brain tissue (Whitaker et al., 2001; Tian et al., 2014). The same studies also confirmed that the expression patterns of the various isoforms throughout the brain were similar between rodents and humans. While Nav1.6 channels are found in most neurons throughout the brain (Whitaker et al., 2001; Tian et al., 2014), Nav1.1 and Nav1.2 are rarely, if ever, co-expressed. Nav1.1 is found primarily in GABAergic interneurons (Yu et al., 2006; Tian et al., 2014), while Nav1.2 and Nav1.6 are found primarily in excitatory neurons (Tian et al., 2014). Subcellularly, Nav1.2 is localized primarily in the dendrites, soma, and proximal axon initial segment (AIS); and Nav1.6 is concentrated in the distal AIS (Tian et al., 2014; Hu et al., 2009). Early in development, before neurons are myelinated, Nav1.2 can be found clustered along the axon at sites that later become nodes of Ranvier; but these clusters are replaced with Nav1.6 clusters once the axons are myelinated (Kaplan et al., 2001). Nav1.3 is also strongly expressed in some regions of the fetal brain, but by adulthood its expression is weak and predominantly somatodendritic (Whitaker et al., 2001; Smith et al., 2018). Nav1.1 expression is low during the prenatal period and increases postnatally, showing a similar subcellular localization to Nav1.3 (Whitaker et al., 2001; Smith et al., 2018). Given the preferential expression of Nav1.6 in the distal AIS and nodes of Ranvier of neurons, Nav1.6 is generally regarded to be the predominant isoform responsible for action potential initiation and propagation (Hu et al., 2009). Nav1.1, Nav1.2, and Nav1.3 have a stronger presence in the dendrites, soma, and proximal AIS, and they are thus believed to be responsible for action potential

backpropagation (Westenbroek, Merrick, anc Catterall, 1989; Trimmer and Rhodes, 2004). Nav1.2 is often found in the AIS and is thus is believed to be involved in action potential initiation (Rush, Dib-Hajj, and Waxmann, 2005; Kaczmarek, 2019). Backpropagation of action potentials into the soma and dendrites of neurons is poorly understood, but it is believed to play a role in synaptic plasticity and synchrony (Kuczewski, Porcher, and Ferrand, 2008; Kuczewski et al., 2008; Spratt et al., 2019; Shin et al., 2019).

Epilepsy

Epilepsy is a devastating set of disorders caused by aberrant bursts of synchronous neuronal activity in the brain. Epilepsy was first associated with voltage-gated sodium (Nav) channels in 1998, when two mutations in the Nav β1 subunit gene, *Scn1b*, were identified as likely pathogenic mutations in two families in which generalized epilepsy with febrile seizures (GEFS+) was known to have been genetically transmitted (Wallace et al., 1998). Since then, mutations in each of the brain voltage gated sodium channel isoforms (Nav1.1, Nav1.2, Nav1.3, and Nav1.6) have been identified in otherwise idiopathic cases of epilepsy (see Noebels, 2019 for review). Some of these epilepsy mutations are passed down in families, but many are *de novo* mutations not present in either parent.

While most epilepsy cases respond well to common antiepileptic drugs, about 38% of epilepsy patients experience persistent seizures under conventional epilepsy treatments (French et al., 2007; Beleza et al., 2009; Loescher et al., 2013; Laxer et al., 2014; Moshe et al., 2015; Sirven et al., 2016). Most of these refractory epilepsies are

9

believed to be manifestations of a genetic defect (Mercimek-Mahmutoglu et al., 2015).

Mutations in 18 genes, including genes encoding voltage-gated sodium channels (Nav

channels) expressed in the brain (*SCN1A, SCN1B, SCN2A,* and *SCN8A,* encoding Nav1.1 α

and β subunits, Nav1.2 α subunit, and Nav1.6 α subunit), have been identified in several

types of epilepsy (Nicita et al., 2012). Since Nav1.2 and Nav1.6 are predominantly

expressed in excitatory neurons, it is believed that epileptic mutations in these channel

isoforms typically cause the channels to conduct too much sodium current into the

affected neurons, resulting in neuronal hyperexcitability. The hyperexcitability leads to

the inappropriate bursts of action potential firing characteristically seen in epileptic

seizures. Mutations that enhance Nav channel function or induce an aberrant function

in the channel are generally (and hereafter) referred to as gain-of-function effects.

Alternately, since Nav1.1 is primarily expressed in inhibitory interneurons, which act to

decrease excitation in their postsynaptic excitatory neurons, epileptic mutations in this

isoform usually cause a decrease in the conductance of the sodium current into the

interneurons; these are generally (and hereafter) referred to as loss-of-function effects.

Affected interneurons are not as excitable as healthy (WT) neurons and do not fire

action potentials as often as they should, and thus the postsynaptic excitatory neurons

are disinhibited and can become hyperexcitable.

The opening of Nav1.2 and Nav1.6 channels in the AIS allows entry of sodium

into neurons and is responsible for the initiation and propagation of action potentials

down the axons (Catterall et al., 2005). If these voltage-gated sodium channels allow

too much sodium to enter the cell, the resting membrane potential may be elevated,

thus reducing the action potential firing threshold. This means that small depolarizing

postsynaptic potential changes, which would not bring the potential past the threshold

voltage in a healthy cell, may bring the potential past the threshold value and cause

action potentials to be fired. This would enhance repetitive firing (e.g. increased

frequency and duration of action potential firing) in these neurons in response to

depolarizing currents, leading to an abnormally large and/or sustained neurotransmitter

release (Wang et al., 2016). In epilepsy, the chronically elevated resting membrane

potentials of excitatory (glutamatergic) neurons leads to aberrant glutamate release,

which excites downstream neurons and results in the seizure phenotype (During et al.,

1993; Broomfield et al., 2006).

Nav1.2 and Molecular Mechanisms of Epilepsy

Mutations in *SCN2A* , the gene encoding the pore-forming α subunit of the

Nav1.2 channel, can lead to multiple types of epilepsy including Dravet Syndrome,

genetic epilepsy with febrile seizures plus (GEFS+), benign familial neonatal-infantile

seizures (BFNIS), early onset epileptic encephalopathies (EOEE), and Ohtahara Syndrome

(Brunklaus et al., 2014; Shi et al., 2012). These mutations can modify different

parameters of channel function, including the voltage-dependence of gating (e.g. the

voltage dependence of activation and inactivation), the kinetics of gating (e.g. the time

constant for fast inactivation), and/or the transient current (INaT) magnitude (e.g. INaT

peak amplitude, INaT peak density). Additionally, some of these epileptic *SCN2A*

mutations induce or alter existing aberrant inward sodium currents, such as persistent,

resurgent, and gating pore currents (Rogawski et al., 2004; Jarecki et al., 2010; Hargus et

al., 2011; Hargus et al., 2013; Lewis and Raman, 2014). Since the Nav1.2 channel isoform is primarily expressed in glutamatergic neurons, epilepsy mutations in this protein are believed to cause a net augmentation of the channel function, leading to hyperexcitability and inappropriate action potential firing.

Mutations in *SCN2A* that confer a loss of channel function, which typically leads to reduced neuronal excitability, have also been implicated in autism. Most of the *SCN2A* mutations that have been reported which result in premature truncation of the protein have been associated with autism. All such mutations that have been studied in vitro have been shown to produce non-conducting channel fragments (Kamiya et al., 2004; Ben-Shalom et al., 2017). Two of these mutations have been shown to diminish the function of WT channels when mutant and WT channels were coexpressed; and most or all other *SCN2A* mutations that have been found to have exclusively loss-of-function effects are associated with a clinical diagnosis of autism (Kamiya et al., 2004; de Rubies et al., 2014; Ben-Shalom et al., 2017; Wolff et al., 2017). Among *SCN2A* mutations associated with epilepsy or seizures, autism diagnoses were reported in all cases associated with mutations that have been shown to produce exclusively loss-of-function effects, and only in one case of a mutation with a mix of gain-of-function and loss-of-function effects (Scalmani et al., 2006; Misra et al., 2008; Wolff et al., 2017). Functional modeling of the impact of *SCN2A* mutations on neuronal excitability predicted that several mutations implicated in autism decrease neuronal excitability, while several associated with epilepsy increase neuronal excitability (Ben-Shalom et al., 2017). This suggests that *SCN2A* mutations that result in a loss of channel function

12

typically lead to decreased neuronal excitability and autism (which is sometimes accompanied by seizures), while mutations that enhance the channel function (i.e. have gain-of-function effects) or have mixed effects on channel function tend to cause neuronal hyperexcitability and epilepsy (which is rarely associated with a diagnosis of autism).

Over 250 mutations in the *SCN2A* gene have been implicated in published cases of epilepsy (Fig. 2A), but only 21 (~8.5%) have been studied and characterized *in vitro* (see Table 1). Of these 21 mutations, 10 have been reported to cause only gain-of-function effects, including increased current density, hyperpolarized voltage dependence of activation, depolarized voltage dependence of fast inactivation, slowed fast inactivation, accelerated recovery from inactivation, increased persistent currents, and increased resurgent currents. Persistent current, also called late current, is the current that occurs after most of the Nav channels have opened and inactivated. This is due to either incomplete inactivation or brief dissociations of the inactivation particle from the central pore (Fig. 3A). Resurgent currents occur when there is an intracellular blocking molecule present, which binds to the central pore upon depolarization, blocking the transient current and hindering the interaction of the inactivation particle with the central pore. Upon repolarization, the blocking molecule dissociates and current briefly resurges through the central pore before it is again cut off by the inactivation particle (Fig. 3B-C).
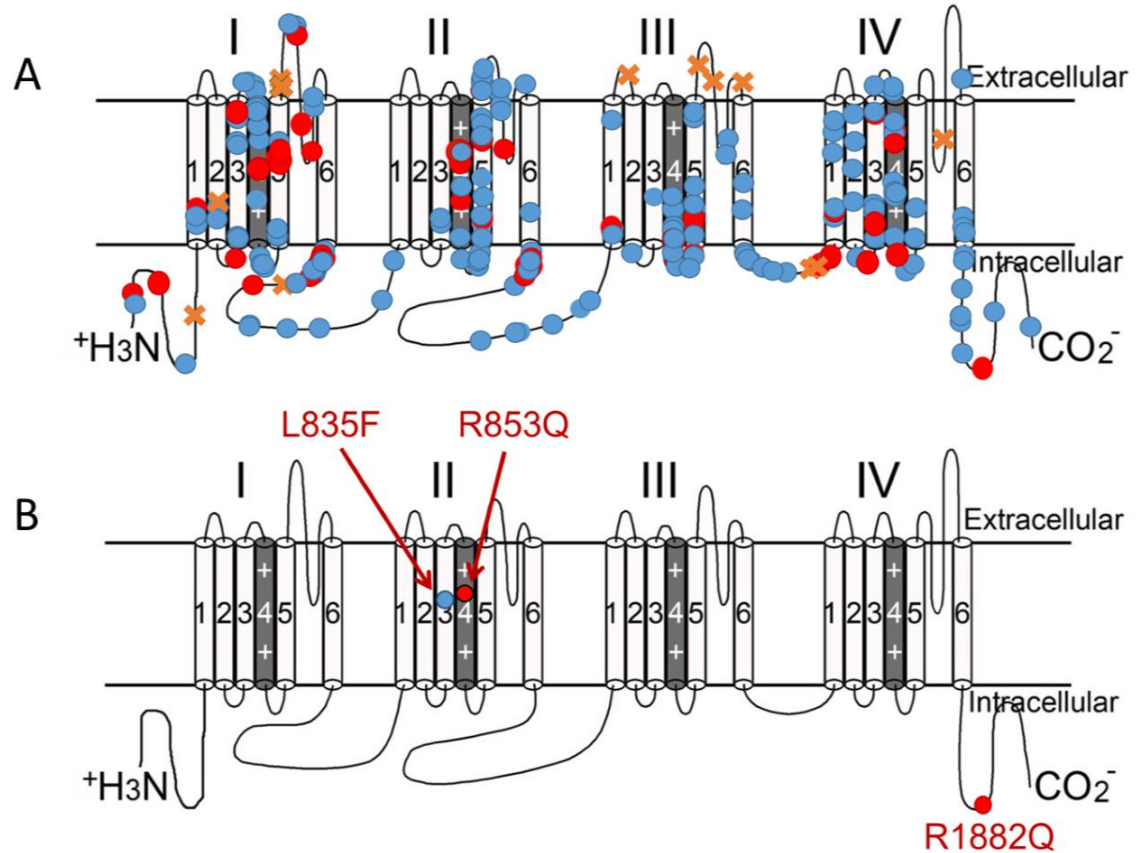
Figure 2. SCN2A/Nav1.2 epilepsy mutations. (A) Schematic of Nav1.2 showing sites of published epilepsy-linked mutations. Blue circles denote mutations reported only once; red circles denote mutations reported in multiple patients; red-orange "X"'s denote truncation mutations in patients with reported epilepsy. (B) Schematic of Nav1.2 showing locations of the three epilepsy mutations characterized in this study. Images in (A) and (B) adapted with permission from figure 1A in "Gating Pore Currents Demonstrate Selective and Specific Modulation of Individual Sodium Channel Voltage-Sensors by Biological Toxins" by Y Xiao, K Blumenthal, and TR Cummins, 2014, *Molecular Pharmacology, 86*, p. 160. Copyright 2014 by the American Society for Pharmacology and Experimental Therapeutics .
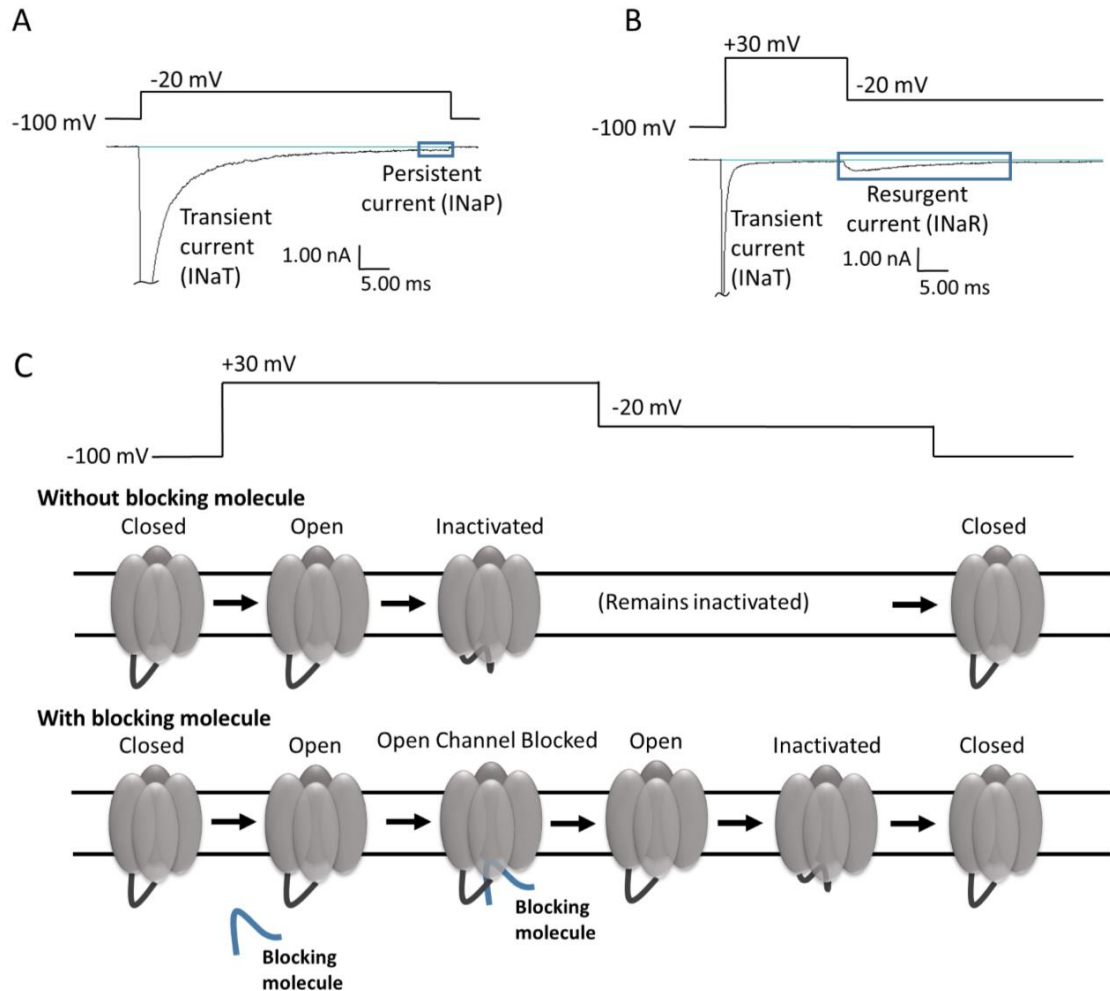
Figure 3. Persistent and resurgent currents. (A) A raw current trace from an HEK cell expressing hNav1.2 cDNA. Peak persistent current (blue box) was measured as the average current over the last 5 ms of a 50 ms depolarization pulse (shown above the trace). Adapted from Figure 1B in (Mason and Cummins, 2020). (B) A raw current trace from an HEK cell expressing hNav1.2 cDNA. Peak Resurgent current (blue box) was measured as the peak current occurring during the repolarization pulse in the resurgent current voltage protocol (single step from the protocol shown above the trace). Adapted from Figure 1A in (Mason and Cummins, 2020). (C) Resurgent current occurs upon repolarization in the presence of a blocking molecule. A single step from the resurgent current voltage protocol is shown (top). When a cell expressing Nav1.2 is depolarized from -100 to +30 mV, the channels open. In the absence of a blocking molecule, they inactivate and remain inactivated until the membrane potential is repolarized to the holding potential of -100 mV, when the channels return to the closed conformation. In the presence of a blocking molecule, the blocking molecule associates with many of the channels before they can inactivate, blocking the central pore and inhibiting the sodium current. When the cell is partially repolarized to -20 mV, the blocking molecule dissociates from the channel, leaving it open briefly and allowing sodium current to come through the central pore before the channel inactivates.

Table 1. Effects of Previously characterized *SCN2A* epilepsy mutations on Nav1.2 channel functions. Reports = patient case reports. Electrophys. = electrophysiology data. With regards to background color: mutations found to have only gain-of-function effects are colored green; mutations found to have a mix of gain– and loss-of-function effects are colored gold; mutations found to have only loss-of-function effects are colored red.

Mutation	Number of Published Reports	Effects on Nav1.2 Function	Report Sources	Electrophys. Sources
R188W	3	Slows inactivation	Sugawara et al., 2001; Ito et al., 2004	Sugawara et al., 2001
M252V	1	Increases persistent current, faster recovery from slow inactivation (neonatal splice variant), increases neuronal firing acc. to neuronal computer model	Liao et al., 2010	Liao et al., 2010
V261M	3	Increases persistent current (adult splice variant), faster recovery from fast inactivation, faster recovery from slow inactivation (neonatal splice variant), increases neuronal firing acc. to neuronal computer model	Liao et al., 2010; Moller et al., 2016; Wolff et al., 2017	Liao et al., 2010
A263V	9	Increases persistent sodium current	Liao et al., 2010; Touma et al., 2013; Schwarz et al., 2016; Johannesen et al., 2016; Singh et al., 2016; Moller et al., 2016; Wolff et al., 2017	Parrini et al., 2017
V423L	2	Increases persistent current, changes slope of voltage dependence of activation, doubles window current	Wolff et al., 2017	Wolff et al., 2017
I1473M	1	Hyperpolarizes voltage dependence of activation (14 mV)	Sawaishi et al., 2002; Ogiwara et al., 2009	Ogiwara et al., 2009; modeled in Ben-Shalom et al., 2017
Y1589C	9	Increases persistent current, depolarizes voltage dependence of inactivation, slows fast inactivation, accelerates recovery from inactivation	Lauxmann et al., 2013	Lauxmann et al., 2013

F1597L	1	Hyperpolarizes voltage dependence of activation, slows fast inactivation, accelerates recovery from fast inactivation	Wolff et al., 2017	Wolff et al., 2017
R1882G	2	Hyperpolarizes voltage dependence of activation (4 mV)	Schwarz et al., 2016	Schwarz et al., 2016
R223Q	2+	Depolarizes voltage dependence of activation (4 mV, LOF) and inactivation (3.5 mV, GOF) curves; slows current activation and decay; Larger area under curve for AP-clamp	Berkovic et al., 2004; Zara et al., 2013	Scalmani et al., 2006
E1211K	3	Hyperpolarizes voltage dependence of activation (18 mV) (GOF) and inactivation (22 mV) (LOF), slows recovery from inactivation (LOF)	Ogiwara et al., 2009; Wong et al., 2015; Wolff et al., 2017	Ogiwara et al., 2009
R1312T	1	Hyperpolarizes fast (small shift) and slow inactivation (big shift) (LOF), slows recovery from fast inactivation (GOF), reduces use-dependent inactivation to less than 50% of WT levels (GOF), hyperpolarizes in voltage dependence of activation (small shift) (GOF); window current unchanged	Shi et al., 2009	Lossin et al., 2012
R1319Q	13	Slows activation and decay, depolarizes voltage dependencies of activation (2.6 mV) and inactivation (3.8 mV); larger area under curve for AP-clamp	Berkovic et al., 2004; Wolff et al., 2017	Scalmani et al., 2006
		Depolarizes voltage dependence of activation (3.9 mV), reduces current density and surface expression		Misra et al., 2008
L1330F	1 (+3 affected family members)	Depolarizes voltage dependence of inactivation (GOF)	Heron et al., 2002	Scalmani et al., 2006
		Reduces surface expression (LOF), decreases channel availability during repetitive stimulation (LOF)		Misra et al., 2008

L1563V	1	Hyperpolarizes voltage dependence of activation (GOF), faster activation kinetics at some voltages (GOF)	Heron et al., 2002	Scalmani et al., 2006
		Depolarizes voltage dependence of inactivation (LOF)		Xu et al., 2007
		Depolarizes voltage dependence of inactivation (LOF), reduces current density (LOF), reduces surface expression (LOF)		Misra et al., 2008
D12N	1	Faster channel inactivation	Iossifov et al., 2014	Ben-Shalom et al., 2017
D82G	1	Depolarizes voltage dependence of activation (3.3 mV)	De Rubeis et al., 2014	Ben-Shalom et al., 2017
R102*	1	Hyperpolarizes voltage dependence of inactivation; IHC results suggest that mutant channel exerts dominant-negative effect on WT channel, since mutation changes localization of channel in HEK cells	Kamiya et al., 2004	Kamiya et al., 2004
R379H	2	Non-conducting; co-expression with WT channels had no effect on WT channel function	De Rubeis et al., 2014	Ben-Shalom et al., 2017
G899S	1	Depolarizes voltage dependence of activation; change of slope of steady-state activation curve	Wolff et al., 2017	Wolff et al., 2017
P1622S	1	Hyperpolarizes voltage dependence of fast inactivation	Wolff et al., 2017	Wolff et al., 2017

Persistent and resurgent current have both been shown to naturally occur in mammalian neurons. Persistent currents have been observed in many populations of neurons in mammalian brains, including subicular neurons from patients with temporal lobe epilepsy (Vreugdenhil et al., 2004). Persistent currents have been shown to occur in the soma and proximal processes of healthy adult rat CA1 pyramidal cells (Yue et al., 2005); which have been shown to strongly express Nav1.2 (Gong et al., 1999). Resurgent current has been shown to occur in brain regions that have been reported to

express Nav1.2, including the globus pallidus (Gong et al., 1999 (Nav1.2); Yu et al., 2003; Mercer et al., 2007 (INaR)), dentate gyrus (Whitaker et al., 2001 (Nav1.2); Yu et al., 2003; Castelli, Biella, et al., 2007 (INaR)), and hippocampal CA1 pyramidal neurons (Whitaker et al., 2001; Liao, Deprez, et al., 2010 (Nav1.2); Yu et al., 2003; Castelli, Biella, et al., 2007; Buffington & Rasband, 2013 (INaR)).   Though no study has definitively shown that human neurons expressing Nav1.2 also express resurgent current, recordings from mouse DRG neurons have demonstrated that Nav1.2 channels can produce resurgent currents in a neuronal background (Rush et al., 2005). Since resurgent current requires a blocking molecule, there must be at least one blocking molecule endogenously expressed in these neuronal populations. So far, only two such proteins endogenous to neurons have been identified as responsible for generating resurgent currents: Navβ4 and FGF14b. It has been shown that Navβ4 and FGF14b, which are both endogenous to mouse cerebellar Purkinje neurons, are responsible for generating the endogenous resurgent current seen in these neurons (Wang et al., 2002; Grieco et al., 2005; Bant & Raman, 2010; Yan et al., 2014; White et al., 2019). A peptide from the intracellular portion of the Navβ4 protein (KKLITFILKKTREK-OH), referred to as the Navβ4 peptide, has been shown to induce resurgent current in multiple cell types expressing Nav channels (Aman et al., 2009; Grieco et al., 2005; Wang et al., 2006; Kim et al., 2010; Lewis and Raman, 2011; Thiele et al., 2011 , Patel et al., 2015). There may also be additional endogenous molecules in neurons that act as blocking molecules to induce resurgent currents.

Enhancement of persistent, resurgent, and gating pore currents are believed to cause hyperexcitability in affected neurons. Persistent currents have been shown to support burst firing in neurons from mammalian brains (Yue et al., 2005; Van Drongelen et al., 2006). Resurgent currents have been identified as drivers of both repetitive action potential activity and spontaneous action potential generation (Raman and Bean, 1997; Bant and Raman, 2010; Khaliq et al., 2003; Barbosa et al., 2015; Xiao et al., 2019). Increases in both persistent and resurgent currents through Nav channels have been correlated with increased action potential frequency and burst firing (Raman & Bean, 1997; Khaliq et al., 2003; Afshari et al., 2004; Yue et al., 2005; Van Drongelen et al., 2006; Kim et al., 2010; Hargus et al., 2013; Barker et al., 2017).

Persistent currents have been shown to be increased in rat hippocampal neurons from multiple epilepsy models (Royeck 2015 & others); and large persistent currents have been observed in subicular (hippocampal) neurons from human epileptic patients (Vreugdenhil et al. 2004). Several *SCN2A* epilepsy mutations (Liao et al., 2010 (M252V, V261M); Lauxmann et al., 2013; Schwarz et al., 2016; Parrini et al., 2017 (A263V); Wolff et al., 2017) have also been shown to increase persistent currents through Nav1.2. Resurgent currents are also enhanced by pro-excitatory disease mutations in other voltage-gated sodium channel isoforms which are associated with pain, myotonia congenital, long-QT syndrome, and *SCN8A* epilepsies (Jarecki et al., 2010; Patel et al., 2016; Xiao et al., 2019). Ours is the first study to investigate the impact of *SCN2A* disease mutations on resurgent currents.

Augmentation of persistent currents is often accompanied by augmentation of resurgent currents (Thiele et al., 2011; Barker et al., 2017). This concurrent augmentation has been seen in hippocampal neurons after induction of epilepsy in three rodent models (Hargus et al., 2013; Barker et al., 2017; Ottolini et al., 2017; Shao et al., 2017) and is associated with neuronal hyperexcitability and repetitive firing (Barker et al., 2017; Hargus et al., 2013; Van Drongelen et al., 2006; Yue et al., 2005; Kim et al., 2010; Raman and Bean, 1997; Khaliq et al., 2003; Afshari et al., 2004).

Six of the 21 *SCN2A* mutations characterized so far are reported to have only loss-of-function effects, and five have been shown to have a combination of gain- and loss-of-function effects. Loss-of-function effects, which diminish the channel function, include faster inactivation, depolarized voltage dependence of activation, hyperpolarized voltage dependence of inactivation, slowed recovery from inactivation, and decreased persistent currents; and they are believed to decrease neuronal excitability by decreasing the buildup of sodium ions in affected neurons. Since Nav1.2 is believed to be primarily expressed in glutamatergic neurons, the idea that some epilepsy mutations in this channel isoform decrease [glutamatergic] neuronal excitability challenges the dogma that the pathogenic effects of all epilepsy mutations in this isoform must enhance neuronal excitability by enhancing or augmenting the intracellular accumulation of sodium ions. Thus, any time loss-of-function effects are found to result from Nav1.2 epilepsy mutations, they complicate the interpretation of the overall mutation effects. When loss-of-function effects are revealed alongside gain-of-function effects, it can often be reasonably argued that the gain-of-function effects

likely prevail over the loss-of-function effects, resulting in a net gain of function and

enhancement of neuronal excitability. Other possible interpretations of a mutation with

mixed effects include that it is not responsible for the epilepsy, that some other protein

or molecule that is not accounted for in the experimental studies modifies the channel

activity to produce a net enhancement of channel function, or that there is another

functional effect of the mutation that has not been considered. One such effect that a

Nav disease mutation may have on the channel is the induction of a gating pore current.

It has been shown that the mutation of voltage-sensing residues in multiple Nav

channels, including Nav1.4 and Nav1.5 disease mutations, induces a cationic inward leak

current that is absent in wild-type channels (Sokolov et al. 2005, 2007, 2008, 2010;

Struyk et al., 2007; Wu et al., 2011; Gosselin-Badaroudine et al., 2012; Gamal El-Din et

al., 2014; Xiao, Blumenthal, and Cummins, 2014; Moreau et al., 2015; Jiang et al., 2018).

Molecular dynamic simulations of these mutations support the idea that they create an

anomalous pore, separate from the central pore, that supports cationic current (Fig. 4;

Gosselin-Badaroudine et al., 2014; Jiang et al., 2018). Since the gating pore is

structurally distinct from the central pore, gating pore currents are unimpeded by

tetrodotoxin (TTX), which binds within the central pore and inhibits transient currents.

These gating pore currents have primarily been observed in *Xenopus* oocytes expressing

the channels of interest, though they have also been observed in HEK cells expressing

Nav1.5 (Xiao, Blumenthal, and Cummins, 2014). Only one study has demonstrated that

mutations of voltage-sensing arginine residues in Nav1.2 can generate gating pore

currents (Sokolov et al, 2005). A study of the bacterial Nav channel, NaChBac, suggested
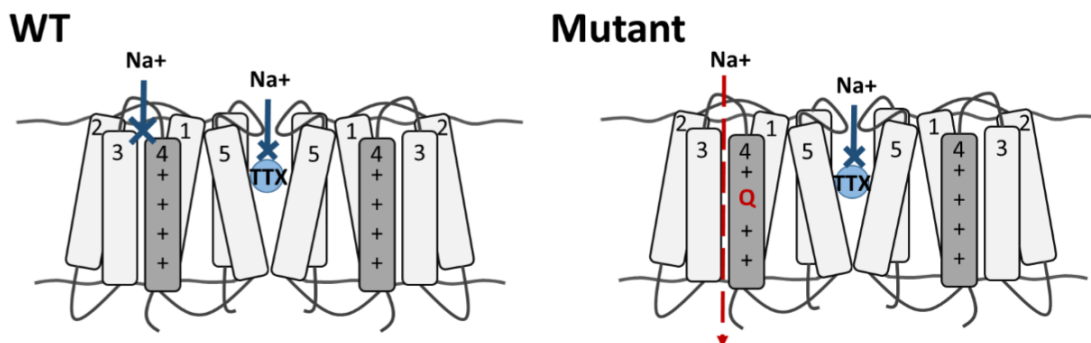
Figure 4. Mutation of S4 voltage-sensing residues creates a gating pore through which cations can pass. In the wild-type (WT) channel (left), sodium cannot pass through the voltage-sensing domain. When one of the voltage-sensing S4 residues is neutralized (right), a pore is created in the voltage-sensing domain that allows sodium – and possibly other cations – to leak into the cell. This gating pore is structurally distinct from the central pore, where tetrodotoxin (TTX) binds to inhibit transient sodium currents. Therefore, gating pore current can be isolated by saturating the sodium channels with TTX to block all transient currents.

that neutralization mutations of the first or second arginine residues (from the extracellular side of the membrane) in the voltage sensing segment can result in a gating pore that is open when the channel is in the resting state and closed when the channel is open or inactivated. Alternatively, it suggested that a neutralizing mutation of the third arginine residue can result in a gating pore that opens when the channel is open or inactivated and closed when the channel is in the resting state (Gamal El-Din et al., 2014). This phenomenon was confirmed, for the two outermost arginine residues, in rat Nav1.2 (Sokolov et al., 2005), though no resurgent current was observed when the third arginine residue was mutated.

Aberrant trafficking and cell surface expression of Nav channels is also believed to contribute to neuronal hyperexcitability (Mantegazza et al., 2010; Rusconi et al., 2007). This is evidenced by the reduced surface expression of BFNIS Nav1.2 mutants R1319Q, L1330F, and L1563V (loss-of-function mutations) as compared to wild-type

Nav1.2 channels (Misra et al., 2008) and the increased expression of these channels in granule cells with the gain-of-function mutation A263V (Liao, Anttonen, et al., 2010). Rat models of temporal lobe epilepsy also demonstrate changes in Nav channel expression and localization that are associated with changes in neuronal excitability and Nav channel function. Hippocampal neurons from rat models of temporal lobe epilepsy have reduced mRNA expression of Nav1.2 & Nav1.3 (Aronica et al., 2001) and altered Nav gating properties (Ketelaars et al., 2001) after induction of status epilepticus in the rats. The mEC layer II neurons from these rats also showed increased action potential firing, increased persistent and resurgent Nav currents, increased staining of Nav1.6 at the axon initial segment, and increased staining of Nav1.2 in the cell bodies, compared to the same population of neurons from age-matched control animals (Hargus et al., 2011). These findings suggest that changes in Nav1.2 localization and trafficking to the plasma membrane may contribute to the pathophysiology of some forms of epilepsy.

Antiepileptic Drug Strategies

Since epilepsy is characterized by inappropriate excitatory signaling in the brain, the overarching goal of antiepileptic therapies is to restore the proper balance of excitatory and inhibitory signaling in the brain. There are two primary strategies that are employed to achieve this aim: inhibiting excitatory neuron signaling and enhancing inhibitory neuron signaling. There are over 30 FDA-approved antiepileptic drugs, most of which have mechanisms of action that fall under one of those two umbrella strategies. Some drugs act only to inhibit excitatory signaling (including the inhibition of

neurotransmitter release), some act only to enhance inhibitory signaling, and some employ both strategies.

Since Nav1.2 is predominantly expressed in excitatory neurons, and since mutations in this protein are generally believed to cause epilepsy through gains of channel function, patients whose epilepsy is reasonably attributable to a *SCN2A* (Nav1.2) mutation are generally expected to respond well to sodium channel blockers, which act to inhibit excitatory signaling. Carbamazepine, lacosamide, oxcarbazepine, eslicarbazepine acetate, phenytoin, lamotrigine, and rufinamide all inhibit Nav channels as their primary mechanism of action, though not necessarily their only mechanism of action. These drugs have all been shown to be state- and frequency-dependent blockers, meaning that they bind preferentially to the inactivated conformation of the channels and that they have a high potency for hyperactive channels. Thus, they bind to inactivated channels and slow their recovery from inactivation, reducing the overall channel availability for the generation of subsequent action potentials. This reduces the occurrence of high-frequency or burst firing that is associated with epilepsy, without impeding normal neuronal firing. Valproate, felbamate, topiramate, and zonisamide are antiepileptic drugs that have been shown to block Nav channels; though they are all at least suspected to also block calcium channels, and the former three (valproate, felbamate, and topiramate) have also been shown to enhance inhibitory (GABA) signaling.

Carbamazepine, phenytoin, valproate, and topiramate are some of the most frequently prescribed drugs for patients with *SCN2A*-associated epilepsy. Phenytoin has

been reported to have achieved seizure freedom for seven patients with *SCN2A*

epilepsy, including two with Ohtahara Syndrome. However, thirteen other *SCN2A*

epilepsy patients found it unhelpful, and it even exacerbated the seizure phenotype in

one patient. Other sodium channel blockers that have been reported to grant seizure

freedom to *SCN2A* epilepsy patients as monotherapies include carbamazepine,

valproate, and topiramate. Five *SCN2A* epilepsy patients have been reported to have

achieved seizure freedom with a combination of two drugs, at least one of which is a

sodium channel blocker; and two more patients have had the same result with a

combination of three antiepileptic drugs, at least one of which is a sodium channel

blocker. Yet, despite the efficacy of these sodium channel blockers in some *SCN2A*

epilepsy patients, they prove insufficient to block seizures in others. Furthermore, these

AEDs, which some patients may need to take for life, are associated with adverse

neurological effects such as fatigue, dizziness, and memory problems. These and other

adverse effects of the AEDs sometimes severely decrease the patients' qualities of life;

therefore, there is a need for new AEDs that can block the mechanism of

epileptogenesis without producing devastating adverse effects.

One of the newest antiepileptics, Brivaracetam, is available as a drug called

Briviact (UCB, Inc.), which has been approved by the FDA as an antiepileptic for patients

with partial-onset seizures (Drugs.com, 2020). Brivaracetam's primary mechanism of

action seems to be similar to that of Levetiracetam, which targets a protein called SV2A

in the membranes of presynaptic vesicles and blocks neurotransmitter release.

Levetiracetam has also been shown to be a state- and voltage-dependent sodium

channel blocker (Zona et al., 2010). Though another study found brivaracetam to be only weakly effective in blocking voltage-gated sodium channel currents in rat neocortical neurons and human neuroblastoma cells and completely ineffective in adult mouse CA1 neurons (Niespodziany et al., 2015), the drug exhibited good tolerability and efficacy in clinical trials comprised of patients with refractory epilepsy (see Feyissa 2019 for review). Thus, it is unclear whether or not Brivaracetam's antagonism of Nav channels is involved as a secondary mechanism of its antiepileptic action.

An ideal pharmacotherapeutic strategy for any epileptic patient with a pathogenic *SCN2A* mutation may involve selectively targeting the specific pathological biophysical effects of each mutation, which often include the enhancement of aberrant currents such as persistent and resurgent currents. Such a strategy would maintain or restore healthy channel conductance and gating, as is seen in wild-type hNav1.2 channels, so as to prevent aberrant action potential firing without producing sedation or other adverse effects in patients. Though there are a few drugs in development that are selective for Nav1.7 and/or Nav1.8 over other Nav isoforms, there are no sodium channel blockers that are selective for the Nav1.2 isoform, as of 2020. Furthermore, studies suggest that most conventional sodium channel blockers do not preferentially block persistent or resurgent currents, which would be a helpful strategy for epileptic patients with Nav1.2 mutations that enhance persistent and resurgent currents but do not significantly affect the transient current amplitude.

Cannabidiol (CBD), a compound found in marijuana, has been demonstrated to preferentially inhibit resurgent current over transient current in hNav1.6 channels

expressed in HEK cells, while also blocking the enhancement of persistent current by an

epileptogenic hNav1.6 mutation (Patel et al., 2016). Though the primary mechanism of

antiepileptic action of CBD is unclear, it is known to antagonize voltage-gated sodium,

potassium, and calcium channels; and it has shown promise as an antiepileptic

compound in both preclinical and clinical studies (Hill et al., 2014; Mao et al., 2015;

Jones et al., 2010; Patel et al., 2016; Ghovanloo et al., 2018; Devinsky et al., 2016, 2017).

Additionally, clinical trials have shown that CBD, alone or as an add-on treatment,

reduces seizure frequency in many patients with refractory epilepsy (Press, Knupp, and

Chapman, 2015; Devinsky et al., 2016, 2017, 2018; Thiele et al., 2018; Szaflarski et al.,

2018a, 2018b; Savage et al., 2019), which explains why many refractory epilepsy

patients find relief from seizures with the use of medical marijuana, which contains CBD.

In June of 2018, a CBD formulation called Epidiolex (a schedule V drug produced by GW

Pharmaceuticals) became the first form of CBD to gain FDA approval, for the treatment

of refractory Dravet Syndrome and Lennox-Gestaut Syndrome (Drugs.com, 2019; U.S.

Food and Drug Administration, 2018).

One antiepileptic drug that is making its debut in 2020, cenobamate

(YKP3089), has been shown to enhance Nav channel inactivation, preferentially block

persistent sodium current (INaP) over transient sodium current (INaT), and reduce

excitability in acutely dissociated rat CA3 neurons (Nakamura 2019). However, it has

also been shown to be a non-benzodiazepine positive allosteric modulator of $GABA_A$

receptors, as evidenced by its enhancement of $GABA_A$-mediated currents in rat CA1

neurons (Sharma et al., 2018). This compound has been shown to be anticonvulsive in

several rodent models of epilepsy as well as in phase 2 trials in human epilepsy patients

(Bialer et al., 2013, Kasteleijn-Nolst Trenite et al., 2019; Krauss, et al., 2020). Though

there are no completed phase 3 studies of cenobamate, it gained FDA approval in

November of 2019 for the treatment of partial-onset seizures in adults, under the

commercial name Xcopri (SK Biopharmaceuticals).

Another sodium channel blocking compound that has demonstrated

preferential inhibition of INaP over INaT is GS967/Prax330 (Baker et al., 2018; Wengert

et al., 2019). This compound was initially studied as an antiarrhythmic that was found

to block persistent current over transient current in the cardiac sodium channel, Nav1.5,

but it is now being repurposed as an antiepileptic compound due to its brain

permeability and non-selectivity among Nav channel isoforms (Anderson et al., 2014;

Koltun et al., 2016). It has been shown to be antiepileptic in a mouse model of Dravet

Syndrome, which is a type of epilepsy caused by a loss of Nav1.1 function, in the Q54

mouse genetic model of *SCN2A* (Nav1.2) epilepsy, and in mice exhibiting epilepsy due to

the Nav1.6 epilepsy mutations N1768D and R1872W (Anderson et al., 2014, 2017; Baker

et al., 2018; Bunton-Stasyshyn et al., 2019). Given this efficacy shown in mouse models

of genetic epilepsy, GS967/Prax330 will likely continue to be studied as an antiepileptic,

especially if it continues to show preferential inhibition of persistent over transient Nav

current. A phase 1 trial to assess the safety of Prax330 has been completed in Australia,

but the results have not been publicly reported.

Since gating pore current is a novel concept in the pathogenesis of Nav

channelopathies, there are no published studies on the abilities of current AEDs or other

small molecules to block this aberrant current. There are no molecules known to bind

Nav channels at the gating pore, so gating pore currents are unlikely to be targeted by

standard clinical therapies. Thus, novel approaches may be needed to ameliorate the

impact of the gating pore currents produced by some neuronal sodium channel disease

mutations.

Though conventional sodium channel blockers are helpful for some epilepsy

patients, there is still a great need for antiepileptic pharmacotherapies that more

effectively prevent seizures in patients with *SCN2A* epilepsy mutations without

producing disturbing adverse effects. *In vitro* studies that examine the biophysical

effects of epileptic Nav channel mutations and the impacts of various sodium channel

blocking antiepileptic compounds on the affected channel functions will facilitate the

tailoring of antiepileptic therapies to the patients based on the specific effects of their

pathogenic mutation.

Hypothesis and Experimental Approach

In order to better understand how *SCN2A* mutations cause treatment-resistant

epilepsy, we must develop an understanding of how these mutations alter the Nav1.2

channel function. Since less than 10% of the *SCN2A* mutations formally reported to be

implicated in epilepsy have been studied *in vitro*, this study aimed to characterize three

more *SCN2A* mutations in order to expand our understanding of how these mutations

alter channel function and contribute to treatment-refractory epilepsy. Thus, the first

aim of this dissertation was to characterize the effects of three epilepsy mutations on

human Nav1.2 (hNav1.2) channel function.

We chose to characterize one novel *SCN2A*/Nav1.2 mutation that has been reported in an epileptic patient, L835F, and two that have been repeatedly reported in the literature, R853Q and R1882Q. Because the latter two mutations have been reported in many patients whose epilepsy was otherwise idiopathic, I am confident that they are implicated in the pathogenesis of the disease in these patients. The L835F mutation has not been identified as a variant in healthy patients, so it is likely to be epileptogenic. The R853Q mutation is one of the most frequently reported epileptogenic mutation in Nav1.2 and has been identified in patients diagnosed with severe forms of epilepsy including West Syndrome (a.k.a. infantile spasms). These are severe forms of epilepsy that usually have late onsets, are correlated with developmental delays and are refractory to multiple antiepileptic drugs. The R1882Q mutation has been identified in one patient diagnosed with Ohtahara Syndrome, as well as early-onset epileptic encephalopathies (including early infantile epileptic encephalopathy (EIEE) and neonatal onset epileptic encephalopathy (NOEE)). Most of these patients were reported to have severe developmental delays or intellectual impairment, but some of them have been able to effectively reduce their seizure frequency with high doses of phenytoin. The patient with the L835F mutation was diagnosed with a severe early-onset epilepsy. Since these mutations affect different segments of the hNav1.2 protein, which are involved in different aspects of channel function, I hypothesized that these mutations would produce distinct alterations in various aspects of hNav1.2 channel function. The results from the first aim confirmed this hypothesis.

It is well known that Nav disease mutations alter various parameters of channel gating, including transient and persistent current amplitude/density, as well as voltage dependencies and kinetics of activation and inactivation. While the enhancement of persistent and resurgent currents have been shown to underlie neuronal hyperexcitability and have both been associated with Nav1.6 epilepsies, resurgent currents had not been shown to result from any Nav1.2 disease mutations prior to 2019. Additionally, gating pore currents have been shown to be correlated with Nav1.4 disease mutations, but this study is also the first to show that gating pore currents can be generated by Nav1.2 mutations and may be implicated in the pathogenesis of epilepsy.

We chose to study these Nav1.2 mutations by expressing the wild-type or mutant channels in HEK cells, which have few or no endogenous Nav channels, in order to study the transfected channels in isolation. I examined most of the same aspects of Nav channel function as did previous *in vitro* electrophysiological studies of other *SCN2A* epilepsy mutations: transient current magnitude (measured as current amplitude and density), voltage dependencies of activation and fast inactivation, kinetics of fast inactivation, and persistent current magnitude. I found that the L835F, R853Q, and R1882Q mutation each produce a distinct set of effects on Nav1.2 channel function in HEK cells. I also investigated the effects of the R853Q and R1882Q mutations on the amplitude and density of resurgent currents, and found that these two mutations had opposite effects on the resurgent current magnitude. Since point mutations in the DII S4 voltage sensor of Nav1.4 have been shown to produce gating pore currents, and

given the high degree of conservation of this segment among all Nav isoforms, I

predicted that the R853Q mutation similarly creates a gating pore current in the Nav1.2

channel. Gating pore currents have been clearly demonstrated in *Xenopus* oocytes but

are difficult to discern in HEK cells, so I collaborated with the Cannon lab at the

University of California Los Angeles to demonstrate that the R853Q mutation creates a

gating pore current that is absent in wild-type channels.

Novel antiepileptic compounds are needed in order to more effectively

prevent seizures in patients with these and many other epileptogenic *SCN2A* mutations;

and this could be achieved by developing compounds that specifically target the

pathogenic effects of the mutations. Since resurgent current is increasingly being

implicated in the pathogenesis of Nav-associated epilepsy, I sought to identify

compounds that preferentially block resurgent or persistent current over transient

current. Previous studies indicated that CBD can preferentially block the resurgent over

transient Nav1.6 current (Patel et al., 2016) and that GS967 can preferentially block

persistent over transient Nav1.6 current (Baker et al., 2018; Wengert et al., 2019). Since

Nav1.6 and Nav1.2 are both predominantly expressed in excitatory neurons in the brain

and have similar structures and functions, I hypothesized that these compounds would

express the same preferential current inhibition in HEK cells stably expressing wild-type

Nav1.2 channels. Thus, the second aim of this dissertation was to test whether CBD and

GS967 preferentially inhibit resurgent or persistent current in hNav1.2. The results of

my preliminary studies support that hypothesis and suggest that, in HEK cells stably

expressing WT hNav1.2, CBD preferentially inhibits resurgent current over transient

current and GS967 preferentially inhibits persistent current over transient current.

Overall, this dissertation focuses on the biophysical effects of epileptogenic

Nav1.2 mutations. The results of this work expand the scope of pathogenic effects of

SCN2A mutations to include the enhancement of resurgent currents and the induction

of gating pore currents. The results of this research suggest that individual epilepsy

mutations in a single Nav channel gene produce distinct combinations of biophysical

effects on the channel function. Given the large proportion of epilepsy patients whose

seizures are refractory to conventional antiepileptic drugs, this implies that the patients

with these mutations may require tailored pharmacotherapies in order to effectively

suppress their seizures. The results of this work suggest that targeting specific

pathogenic biomechanisms of the mutations, such as resurgent and gating pore

currents, could constitute one novel approach to the identification and development of

more effective and tailored antiepileptic drugs.

II. MATERIALS AND METHODS

DNA Constructs

Codon-optimized human Nav1.2 DNA constructs (wild-type, R1882Q, & R853Q) were designed in-house and synthesized by GenScript (Piscataway, NJ). The amino acid sequence for the synthesized wild-type hNav1.2 cDNA construct corresponds with NG_008143.1 in the NCBI database. The *SCN2A* gene is contained within a pcDNA3.1 vector and preceded by a CMV promoter. Synthesized mutant constructs are identical to wild-type (WT) aside from the single mutation (R1882Q or R853Q). Mutagenesis (QuickChange II kit, Agilent Technologies, Inc.) was performed on the WT channel construct in order to generate the L835F mutant construct. The entire *SCN2A* gene region of this construct was sequenced (ACGT, Inc.) to ensure that no additional mutations were present.

HEK293 Cell Culture

The use of HEK293T cells (hereafter referred to as HEK cells; Dubridge et al., 1987) was approved by the Institutional Biosafety Committee and followed the ethical guidelines for the National Institutes of Health for the use of human-derived cell lines. HEK cells were grown under standard tissue culture conditions (5% CO_2, 37°C) in maintenance media consisting of DMEM supplemented with 10% fetal bovine serum and 1% penicillin/streptomycin.

Transient Transfections

HEK cells were transfected using the calcium phosphate precipitation method. Briefly, calcium phosphate-DNA mixture [2 µg channel construct and 1 µg enhanced

green fluorescent protein (EGFP)] was added to cells in serum-free media for 8-17 hours, after which the cells were washed with maintenance media and the serum-free media was replaced with maintenance media. Transfected cells were identified by presence of fine particulate coating the cells before washing and by expression of EGFP using a fluorescent microscope. Whole-cell patch clamp recordings were obtained 36-48h post-transfection.

Generation of Cell Lines Stably Expressing hNav1.2

Cell lines stably expressing hNav1.2 channels were generated by transfecting cells with the wild-type or mutant channel construct, which contains a gene conferring resistance to geneticin (G418). The calcium phosphate precipitation method of transfection was used, including replacement of media 8-17h post-transfection. 48h post-transfection, the cells were split into a 100mm dish and G418 (500 µg/mL) was added to the media. Media, including G418, was replaced 48h later. Once cell colonies were visible to the naked eye, colonies were picked and re-plated individually as independent cell lines stably expressing hNav1.2. Cell lines stably expressing hNav1.2 were maintained in maintenance media (1X DMEM, 10% FBS, 1% penicillin/streptomycin) containing 500 µg /mL G418.

HEK Electrophysiology

Currents were measured at room temperature (~22°C) using a HEKA EPC 10 amplifier and the Pulse software (v8.80, HEKA Elektronik) for data acquisition. Electrodes were fabricated from 100 µL calibrated pipettes (Drummond Scientific Company, Broomall, PA; cat. # 2-000-100; capillary glass) and fire-polished to a

resistance of 1.0-2.0 MΩ using a P-1000 micropipette puller (Sutter Instrument

Company, Novato, CA). For each cell, a GΩ seal was obtained before breaking into the

whole-cell configuration. Voltage protocols were initiated five minutes after entering

the whole-cell configuration, allowing time for each cell's cytoplasm to equilibrate with

the pipette solution, while also controlling for time-dependent shifts in sodium channel

properties. Voltage errors were minimized by using series resistance compensation (up

to 90%), and passive leak currents were cancelled by P/-5 subtraction. The bath

solution contained (in mM): 140 NaCl, 3 KCl, 1 $MgCl_2$, 1 $CaCl_2$, and 10 HEPES, adjusted to

pH 7.30 with NaOH. The pipette solution contained (in mM): 130 CsF, 10 NaCl, 10

HEPES, and 1 CsEGTA, adjusted to pH 7.30 with CsOH. Navβ accessory subunits were

not co-transfected with the Nav1.2α subunit, which functions independently as a

channel, due to the variability that this would introduce into the experiments and the

lack of information regarding which Navβ subunits are associated with the Nav1.2α

subunits in the affected neurons in the brain. When measuring resurgent currents, the

Navβ4 peptide (KKLITFILKKTREK-OH, used at 200 μM) (Biopeptide Co., Inc., San Diego,

CA), which corresponds to part of the C-terminal tail of the full-length Nav β4 subunit,

was included in the pipette solution in order to induce the resurgent currents. This

peptide has been shown to induce resurgent currents in HEK cells expressing voltage-

gated sodium channels, while, for unknown reasons, the full-length Navβ4 protein is not

sufficient to produce resurgent currents in HEK cells expressing voltage-gated sodium

channels (Aman et al., 2009; Chen et al., 2008).

HEK Voltage Protocols

All HEK cells were held at -100 mV.

Measures pertaining to transient current size, voltage-dependent activation, and persistent current were taken from a voltage protocol consisting of 50 ms test pulses to voltages from -80 to +60 mV, in 5 mV steps (Fig. 5A) for mutation characterization experiments. For pharmacology experiments, these values were derived from the first several sweeps in the inactivation protocol, which consisted of 500 ms hyperpolarizing pulses from -130 - +10 mV followed by a 20 ms depolarizing test pulse to +10 mV (Fig. 5B). Peak current amplitudes, for each voltage, were measured as the minimum value of the current over the entirety of the test pulse. Current densities were calculated by dividing raw current amplitudes by the membrane capacitance value of each cell. The reversal potential was estimated, for each cell, by extrapolation of the ascending limb of the current-voltage (IV) curve. The conductance values were then calculated and normalized within each cell. Persistent currents were measured, in Pulsefit (v8.80, HEKA Elektronik), as an average of the current amplitude over the last 10% of the test pulse, from 45-50 ms.

As mentioned above, inactivation was measured by a 500 ms prepulse step to voltages from -130 to +10 mV, in 10 mV steps, followed by a 20 ms test pulse to +10 mV (Fig. 5B). As with the activation protocol, peak transient current amplitude, for each voltage, was measured as the minimum value of the current over the entirety of the test pulse.
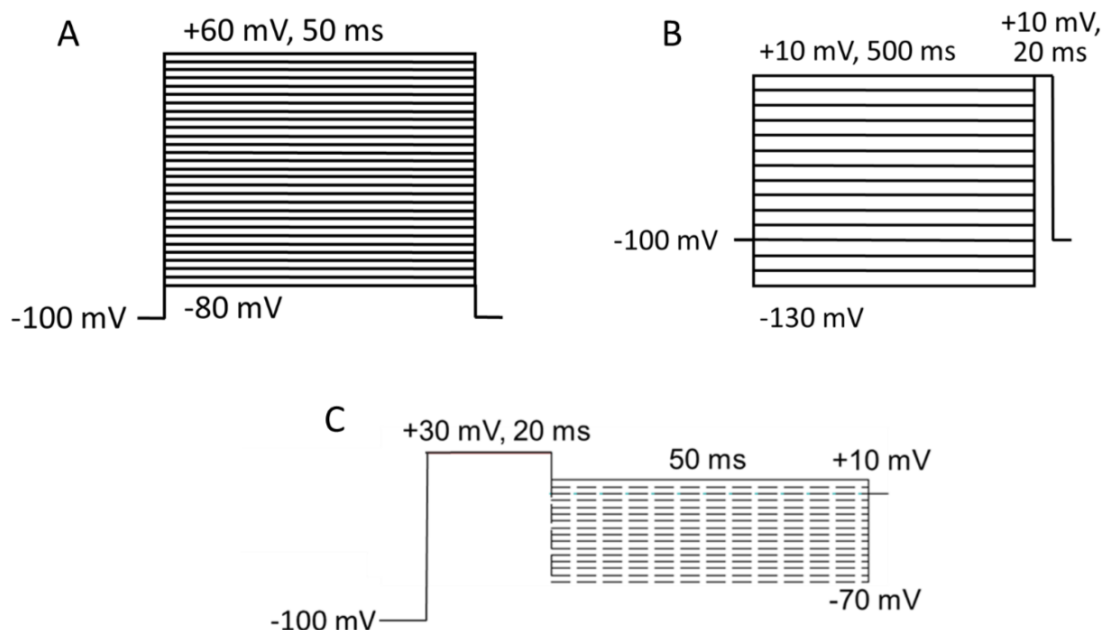
Figure 5. HEK cell electrophysiology voltage protocols. Adapted from Figure 2 in (Mason and Cummins, 2020). Cells were held at -100 mV for all three protocols. (A) Voltage protocol for the analysis of activation, transient currents, persistent currents, and gating pore currents. 50 ms square pulses from -80 to +60 mV, in 5 mV steps. (B) Voltage protocol for the analysis of inactivation and transient currents. 500 ms depolarizing prepulses from -130 to +10 mV, in 10 mV steps, followed by a 20 ms test pulse at +10 mV. (C) Resurgent current protocol.

Resurgent currents were elicited by a 20-ms pulse to +30 mV, followed by a 50-ms repolarization step of voltages from +10 to -65 mV (Fig. 5C). The resurgent current peak amplitude was measured, in Pulsefit, as the largest inward current value elicited during the repolarization step. For pharmacology experiments, in order to improve my confidence in the resurgent current values, each value was the average value from three repeats of each sweep.

Gating pore currents were measured with the same voltage protocol that was used to measure transient current size (with the addition of TTX to the bath solution and the exclusion of Navβ4 peptide from the pipette solution). The gating pore current

amplitude at each voltage step was measured as the average current amplitude from 1-99% of the duration of the test pulse.

Subcloning and Expression in Oocytes

For expression of hNav1.2 in oocytes, the *SCN2A* gene was cut from the pcDNA3.1 vector using the restriction enzymes NotI and NheI and subcloned into the pGEMHE-membrane-mEGFP plasmid (a gift from Melina Schuh, Addgene plasmid #105526 ; http://n2t.net/addgene:105526; RRID:Addgene_105526; Clift et al., 2017), replacing the EGFP gene in that construct with the *SCN2A* gene. The human β1 subunit, also in pGEMHE (Struyk and Cannon, 2007), was co-expressed with hNaV1.2 because it normalizes the inactivation kinetics of voltage-gated sodium channels expressed in *Xenopus* oocytes (Patton et al., 1994). Complementary RNAs were synthesized in vitro with the mMessage mMachine transcription kit (Ambion™). Oocytes were injected with ~ 50 ng of the hNaV1.2 WT or R853Q transcript plus 50 ng of the β1 subunit (four-fold molar excess).

Oocyte Maintenance

Oocytes were harvested from three female *Xenopus laevis* under MS222 anesthesia, in accordance with the guidelines established by the University of California, Los Angeles animal care committee's regulations. After defolliculation in collagenase type I at room temperature for ~ 2 h, oocytes were injected with cRNA and stored at 18 °C in 0.5 x Leibovitz's L-15 medium (Gibco™) supplemented with 1% horse serum, 100 U/ml penicillin, 100 μg/ml streptomycin and 100 μg/ml amikacin.

Oocyte Electrophysiology

Currents were recorded 3-6 days after injection using a cut-open oocyte voltage-clamp with the CA-1B amplifier (Dagan Corp.) in headstage clamp mode, as previously

described (Struyk and Cannon, 2007). The extracellular solution (upper and middle

chambers) contained in mM: 115 Na-methanesulfonate, 3 K-methanesulfonate, 4 Ca-

acetate, 10 HEPES, 0.1 ouabain, and 0.005 TTX, pH 7.4 with NaOH. The internal solution

(lower chamber) contained in mM: 120 K-methanesulfonate, 10 EGTA, 10 HEPES, pH 7.4

with methanesulfonic acid. The lower surface of the oocyte was permeabilized by brief

exposure to internal solution supplemented with 0.1% saponin.

Oocyte Voltage Protocols

To record gating pore current, an oocyte was held at -100 mV and a series of 200

ms voltage steps from -140 to +40 mV was applied. No on-line leak subtraction was

used. Instead, a linear fit of the (total) steady-state IV for test potentials from -20 mV to

+10 mV obtained to estimate the nonspecific linear current, which was subtracted to

obtain the gating pore current (see Fig. 11).   Charge displacement current was recorded

by application of a series of 20 ms test depolarizations from -140 mV to +40 mV from a

holding potential of -100 mV. The membrane capacitance was analog compensated

with the amplifier circuitry, and the residual linear leakage current suppressed by P/N

on-line leak subtraction of the current elicited by a depolarization from -120 mV to -100

mV. The charge displacement current was integrated digitally to obtain on-gating

charge, Q_{on}.

Pharmacology Methods

HEK293 cells stably expressing WT hNav1.2 channels were cultured in

maintenance media (DMEM with 10% FBS and 1% penicillin/streptomycin) containing

G418 (500 µg/mL). Cells were used 2 days (36-52h.) after splitting. The cells to be

studied were pre-incubated at 37°C for 15 minutes in either plain DMEM (untreated controls) or DMEM containing the pharmacological treatment (vehicle or vehicle + compound). Following the preincubation, the DMEM media was removed and replaced with HEK bath solution (recipe provided in previous "HEK Electrophysiology" section). Vehicle and compound treatments were added to the bath solution for those groups, at the same concentrations as in the preincubation.

Tested compounds included cannabidiol (CBD, Cayman Chemicals) and GS967 (Cayman Chemicals). Cannabidiol was dissolved in methanol at a stock concentration of 1 mM and stored at -20°C. GS967 was dissolved in dimethyl sulfoxide (DMSO) at a stock concentration of 1 mM and stored at -20°C. Both compounds were used at 1 µM final concentrations. Stock solutions were stored as 2 µL aliquots, one of which was diluted in each DMEM preincubation (2 mL) and each bath solution (2 mL) for each 35mm dish of cells, yielding a final solution comprised of 0.1% vehicle or compound solution.

Since the pharmacology experiments investigated the compounds' abilities to preferentially inhibit resurgent current over transient current, Navβ4 peptide (200 µM) was included in the pipette solution to induce resurgent currents.

For these experiments, transient currents were measured as the peak transient current elicited by the inactivation protocol (Fig. 5B), and peak persistent currents were also measured as the average current over the last 10% of the depolarization test pulse (from 18-20 ms) from this protocol. Peak resurgent currents were measured from the resurgent current protocol (Fig. 5C), as described above.

Statistics and Analysis

Electrophysiological data were analyzed using Pulsefit (v.8.80, HEKA Elektronik), Microsoft Excel, Origin (v9.1, OriginLab Corp.), and GraphPad Prism (v.7.03, GraphPad Software, Inc.). All data points are presented as mean ± standard error of the mean (SEM), and *n* is the number of cells from which contributing data was collected. Current density and conductance were calculated as previously described (Cummins et al., 1994; also see subsection above entitled "HEK Cell Voltage Protocols"). Activation and inactivation midpoints were estimated by fitting the current-voltage (IV) plot and inactivation curve for each cell to a current-voltage equation and the Boltzmann equation, repspectively, in Pulsefit. Inactivation time constants were estimated by fitting the decay portion of each sodium current trace to a single-exponential equation in Pulsefit.

The normality of data distribution was evaluated with the Shapiro-Wilk normality test. If the data was normally distributed, a parametric test was used; if the data was not normally distributed, a nonparametric test was used. For data comparisons spanning multiple voltages, a two-way ANOVA with the Sidak's multiple comparisons test was used. For single-measure comparisons between HEK cells expressing WT and L835F mutant channels, student's t tests or Mann-Whitney (nonparametric) tests were used. When a single measure was compared between the control and two conditional groups, as in the data comparing HEK cells expressing WT, R853Q mutant, and R1882Q mutant channels, and in the datasets comparing untreated cells with vehicle- and compound-treated cells, the data for all groups were collected concurrently, so these

single measurements were compared with one-way ANOVAs. If the data was normally distributed, an ordinary one-way ANOVA with Dunnett's multiple comparisons test was used; if the data was not normally distributed, the nonparametric Kruskal-Wallis with Dunn's multiple comparisons test was used. Statistical significance was set at $\alpha = 0.05$. Unless otherwise stated, p values reported for ANOVAs are the p values obtained from the post-test, and a significant p value ($p < 0.05$) was obtained in the ANOVA test. For all figures, unless otherwise specified, * $p < 0.05$, ** $p < 0.01$, *** $p < 0.001$, and **** $p < 0.0001$. Data from oocytes only included two groups, wild-type and R853Q, and therefore a nonparametric Mann-Whitney test was used for the single-measure comparison of Q_{max} values obtained from oocytes.

III. RESULTS

To investigate the functional effects of the L835F, R853Q, and R1882Q mutations on hNav1.2 channel function, the biophysical properties of wild-type and mutant voltage-gated sodium channels were characterized using whole-cell voltage clamp electrophysiology. The channel constructs were transiently expressed in HEK cells, which I have found to express little to no endogenous voltage-gated sodium current (-207.1 ± 33.64 pA, n = 10). Therefore, most of the voltage-gated inward current that I see, which, on average, is many times the amplitude of the average endogenous current, can be attributed to the wild-type or mutant channels for which the DNA was transfected.

Effects of the L835F Mutation on hNav1.2 Channel Function

Compared to wild-type (WT), the L835F mutation did not significantly alter average peak transient current density elicited by voltage steps between -80 and +65 mV (Fig. 6A-B, two-way ANOVA p = 0.0532, Sidak's multiple comparisons p > 0.99 at all tested membrane potentials, n = 11 WT, 18 L835F), maximum peak transient current density (an average of the maximum peak transient current density values for individual cells, WT -0.43 ± 0.07 nA/pF, L835F -0.47 ± 0.06 nA/pF, n = 11 WT, 18 L835F; p = 0.5968), or the average maximum peak transient current amplitude (an average of the maximum peak transient current amplitude values for individual cells, WT -8.19 ± 1.34 nA, R853Q -7.31 ± 0.92 nA, n = 12 WT, 16 L835F; p = 0.5785). Thus, the L835F mutation has no effect on transient hNav1.2 current amplitudes or densities in HEK cells.
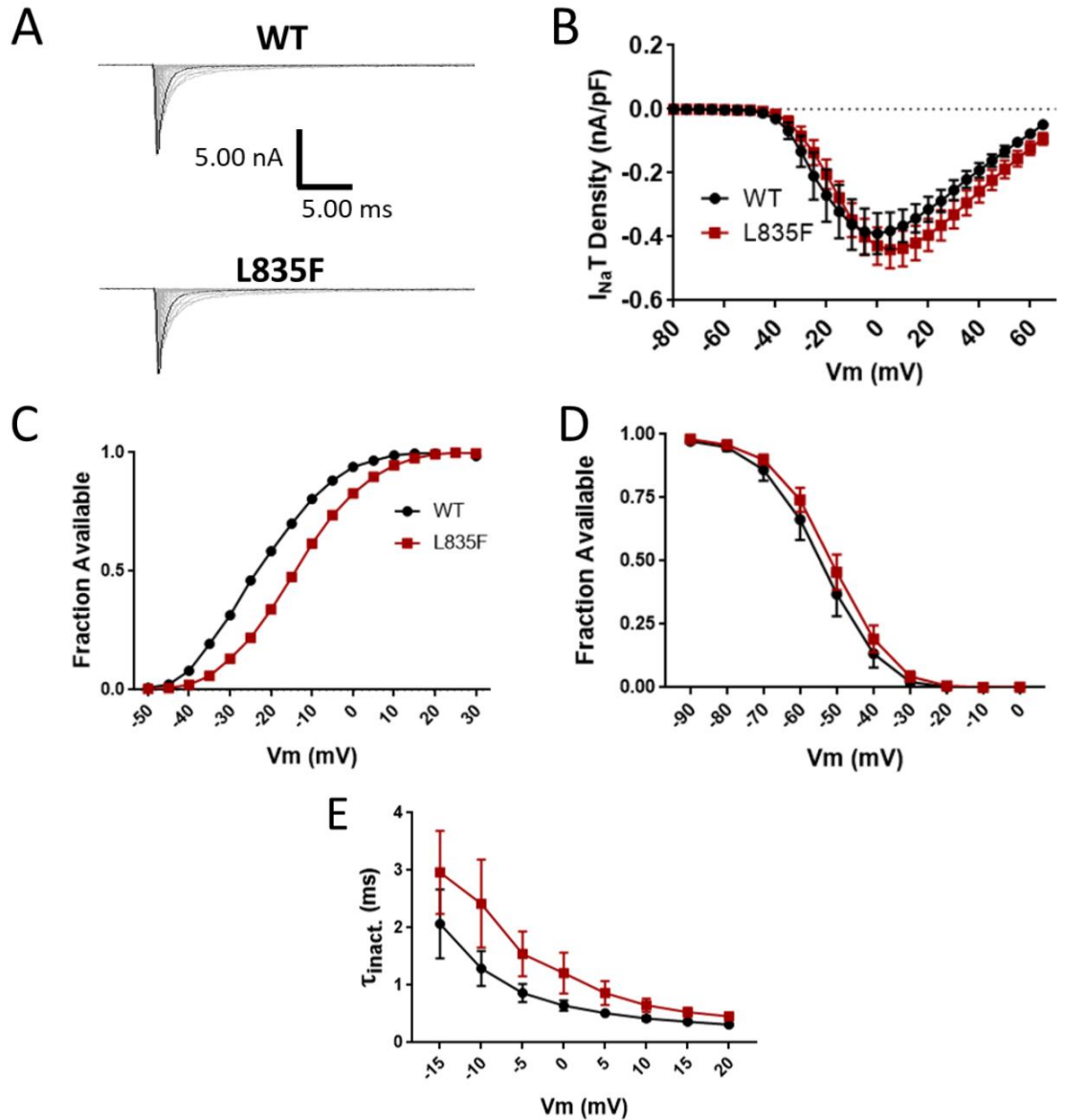
Figure 6. The L835F mutation does not significantly alter hNav1.2 transient current or gating properties. (A) Representative raw current trace families elicited by voltage steps from -80 to +60 mV. (B) Average current densities elicited by voltage steps from -80 to +60 mV. (C) Activation curves. Conductance was calculated as G/Gmax, where G = I/(Vm-Vrev), Vrev = reversal potential, and Gmax = maximum inward conductance across all tested voltages. (D) Inactivation curves. Fraction available was calculated as I/Imax for each cell at each voltage step. (E) Time constants of fast inactivation were calculated by fitting the decay portion of each current trace to a single-exponential equation in PulseFit (HEKA).

The voltage dependence of activation and inactivation were assessed using step

depolarizations as seen in the voltage protocols (Fig. 5A-B). The L835F mutation

46

produced depolarizing shifts in the voltage dependence of activation (Fig. 6C, two-way

ANOVA p = 0.0004; Sidak's multiple comparisons, p > 0.2500 at all tested membrane

potentials), and the average estimated activation midpoint (WT -19.03 ± 3.10, L835F -

11.99 ± 2.41, n = 12 WT, 18 L835F; p = 0.0861) for hNav1.2 channels transiently

expressed in HEK cells. The L835F mutation did not significantly alter the voltage-

dependence of fast inactivation (Fig. 6D, two-way ANOVA p = 0.1404, n = 12 WT, 16

L835F), the average estimated midpoint of inactivation (WT -53.98 ± 2.77 mV, L835F -

50.05 ± 2.14 mV, n = 12 WT, 17 L835F; p = 0.2636), or the kinetics of inactivation (Fig.

6E, two-way ANOVA p = 0.0085; Sidak's multiple comparisons p = 0.2946 - >0.9999 at all

tested voltages). Thus, the L835F mutation had only a small depolarizing effect on

hNav1.2 activation and no effect on inactivation in HEK cells.

The persistent component of the transient current was measured as the average

current amplitude during the last 10% of each depolarization pulse in the activation

protocol (Fig. 5A).   As shown in the representative traces (Fig. 7A), the L835F mutation

increased the average inward persistent current densities at voltages positive to -35 mV

(Fig. 7B, p = 0.0136 at -30 mV, p = 0.0336 at -20 mV, p < 0.01 from -15 - +10 mV, n = 11

WT, 18 L835F).   This increase in persistent current was further supported by an increase

in the average persistent current amplitude during the voltage step that elicited the

peak transient current amplitude for each cell (WT -31.60 ± 7.54 pA, L835F -57.26 ± 5.21

pA, n = 12 WT, 18 L835F; p = 0.0072; data not shown). To normalize the persistent

current amplitudes to overall expression levels, I also plotted persistent current

amplitude as a percentage of the maximum peak transient current amplitude of the

cells (values calculated for individual cells, average values plotted in Fig. 7C). This

analysis revealed that the persistent current was increased by the L835F mutation at

voltages positive to -35 mV, compared to persistent current in the wild-type channel

(Fig. 7C, p = 0.0569 at +5 mV, p = 0.0002 at +10 mV). Thus, the L835F mutation

increased persistent hNav1.2 currents in HEK cells. The effects of this mutation on

resurgent currents has not been studied, but I would expect the increase in persistent

currents to be accompanied by either no change or an increase in peak resurgent

current density and/or in peak resurgent current expressed as a percentage of peak

transient current.

The results of this experiment are reported in Table 2.
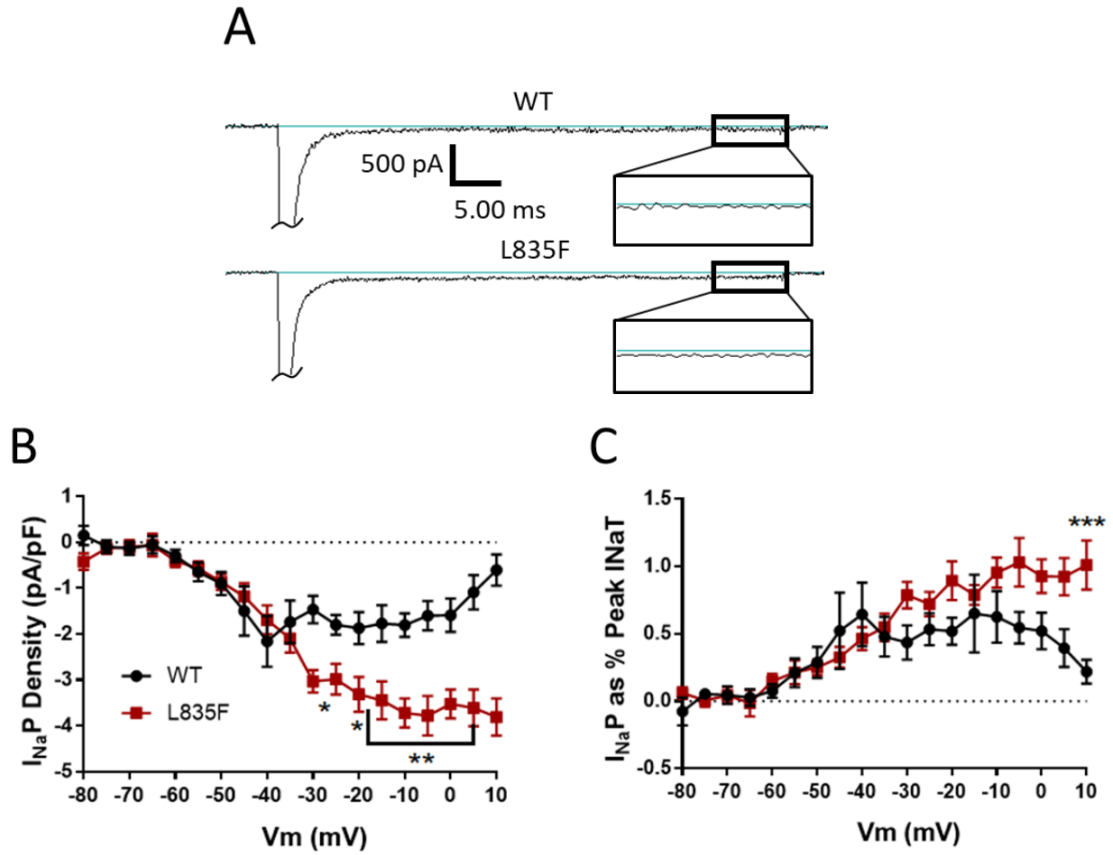
Figure 7. The L835F mutation enhances persistent currents. (A) Representative raw current traces from a voltage step to -5 mV. Persistent current, boxed (time, 4.26x zoom), was measured as the average current over the last 10% (i.e. 5 ms) of the voltage step. Inset: the portion of the trace (45-50 ms into depolarization) that was averaged to measure persistent current. (B) Average persistent current densities during the last 10% of voltage steps from -80 to +60 mV. (C) Average persistent current amplitudes normalized to maximum peak transient current amplitudes.

Table 2. Summary of current magnitudes and gating parameters of WT and L835F mutant channels.

	WT	L835F	L835F effect
Peak Transient Current Amplitude	-8.19 ± 1.34 nA	-7.31 ± 0.92 nA	None (unpaired t test, p = 0.5785)
Peak Transient Current Density	-0.425 ± 0.07 nA/pF	-0.474 ± 0.06 nA/pF	None (unpaired t test, p = 0.5968)
Activation Midpoint	-19.03 ± 3.10 mV	-11.99 ± 2.41 mV	Depolarizing shift (ns, unpaired t test, p = 0.0861)
Inactivation Midpoint	-53.98 ±2.77 mV	-50.05 ± 2.14 mV	Slight depolarizing shift (ns, unpaired t test, p = 0.2636)
Peak Persistent Current Amplitude	-54.64 ± 6.84 pA	-78.90 ± 8.34 pA*	Increased* (Mann-Whitney test, p = 0.0310)
Peak Persistent Current as % Peak INaT	0.8521 ± 0.15 %	1.389 ± 0.25 %*	Increased* (outlier removed, Mann-Whitney test, p = 0.0476)

*Significant difference ($p < 0.05$) vs. WT

Effects of the R853Q Mutation on hNav1.2 Channel Function

The R853Q mutation decreases transient current and enhances fast inactivation

The experiments characterizing the R853Q and R1882Q mutations were not performed contemporaneously with the experiment characterizing the L835F mutation, so separate WT groups were used for the two sets of characterization experiments. This way, the data from cells expressing each mutant was compared to contemporaneous data from cells expressing WT channels. In the presence of the Navβ4 peptide in the pipette solution, the R853Q mutation decreased the average peak transient current density, compared to wild-type (Fig. 8A-B, $p < 0.05$ from -30 - +30 mV), as well as the average maximum peak transient current density (WT-0.55 ± 0.05 nA/pF, R853Q -0.28 ±

0.04 nA/pF, n = 40 WT, 15 R853Q; p = 0.0033). The R853Q mutation also resulted in a

reduction of maximum peak transient current amplitude (WT -8.75 ± 0.76 nA, R853Q -

3.82 ± 0.54 nA, n = 41 WT, 16 R853Q; p = 0.0045). Thus, the R853Q mutation decreased

transient hNav1.2 current amplitudes and densities in HEK cells.

The same voltage protocols that were used to study activation and inactivation

in the L835F mutant were used to study these parameters for the R853Q mutant (Fig.

5A-B). The R853Q mutation did not significantly alter the voltage-dependence of

activation for hNav1.2 channels (Fig. 8C, p > 0.99 at all tested membrane potentials).

This was supported by a lack of significant difference in average estimated activation

midpoints (WT -26.5 ± 1.48, R853Q -25.11 ± 1.81, n = 41 WT, 16 R853Q; one-way

ANOVA p = 0.79). However, the mutation produced hyperpolarizing shifts in both the

voltage-inactivation relationship (Fig. 8D, p = 0.0001 at -70 and -60 mV) and the average

estimated inactivation midpoint (WT -65.01 ± 1.27 mV, R853Q -71.46 ± 1.62 mV, n = 40

WT, 16 R853Q; p = 0.016). The speed of fast inactivation, measured as a time constant,

was unaltered by the R853Q mutation (Fig. 8E, p > 0.99 at all tested membrane

potentials). Thus, the R853Q mutation had no effect on hNav1.2 activation but

enhances inactivation in HEK cells.
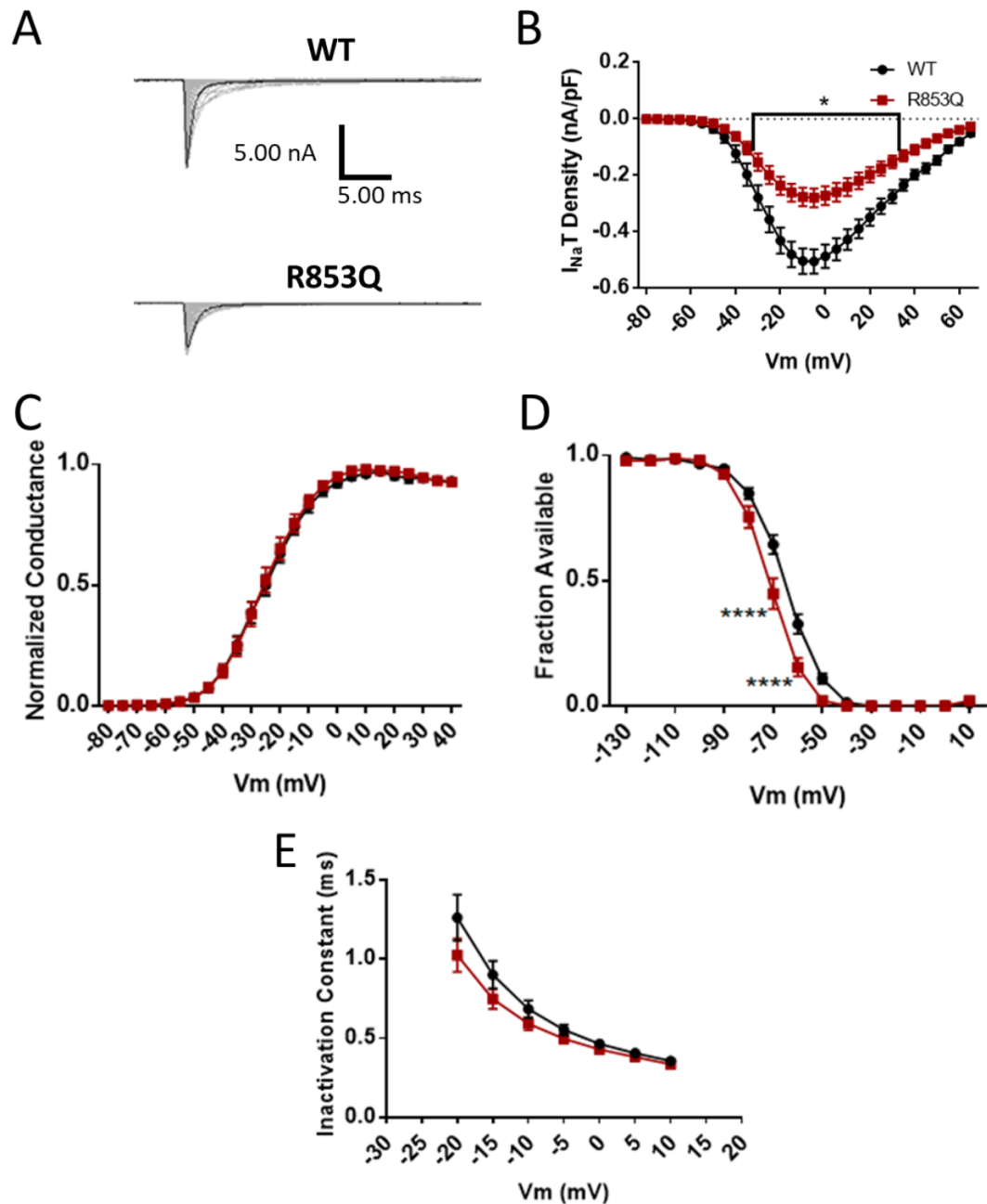
Figure 8. The R853Q mutation reduces transient current size and enhances inactivation. Adapted from Figure 4 in (Mason et al., 2019). (A) Representative raw current trace families elicited by voltage steps from -80 to +60 mV. (B) Average current densities elicited by voltage steps from -80 to +60 mV. (C) Activation curves. Conductance was calculated as G/Gmax, where G = I/(Vm-Vrev), Vrev = reversal potential, and Gmax = maximum inward conductance across all tested voltages. (D) Inactivation curves. Fraction available was calculated as I/Imax for each cell at each voltage step. (E) Time constants of fast inactivation were calculated by fitting the decay portion of each current trace to a single-exponential equation in PulseFit (HEKA).

The R853Q mutation decreases persistent and resurgent currents

Persistent current was measured in the same manner for the R853Q mutant

channel as for the L835F mutant and wild-type channels. As shown in the

representative traces (Fig. 9A), the R853Q mutation reduced the average inward

persistent current densities between voltages of -60 mV to +10 mV (Fig. 9B, p = 0.0028 –

0.05 from -35 - +5 mV). This reduction in persistent current was further supported by a

reduction in the average persistent current amplitude during a -30-mV depolarization

(WT -44.97 ± 4.15 pA, R853Q -12.78 ± 4.27 pA, n = 40 WT, 16 R853Q; p = 0.0008). When

normalized to the maximum peak transient current amplitudes for individual cells, the

persistent current was reduced, though not significantly, by the R853Q mutation,

compared to persistent current in the wild-type channel (Fig. 9C, p > 0.10 at all tested

membrane potentials). This reduction was supported by analysis of the average

persistent current during a -30 mV step, as percent of peak transient current, which

showed a significant reduction in this value with the R853Q mutation, compared to wild-

type (WT 0.57 ± 0.05 %, R853Q 0.26 ± 0.10, n = 40 WT, 16 R853Q; p = 0.037). Thus, the

R853Q mutation decreased persistent hNav1.2 currents in HEK cells.
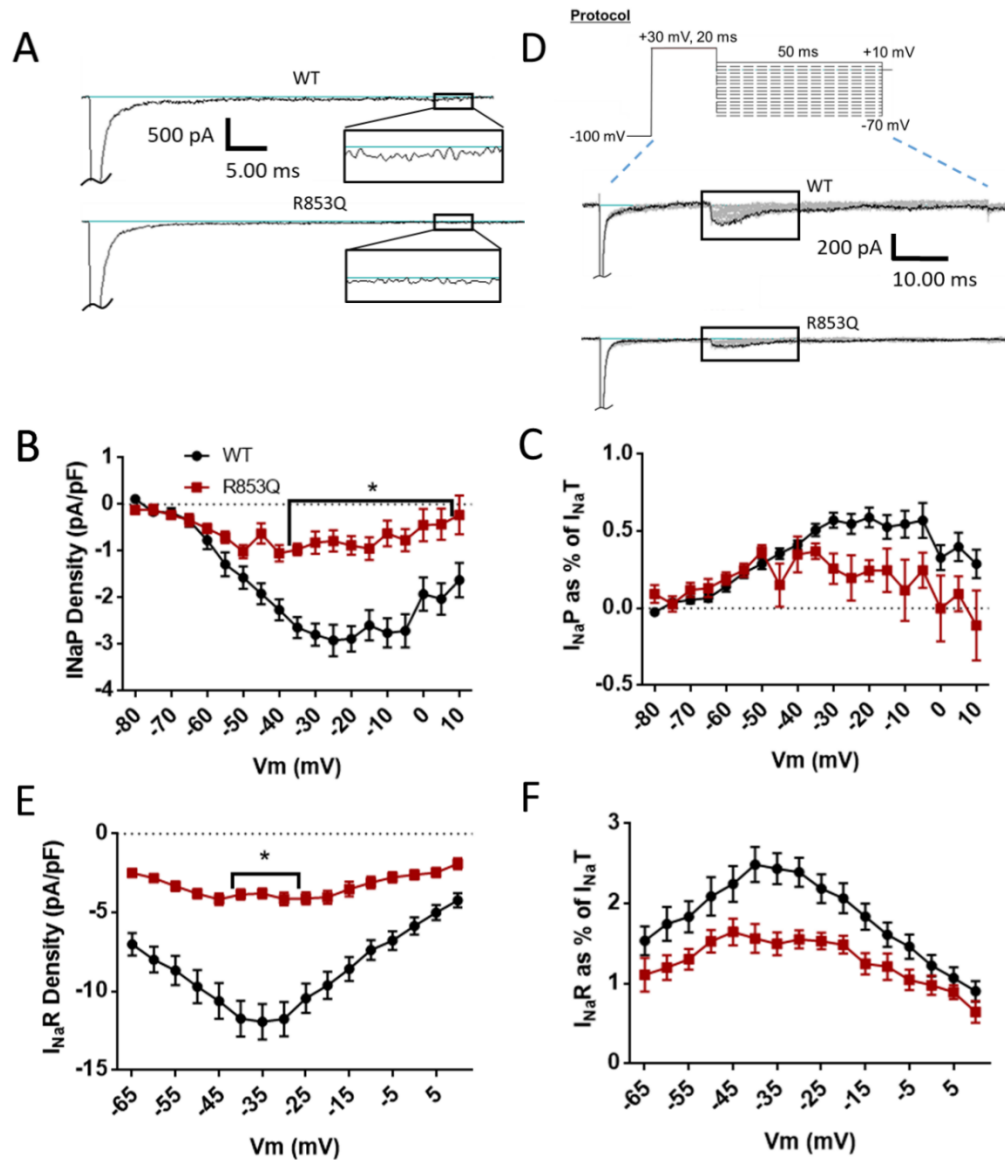
Figure 9. The R853Q mutation reduces persistent and resurgent currents. Adapted from Figure 5 in (Mason et al., 2019). (A) Representative raw current traces from a voltage step to -15 mV. Persistent current, boxed (~5x), was measured as the average current over the last 10% (i.e. 5 ms) of the voltage step. Inset: the portion of the trace (45-50 ms into depolarization) that was averaged to measure persistent current. (B) Average persistent current densities during the last 10% of voltage steps from   -80 to +10 mV. (C) Average persistent current amplitudes normalized to maximum peak transient current amplitudes. (D) Resurgent current voltage protocol (top) and representative resulting raw current trace families (middle and bottom); resurgent current indicated by boxes. (E) Average peak resurgent current densities over a range of voltages from -65 to +5 mV. (F) Average peak resurgent current amplitudes normalized to maximum peak transient current amplitudes. For (B, C, E), and (F), values were calculated for each individual cell and averaged for each group.

Resurgent sodium currents have not been studied with Nav1.2 disease

mutations, though they have been associated with other diseases (Xiao et al., 2019,

Jarecki et al., 2010, Hargus et al., 2011, Tanaka et al., 2016, Patel et al., 2016). To induce

resurgent current through Nav1.2 in HEK cells, the Navβ4 peptide (200 μM) was

included in the pipette solution. Cells were depolarized to +30 mV briefly, to open the

channel and allow the peptide time to block the central pore, followed by a longer

repolarization to voltages ranging from -65 to +10 mV (Fig. 5C; 9D, top). Resurgent

current occurs during the repolarization step, after the transient current is inactivated,

when the peptide unbinds and a small inward current occurs between the unbinding of

the peptide and the binding of the inactivation particle to the pore. Compared to cells

expressing wild-type hNav1.2 channels, cells expressing R853Q mutant channels

exhibited a significant reduction in average resurgent current densities (Fig. 9D-E, p =

0.0058 – 0.0137 from -40 - -30 mV), which also manifested as a reduction when the

maximum peak resurgent current amplitudes were normalized to the maximum peak

transient current amplitudes for individual cells (Fig. 9F, p = 0.0972 at -35 mV, p > 0.10

at all other tested membrane potentials). These results were supported by analysis of

the average resurgent current amplitudes during a -30 mV pulse, which revealed a

significant reduction in the average peak resurgent current amplitude (WT -178.40 ±

15.33 pA, R853Q -61.33 ± 7.26, n = 39 WT, 16 R853Q; p < 0.0001) and a nearly-

significant reduction in the average peak resurgent current amplitude expressed as a

percentage of peak transient current amplitude (WT 2.39 ± 0.18 %, R853Q 1.55 ± 0.11

%, n = 39 WT, 16 R853Q; p = 0.0389). Thus, the R853Q mutation decreases resurgent hNav1.2 currents in HEK cells.

The R853Q mutation forms a gating pore that passes current at negative membrane potentials

All of my data up to this point suggests that the R853Q mutation confers a loss of function on the hNav1.2 channel. Since the seizures and choreoathetosis (a specific form of irregular involuntary movements) associated with the R853Q mutation suggest a possible neuronal gain of function effect, I hypothesized that this mutation increases channel activity via the formation of a gating pore conductance. Such a pore, which is structurally distinct from the central pore, can allow some monovalent cations to leak into the cell through the domain II voltage sensor, which contains the R853Q mutation (Fig. 4).

To assess the effects of the R853Q mutation on the gating pore current, cells expressing wild-type or R853Q mutant hNav1.2 were treated with TTX and subjected to a series of voltage steps, in the absence of the Navβ4 peptide. Such experiments in HEK cells yielded inconsistent results which were difficult to interpret. Since *Xenopus* oocytes are much larger and can express more copies of the transfected Nav channel, the peak current amplitude in oocytes is much larger (~1,000x) than that recorded from HEK cells. Due to the large magnitudes of currents in oocytes, including gating pore current, this expression system allows rigorous quantification of any differences in gating pore current amplitude between wild-type and R853Q mutant hNav1.2 channels. The optimized hNav1.2 wild-type and R853Q mutant channel constructs were subcloned

from the pcDNA3.1 vector into a pGEMHE vector that could be used for sodium channel

expression in oocytes. To estimate relative plasma membrane expression levels of wild-

type and R853Q mutant hNav1.2 channels, the average maximal gating charge (Q_{max}) of

oocytes expressing wild-type or R853Q mutant hNav1.2 channels was measured in the

presence of TTX. The peak Q_{max} was significantly reduced by the R853Q mutation,

compared to wild-type (Fig. 10A, WT 0.85 ± 0.12 nC, n = 5; R853Q 0.44 ± 0.06 nC, n = 6;

$p < 0.0001$ at all voltages positive to 0 mV). The magnitude of this reduction of Q_{max}

(~50%) suggests that the plasma membrane expression level of the channels is reduced

by the R853Q mutation, consistent with the reduced amplitude of the transient inward

sodium current in HEK cells. Normalizing the Q(V) curves to Q_{max} for each cell and

plotting the average across cells revealed no significant change in the midpoint or slope

of the gating charge-voltage relationship between wild-type -expressing and R853Q-

expressing oocytes (Fig. 10B). The gating charge movement reflects the movement of

the S4 (voltage-sensing) segments during activation, these results suggest that the

R853Q mutation does not alter the voltage dependence of voltage sensor movement,

with regards to activation.
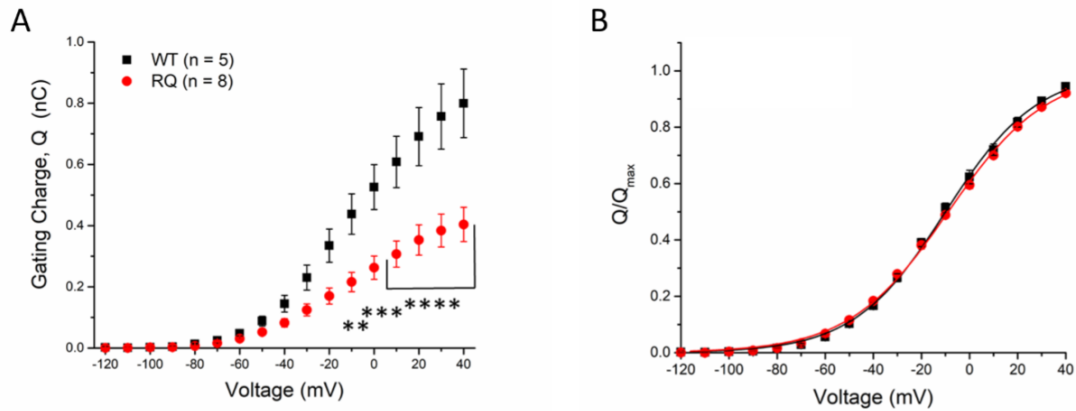
Figure 10. R853Q reduces channel surface expression. Published as Figure 6 C-D in (Mason et al., 2019). (A) Average gating charge (Q) values measured from oocytes expressing either WT (black squares) or R853Q (red circles) hNav1.2. The average Q value at +40 was recorded as Qmax for each group. (B) Voltage dependence of gating charge movement is shown as a normalized gating charge-voltage relationship. Average gating charge (Q) across a range of membrane potentials were normalized to the average Qmax value for each group.

To measure gating pore current, the total leak current in oocytes expressing wild-type or mutant hNav1.2 was measured over a range of membrane potentials (-120 to +40 mV) in the presence of TTX, which blocked the central pore and prevented transient current conduction (see raw traces in Fig. 11A-B). In order to isolate the gating pore current, the average nonspecific leak current was subtracted from the total leak current. The average nonspecific leak was estimated by fitting the steady-state current-voltage (I-V) curve (range -20 to + 10 mV, end of 200 ms pulse) with a line (Fig. 11C-D, dotted lines) and subtracted from the total leak current (11C-D, data points) to generate gating pore current I-V curves for oocytes expressing wild-type and R853Q channels (Fig. 11E-F). Compared to oocytes expressing wild-type channels, R853Q-expressing oocytes demonstrated an inwardly-rectifying current that diverges from the nonspecific leak current at hyperpolarized potentials (Fig. 11E-F). This anomalous inward-rectifying current presumably exists due to the formation of a gating pore in the mutant channel,

as supported by dramatically increased current amplitude in the presence of extracellular guanidinium (Fig. 12), which has been reported for gating pore currents in R/X mutations of S4 in Nav1.4 (Sokolov et al., 2010).

To further confirm that the inwardly-rectifying current in the R853Q mutant channels is conducted by the gating pore, and not an endogenous conductance, the Q_{max} for each cell was plotted against the measured gating pore current at -120 mV. This plot (Fig. 13A) revealed a linear correlation between inward current amplitudes and the corresponding maximal gating charge displacement in individual oocytes for the R853Q mutant channel (Pearson's R = –0.974, R^2 (adjusted) = 0.943), but not for the wild-type channel. This suggests that a gating pore current that is dependent on channel density is present in the R853Q mutant form of hNav1.2 but essentially absent in the wild-type form.

To facilitate the comparison of gating pore currents in oocytes with different levels of channel expression on the plasma membranes, leak-subtracted currents were normalized to Q_{max} for each oocyte. The average normalized I-V relationships of wild-type - and R853Q-expressing oocytes revealed a substantial increase in hyperpolarization-activated inward current in R853Q-expressing oocytes compared to wild-type -expressing oocytes (Fig. 13B). These data provide strong support for the theory that a gating pore current exists in the R853Q mutant channel at membrane potentials negative to -30 mV.
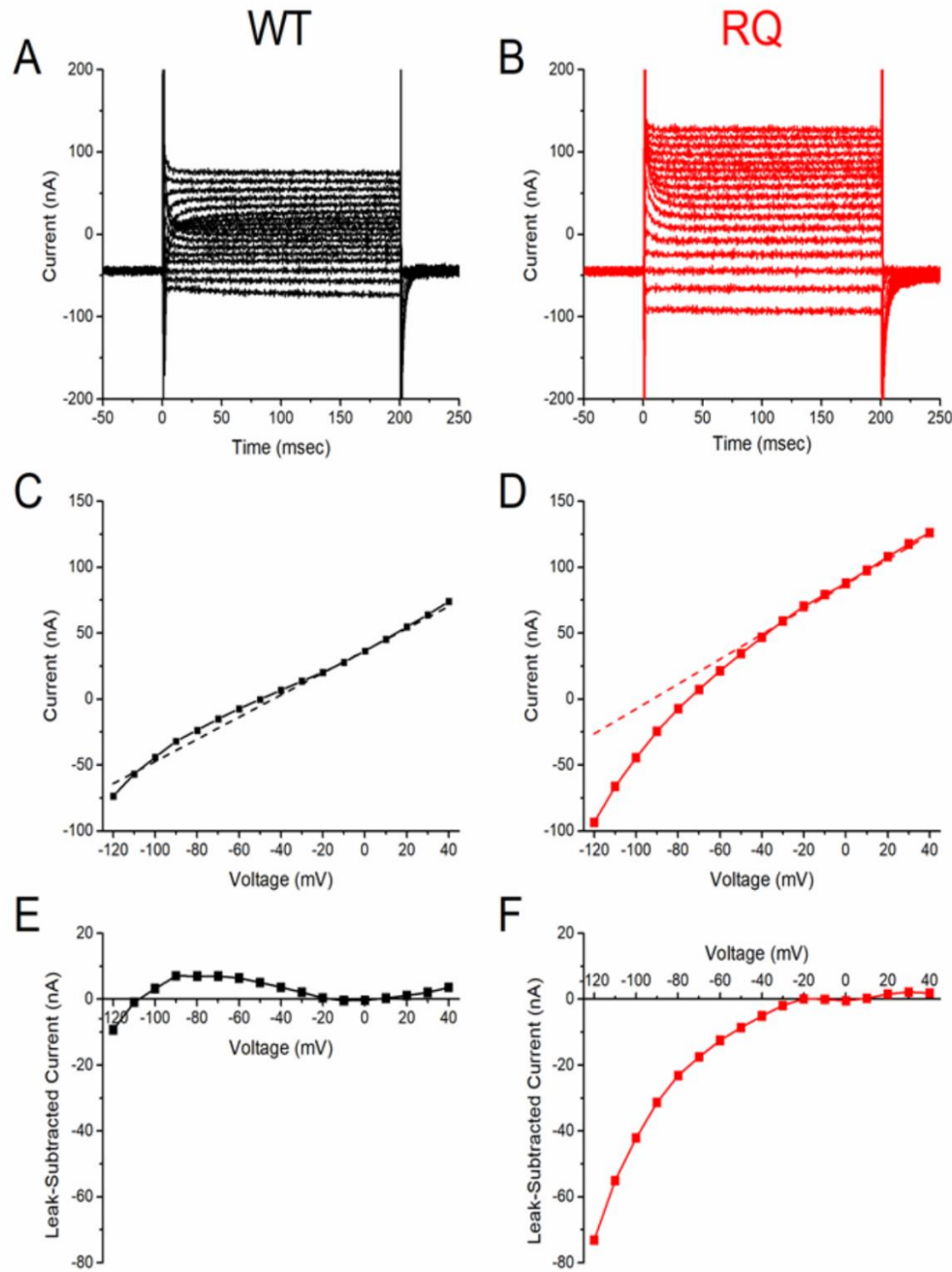
Figure 11. R853Q creates a voltage-sensitive inward leak current. Published as Figure 7 in (Mason et al., 2019). Single-cell representative data (n = 1 WT, 1 R853Q). (A-B) Representative raw leak current traces measured from oocytes expressing either WT (black) or R853Q (red) hNav1.2. (C-D) Leak current-voltage (IV) relationships of the representative cells. Leak subtraction was performed for each cell by fitting the steady-state IV (range -20 to + 10 mV, end of 200 msec pulse) with a line (dotted lines). (E-F) Nonspecific leak-subtracted current-voltage (IV) relationships, interpreted as gating pore current-voltage (IV) relationships, of the representative cells.
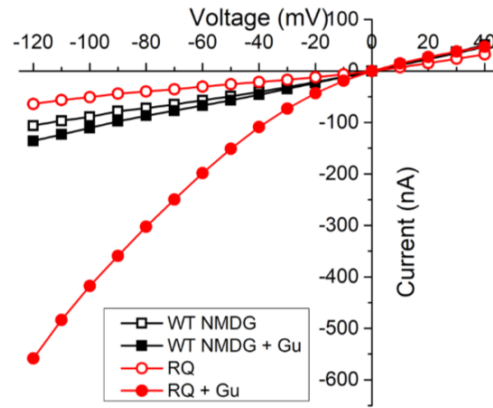
Figure 12. R853Q-induced gating pore is permeable to guanidinium. Published as Figure 8 in (Mason et al., 2019). Single-cell representative data (n = 1 WT, 1 R853Q). Leak currents in oocytes expressing either WT (black squares) or R853Q (red circles) hNav1.2 in the absence (empty symbols) and presence (filled symbols) of guanidinium, a cation believed to be permeant to the gating pore created by the R853Q mutation in Nav1.2.
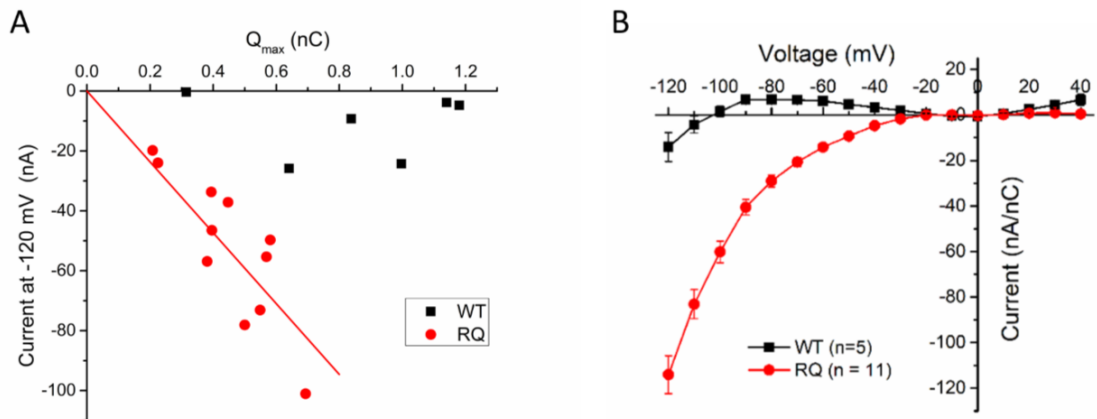
Figure 13. R853Q creates gating pore current. Adapted from Figure 9 in (Mason et al., 2019). (A) Distance of gating charge movement (Qmax) was plotted against the gating pore current amplitude measured at -120 mV for each cell. (B) Average leak-subtracted (i.e. gating pore) current was normalized to Qmax for each cell and the normalized gating pore current-voltage (IV) relationships for WT (black squares) and R853Q (red circles) were plotted.

Effects of the R1882Q Mutation on hNav1.2 Channel Function

The R1882Q mutation impairs fast inactivation

In HEK cells transiently expressing hNav1.2, and with the Navβ4 peptide in the pipette solution, the R1882Q mutation had no effect on the average peak transient current density (Fig. 14A-B, $p > 0.40$ at all tested membrane potentials). It also had no effect on the average maximum peak transient current density (WT -0.55 ± 0.05 nA/pF, R1882Q -0.51 ± 0.07 nA/pF, n = 40 WT, 22 R1882Q; $p = 0.80$) or the average maximum peak transient current amplitude (WT -8.75 ± 0.76 nA, R1882Q -8.89 ± 1.14 nA, n = 41 WT, 27 R1882Q; $p > 0.99$). Thus, the R1882Q mutation did not alter transient hNav1.2 current amplitudes or densities in HEK cells.

The same voltage protocols that were used to study activation and inactivation in the previous two mutants were used to study these parameters for the R1882Q mutant (Fig. 5A-B). The R1882Q mutation produced no significant shift in the conductance curve of Nav1.2, compared to wild-type (WT) (Fig. 14C, $p > 0.40$ at all tested membrane potentials) and had no effect on the average midpoint of activation (WT -26.50 ± 1.48 mV, R1882Q -24.77 ± 2.76 mV, n = 41 WT, 24 R1882Q; one-way ANOVA $p = 0.79$). The R1882Q mutation produced a significant depolarizing shift in the fast inactivation curve (Fig. 14D, $p = 0.0001$ from -70 - -50 mV, $p = 0.040$ at -40 mV), which was reflected in the depolarization of the average inactivation midpoint (WT -65.01 ± 1.27 mV, R1882Q -57.34 ± 2.05 mV, n = 40 WT, 20 R1882Q; $p = 0.0017$). The R1882Q mutation also slowed inactivation, as evidenced by increased inactivation time constants at voltages from -20 to +10 mV (Fig. 14E, $p < 0.0001$ at -20 and -15 mV, $p =$
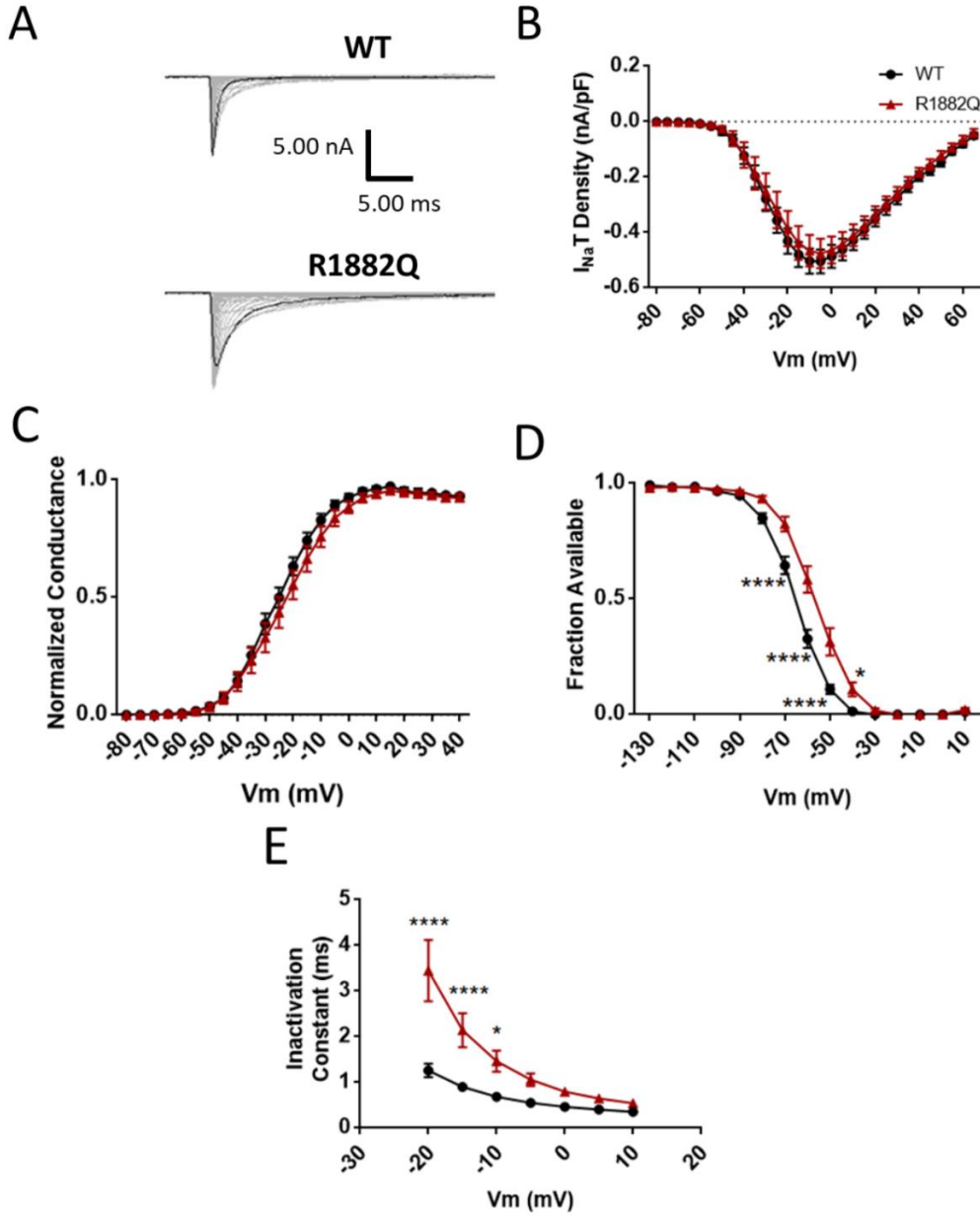
Figure 14. The R1882Q mutation has no effect on transient current magnitude and impairs inactivation. Adapted from Figure 2 in (Mason et al., 2019). (A) Representative raw current trace families elicited by voltage steps from -80 to +60 mV. (B) Average current densities elicited by voltage steps from -80 to +60 mV. (C) Activation curves. Conductance was calculated as G/Gmax, where G = I/(Vm-Vrev), Vrev = reversal potential, and Gmax = maximum inward conductance across all tested voltages. (D) Inactivation curves. Fraction available was calculated as I/Imax for each cell at each voltage step. (E) Time constants of fast inactivation were calculated by fitting the decay portion of each current trace to a single-exponential equation in PulseFit (HEKA).

0.0185 at -10 mV). Thus, the R1882Q mutation had no effect on hNav1.2 activation but

impaired inactivation in HEK cells.

The R1882Q mutation increases persistent and resurgent currents

Persistent current was measured in the same manner for the R1882Q mutant

channel as for the previous two mutants. The R1882Q mutation increased average

persistent current densities at voltages from -65 to +5 mV (Fig. 15A-B, $p = 0.0001$ from -

50 to -25 mV, $p = 0.0016$ at -20 mV, $p = 0.0526$ at -15 mV). When analyzed at a single

voltage of -30 mV, the average persistent current amplitude was increased for the

R1882Q mutant, compared to wild-type (WT -44.97 ± 4.15 pA, R1882Q -100.80 ± 16.53

pA, n = 40 WT, 27 R1882Q; $p = 0.029$). When normalized to the maximum peak

transient current amplitudes for individual cells, the persistent current was still

increased for the R1882Q mutant channel at most voltages from -65 to +5 mV (Fig. 15C,

$p < 0.05$ from -35 to -20 mV), compared to the wild-type channel. When the persistent

current, as percent of transient current, was analyzed at -30 mV, the significant increase

caused by the R1882Q mutation was again observed (WT 0.57 ± 0.05 %, R1882Q 1.15 ±

0.13, n = 40 WT, 27 R1882Q; $p < 0.0001$). Thus, the R1882Q mutation enhanced

persistent hNav1.2 currents in HEK cells.
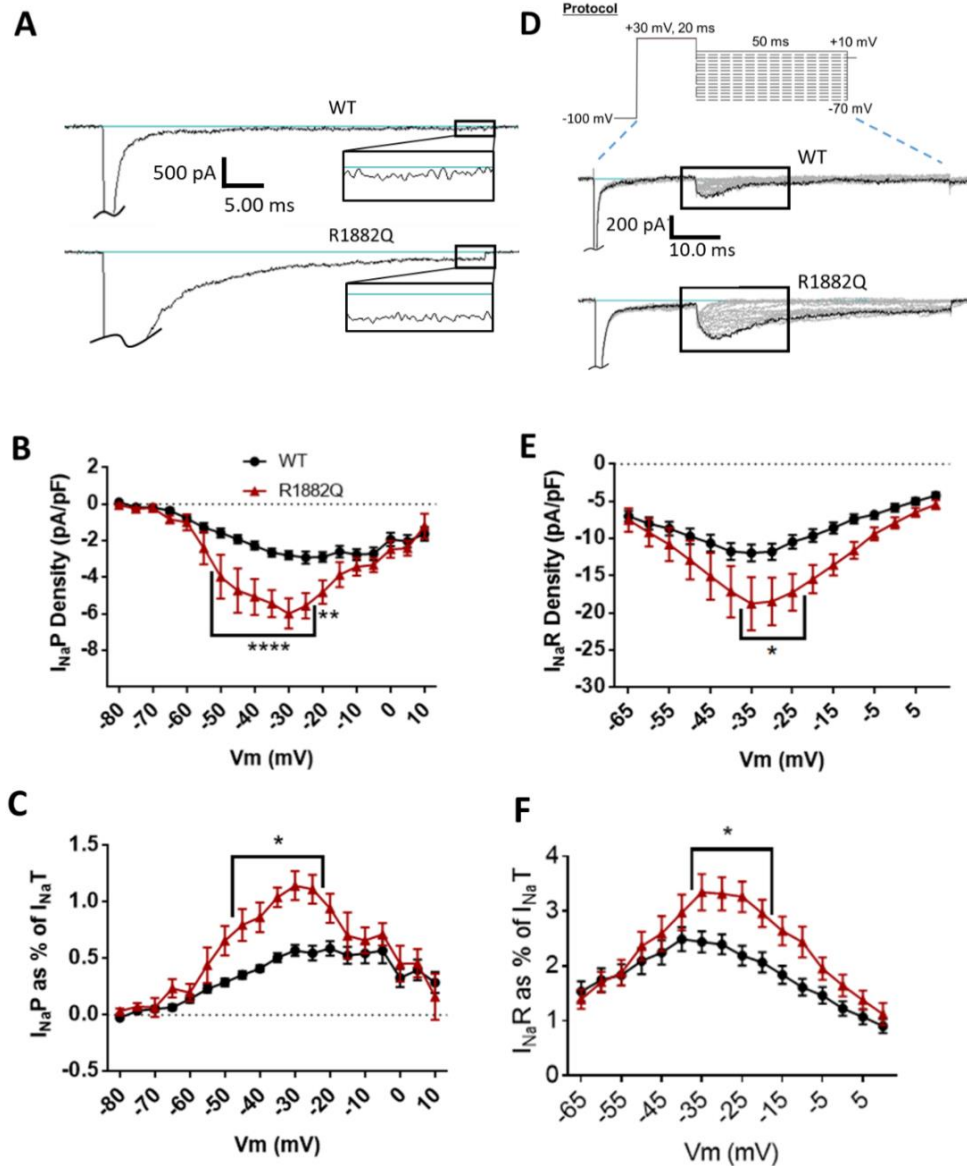
Figure 15. The R1882Q mutation enhances persistent and resurgent currents. Adapted from Figure 3 in (Mason et al., 2019). (A) Representative raw current traces from a voltage step to -15 mV. Persistent current, boxed (~5x), was measured as the average current over the last 10% (i.e. 5 ms) of the voltage step. Inset: the portion of the trace (45-50 ms after depolarization) that was averaged to measure persistent current. (B) Average persistent current densities during the last 10% of voltage steps from -80 to +10 mV. (C) Average persistent current amplitudes normalized to maximum peak transient current amplitudes. (D) Resurgent current voltage protocol (top) and representative resulting raw current trace families (middle and bottom); resurgent current indicated by boxes. (B) Average peak resurgent current amplitudes over a range of voltages from -65 to +5 mV. (E) Average peak resurgent current densities over a range of voltages from -65 to +5 mV. (F) Average maximum peak resurgent current amplitudes normalized to maximum peak transient current amplitudes. For (B, C, E), and (F), values were calculated for each individual cell and averaged for each group.

Resurgent current was measured in the same manner for the R1882Q mutant

channel as for the R853Q mutant and wild-type channels (protocol in Fig. 5C and 15D,

top). The R1882Q mutation increased average resurgent current densities at voltages

from -65 to 0 mV (Fig. 15D, E, $p = 0.0082 – 0.046$ from -35 - -20 mV). When analyzed at

a single voltage of -30 mV, the average maximum resurgent current amplitude was

increased for the R1882Q mutant, compared to wild-type (WT -178.40 ± 15.33 pA,

R1882Q -284.80 ± 45.71 pA, n = 39 WT, 25 R1882Q; Kruskal-Wallis test, $p < 0.0001$,

Dunn's multiple comparisons test, WT vs. R1882Q, $p = 0.3432$). When the resurgent

current, as percent of transient current, was analyzed at -30 mV, the R1882Q mutation

still increased the value, compared to wild-type (WT 2.39 ± 0.18 %, R1882Q 3.35 ± 0.31

%, n = 39 WT, 25 R1882Q; $p = 0.0050$). When normalized to the maximum peak

transient current amplitudes for individual cells, the resurgent current was, again,

increased by the R1882Q mutation at voltages from -65 to -5 mV (Fig. 15F, $p = 0.0053 –$

0.0446 from -35 - -20 mV). Thus, the R1882Q mutation enhanced hNav1.2 resurgent

currents in HEK cells.

The results of this experiment, encompassing the R853Q and R1882Q mutations,

are reported in Table 3.

Table 3. Summary of current magnitudes and gating parameters of WT, R853Q, and R1882Q mutant channels.

	WT	R853Q	R1882Q
Peak Transient Current ($I_{Na}T$) Amplitude	-8.75 ± 0.76 nA	-3.82 ± 0.54 nA*	-8.89 ± 1.14 nA
Peak Transient Current Density	-0.5515 ± 0.05 nA/pF	-0.2816 ± 0.04 nA/pF*	-0.5109 ± 0.07 nA/pF
Activation Midpoint	-26.50 ± 1.48 mV	-25.11 ± 1.81 mV	-24.77 ± 2.76 mV
Inactivation Midpoint	-65.01 ± 1.27 mV	-71.46 ± 1.62 mV*	-57.34 ± 2.05 mV*
Peak Persistent Current ($I_{Na}P$) Amplitude	-69.87 ± 5.81 pA	-27.24 ± 4.18 pA*	-162.80 ± 21.54 pA*
Persistent Current as % Peak $I_{Na}T$	0.96 ± 0.11 %	0.66 ± 0.05 %	1.93 ± 0.11 %*
Peak Resurgent Current Amplitude	-205.7 ± 17.39 pA	-79.84 ± 6.90 pA*	-342.40 ± 53.28 pA
Resurgent Current as % Peak $I_{Na}T$	2.86 ± 0.24 %	2.09 ± 0.18 %	4.04 ± 0.32 %*

*Significant difference ($p < 0.05$) vs. WT

Transient Transfections without Navβ4 Peptide

In order to strengthen my confidence that the observed effects of the mutations that I observed in HEK cells transiently transfected with the hNav1.2 channels was not due to the presence of Navβ4 peptide, I repeated the characterization experiments with HEK cells transiently expressing WT, R853Q mutant, or R1882Q mutant hNav1.2, in the absence of the peptide.

Effects of the R853Q Mutation in the Absence of Navβ4

In the absence of the Navβ4 peptide, the R853Q mutation reduced the average maximum peak transient current density of hNav1.2 in transiently transfected cells, though the decrease was not significant (WT -0.62 ± 0.08 nA/pF, R853Q -0.34 ± 0.07

nA/pF; n = 18 WT, 9 R853Q; ANOVA p = 0.0686); and it significantly reduced the average

maximum peak transient current amplitude (WT -10.40 ± 1.30 nA, R853Q -5.08 ± 1.01

nA; Dunn's multiple comparisons, WT vs. R853Q p = 0.0298). The R853Q mutation

produced slight, but not significant shifts in the average estimated midpoint of

activation (WT -20.03 ± 1.70 mV, R853Q -16.55 ± 2.42 mV; ANOVA p = 0.4086) and the

average estimated midpoint of inactivation (WT -56.83 ± 1.55 mV, R853Q -60.53 ± 1.58

mV; Dunn's multiple comparisons, WT vs. R853Q p = 0.3269). Thus, the R853Q

mutation decreased transient currents, slightly depolarized the activation-voltage

relationship, and slightly hyperpolarized the inactivation-voltage relationship in HEK

cells transiently expressing hNav1.2 in the absence of the Navβ4 peptide.

The R853Q mutation slightly reduced, but did not significantly alter, the average

maximum peak persistent current amplitude (WT -74.80 ± 13.00 pA, R853Q -47.06 ±

5.30 pA; Dunn's multiple comparisons, WT vs. R853Q p = 0.4632) and slightly increased,

but did not significantly alter, the average maximum peak persistent current amplitude

expressed as a percentage of the average maximum peak transient current amplitude of

each cell (WT 0.74 ± 0.10 %, R853Q 1.22 ± 0.20 %; Dunn's multiple comparisons, WT vs.

R853Q p = 0.0626). Thus, the R853Q mutation did not appreciably alter persistent

currents in HEK cells transiently expressing hNav1.2 in the absence of the Navβ4

peptide.

Effects of the R1882Q Mutation in the Absence of Navβ4

In the absence of the Navβ4 peptide, the R1882Q mutation increased the

average maximum peak transient current density of hNav1.2 in transiently transfected

cells, though the increase was not significant (WT -0.62 ± 0.08 nA/pF, R1882Q -0.90 ±

0.26 nA/pF; n = 18 WT, 6 R1882Q; ANOVA p = 0.0686); and it did not alter the average

maximum peak transient current amplitude (WT -10.40 ± 1.30 nA, R1882Q -13.97 ± 4.41

nA; Dunn's multiple comparisons, WT vs. R1882Q p > 0.9999). The R1882Q mutation

did not alter the average estimated midpoint of activation (WT -20.03 ± 1.70 mV,

R1882Q -19.80 ± 1.34 mV; ANOVA p = 0.4086) but produced a significant depolarizing

shift in the average estimated midpoint of inactivation (WT -56.83 ± 1.55 mV, R1882Q -

50.38 ± 0.67; Dunn's multiple comparisons, WT vs. R1882Q p = 0.0217). Thus, the

R1882Q mutation did not significantly alter transient currents or the activation-voltage

relationship, but it depolarized the inactivation-voltage relationship in HEK cells

transiently expressing hNav1.2 in the absence of the Navβ4 peptide.

The R1882Q mutation slightly increased, but did not quite significantly alter, the

average maximum peak persistent current amplitude (WT -74.80 ± 13.00 pA, R1882Q -

176.90 ± 53.18 pA; Dunn's multiple comparisons, WT vs. R1882Q p = 0.0620) and

significantly increased the average maximum peak persistent current amplitude

expressed as a percentage of the average maximum peak transient current amplitude of

each cell (WT 0.74 ± 0.10 %, R1882Q 1.38 ± 0.21 %; Dunn's multiple comparisons, WT vs.

R1882Q p = 0.0113). Thus, the R1882Q mutation increases persistent currents in HEK

cells transiently expressing hNav1.2 in the absence of the Navβ4 peptide.

Effects of the R853Q and R1882Q Mutations in Cell Lines Stably Expressing hNav1.2

In order to strengthen my confidence in the observed effects of the mutations

that I observed in HEK cells transiently transfected with the hNav1.2 channels, I

repeated the characterization experiments with HEK cell lines stably expressing WT,

R853Q mutant, or R1882Q mutant channels. All three cell lines were studied in the

absence of the Navβ4 peptide, and the WT and R1882Q cell lines were studied in

additional experiments with the Navβ4 peptide in the pipette solution in order to

examine the effects of the R1882Q mutation on resurgent current in cells stably

expressing the mutant channels. The experiment examining cell lines stably expressing

hNav1.2 in the absence of the Navβ4 peptide were not contemporaneous with the other

three experiments (transiently transfected cells with the Navβ4 peptide, transiently

transfected cells without the peptide, and cell lines stably expressing hNav1.2 with the

peptide).

Effects of the R853Q Mutation on I_{Na} in Cell Lines Stably Expressing hNav1.2

The R853Q mutation significantly reduced peak transient current densities from -

20 to +40 mV (p = 0.0001 – 0.0454, fig. 16A) and maximum peak transient current

density (WT -0.65 ± 0.05 nA/pF; R853Q -0.41 ± 0.04 nA/pF; p = 0.0029) in HEK cells

stably expressing the mutant channel, compared to cells stably expressing the WT

channel. It also significantly decreased maximum peak transient current amplitude (WT

-11.02 ± 0.77 nA, R853Q -8.351 ± 0.72 nA, n = 23 WT, 27 R853Q; p = 0.0414). The

mutation did not significantly alter the voltage dependence of activation (p > 0.10 at all

measured voltages; fig. 16B) or the estimated activation midpoint (WT -23.52 ± 0.92;

70
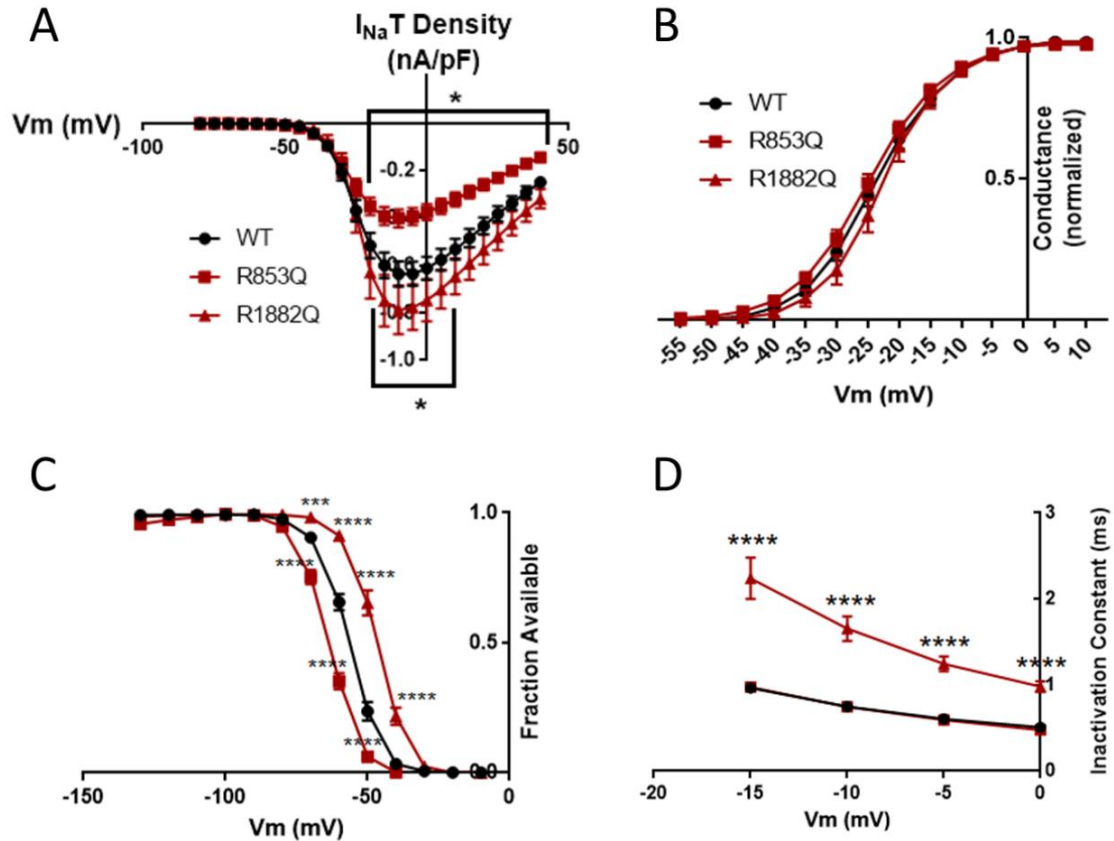
Figure 16. Effects of R853Q and R1882Q on transient current in HEK cell lines stably expressing hNav1.2 in the absence of the Navβ4 peptide. (A) Average current densities elicited by voltage steps from -80 to +40 mV. (B) Activation curves. Conductance was calculated as G/Gmax, where G = I/(Vm-Vrev), Vrev = reversal potential, and Gmax = maximum inward conductance across all tested voltages. (C) Inactivation curves. Fraction available was calculated as I/Imax for each cell at each voltage step. (D) Time constants of fast inactivation were calculated by fitting the decay portion of each current trace to a single-exponential equation in PulseFit (HEKA).

R853Q -24.16 ± 0.76; ANOVA p = 0.5172). It did, however, produce a hyperpolarizing

shift in the voltage dependence of fast inactivation (p = 0.0001 from -70 to -50 mV; fig.

16C) and the estimated midpoint of inactivation (WT -56.31 ± 0.87 mV; R853Q -63.1 ±

0.79 mV; p < 0.0001). The speed of fast inactivation, as evidenced by the inactivation

constants from -15 to 0 mV, was unaltered by the R853Q mutation (p > 0.87 at all

measured voltages; fig. 16D). Thus, the R853Q mutation does not alter the voltage

dependence of activation or the speed of fast inactivation in HEK cells stably expressing

R853Q mutant hNav1.2 channels; though it does decrease transient current amplitudes

and densities and produce a hyperpolarizing shift in the voltage dependence of fast

inactivation.

The R853Q mutation significantly decreased the average maximum peak

persistent current amplitude (WT -88.81 ± 10.83 pA; R853Q -62.62 ± 7.70 pA; p =0.0345)

but did not significantly alter the average maximum peak persistent current measured

as percentage of peak transient current (WT 0.958 ± 0.19%; R853Q 0.89 ± 0.12%; p >

0.9999). Thus, the R853Q mutation slightly reduces persistent currents in HEK cells

stably expressing R853Q mutant hNav1.2 channels, compared to cells stably expressing

WT channels.

Effects of the R1882Q Mutation on I_{Na} in Cell Lines Stably Expressing hNav1.2

In the absence of the Navβ4 peptide, the R1882Q mutation significantly

increased the peak transient current densities, compared to WT, from -15 to +5 mV (Fig.

16A, p = 0.0111 – 0.0442), though it does not significantly alter the maximum peak

transient current density (WT -0.6504 ± 0.05 nA/pF; R1882Q -0.8081 ± 0.10 nA/pF; p =

0.5148) or the maximum peak transient current amplitude (WT -11.02 ± 0.77 nA,

R1882Q -13.73 ± 1.80 nA, n = 23 WT, 13 R1882Q; p = 0.6221). The R1882Q mutation

does not significantly shift the voltage dependence of activation (Fig. 16B, p = 0.0900 at

-30 mV, p = 0.0529 at -25 mV, p > 0.500 at all other measured voltages) or the estimated

midpoint of activation (WT -23.52 ± 0.92; R1882Q -22.48 ± 1.35; ANOVA p = 0.5172).

The R1882Q mutation did, however, produce a depolarizing shift in the voltage

dependence of fast inactivation (Fig. 16C, p = 0.0001 – 0.0010 from -40 to -70 mV) and

the estimated midpoint of inactivation (WT -56.31 ± 0.87 mV; R1882Q -46.59 ± 1.06 mV;

p < 0.0001). The speed of fast inactivation, as evidenced by the inactivation constants

from -15 to 0 mV, was significantly increased by the R1882Q mutation (Fig. 16D, p =

0.0001 at all measured voltages). Thus, the R1882Q mutation does not alter the voltage

dependence of activation but impairs inactivation in HEK cells stably expressing the

mutant channel, compared to cells stably expressing the WT channel.

The R1882Q mutation significantly increased the average maximum peak

persistent current amplitude (WT -88.81 ± 10.83 pA; R1882Q -289.0 ± 36.71 pA; p =

0.0007) and the average maximum peak persistent current measured as percentage of

peak transient current (WT 0.958 ± 0.19%; R1882Q 2.131 ± 0.08%; p = 0.0003). Thus,

the R1882Q mutation significantly increases persistent currents in HEK cells stably

expressing R1882Q mutant hNav1.2 channels, compared to cells stably expressing WT

channels.

Effects of the R1882Q Mutation on I$_{Na}$ in Cell Lines Stably Expressing hNav1.2 in the

Presence of the Navβ4 Peptide

Since the R1882Q mutation increased I$_{Na}$R density in HEK cells transiently

expressing R1882Q mutant hNav1.2 channels, compared to cells transiently expressing

the WT channel, I investigated whether this enhancement of resurgent current and the

other effects of the R1882Q mutation could be observed in HEK cells stably expressing

the mutant channel. Compared to cells stably expressing the WT channel, cells

expressing the R1882Q mutant channel exhibited a slight decrease in the average

maximum peak transient current density (WT -0.947 ± 0.14 nA/pF, n = 13; R1882Q -

0.779 ± 0.06 nA/pF, n = 14; p = 0.2756) and no change in the estimated midpoint of

activation (WT -32.58 ± 1.32 mV; R1882Q -30.47 ± 1.65 mV; p = 0.3298) in the presence

of the Navβ4 peptide. It did, however, cause a significant depolarizing shift in the

estimated midpoint of inactivation (WT -63.17 ± 1.33 mV; R1882Q -54.13 ± 1.30 mV; p =

0.0001). Thus, in the presence of the Navβ4 peptide, the R1882Q mutation does not

alter the voltage dependence of activation but impairs inactivation in HEK cells stably

expressing the mutant channel, compared to cells stably expressing the WT channel.

The R1882Q mutation also significantly augmented the maximum peak

persistent current amplitude (WT -141.9 ± 21.01 pA; R1882Q -239.1 ± 24.63 pA; p =

0.0027) and the maximum peak persistent current measured as a percentage of

maximum peak transient current amplitude (WT 0.95 ± 0.17%; R1882Q 1.72 ± 0.06%; p =

0.0040). There was no difference in maximum peak resurgent current amplitude (WT -

382.7 ± 43.6 pA; R1882Q -368.4 ± 33.4 pA; p = 0.9362) or peak resurgent current

normalized to maximum peak transient current amplitude (WT 2.414 ± 0.32 %; R1882Q

2.723 ± 0.31 %; p = 0.5743). Thus, in the presence of the Navβ4 peptide, the R1882Q

mutation significantly increases persistent currents in HEK cells stably expressing

R1882Q mutant hNav1.2 channels, compared to cells stably expressing WT channels.

Pharmacology: Targeting INaR over INaT

In order to begin identifying compounds that slectively inhibit persistent (INaP)

and resurgent (INaR) sodium currents over transient sodium current (INaT), studies

involving two compounds (CBD and GS967) were performed. Epilepsy mutations in both *SCN8A* and *SCN2A* have now been shown to increase INaR. Since our lab has shown that the enhancement of resurgent current by the *SCN8A*/Nav1.6 epilepsy mutation N1768D can be preferentially inhibited by CBD (Patel et al., 2016), I tested the ability of these compounds to preferentially inhibit INaR in the Nav1.2 channel isoform. I tested the effects of these compounds in cells stably expressing hNav1.2 in the presence of the Navβ4 peptide.

Cannabidiol (CBD) Effects on $I_{Na}T$, $I_{Na}R$, and $I_{Na}P$

Since CBD has been shown to inhibit the enhancement of INaR caused by the Nav1.6 epilepsy mutation N1768D without disturbing the INaT density (Patel 2016), I predicted that CBD would also preferentially inhibit INaR and/or INaP over INaT in HEK cells stably expressing WT Nav1.2. Compared to untreated cells, methanol had no effect on average maximum peak transient current amplitude (untreated -12.53 ± 1.19 nA, n = 9; vehicle (methanol) -12.28 ± 1.31 nA, n = 7; ANOVA p = 0.6805, data not shown) or average maximum peak transient current density (Fig. 17A, untreated -0.67 ± 0.06 nA/pF, n = 9; vehicle (methanol) -0.68 ± 0.06 nA/pF; ANOVA p = 0.3591). CBD (1 µM) had no significant effect on average maximum peak transient current amplitude (-10.54 ± 1.24 nA, n = 8, data not shown) or average maximum peak transient current density (Fig. 17A, -0.54 ± 0.07 nA/pF, n = 8) compared to untreated or methanol-treated cells (ANOVA p = 0.3591). However, when the current densities were averaged within groups at each tested membrane potential, CBD significantly inhibited the transient current
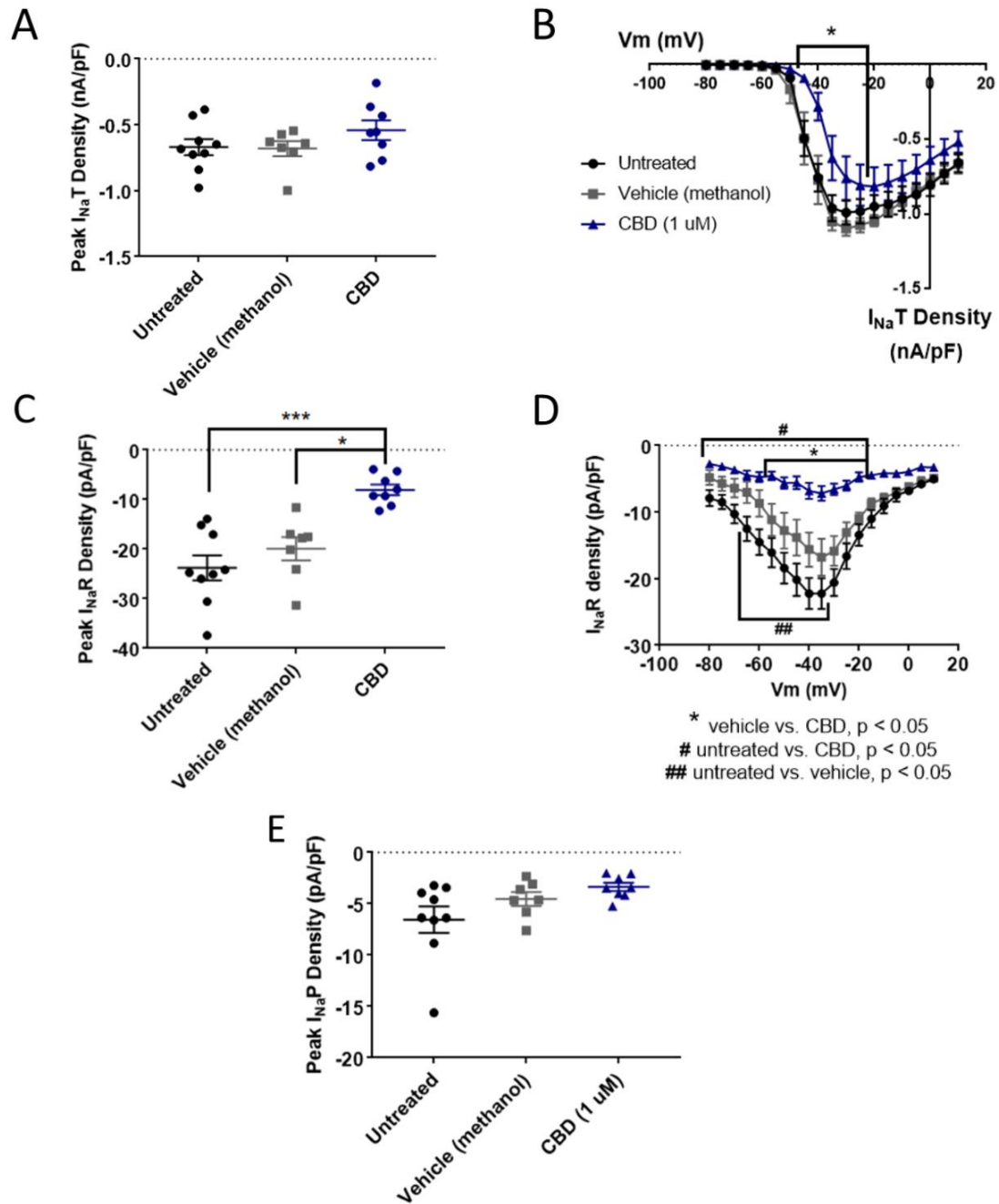
Figure 17. Effects of CBD on WT hNav1.2 in HEK cell lines stably expressing hNav1.2. Published as Figure 4 in (Mason and Cummins, 2020). The Navβ4 peptide was included in the pipette solution for all experiments with CBD. (A) The maximal peak transient current density of each cell is plotted; average and SEM for each group is indicated by bars. (B) The maximal peak resurgent current density of each cell is plotted; average and SEM for each group is indicated by bars. (C) The maximal peak persistent current density of each cell is plotted; average and SEM for each group is indicated by bars. (D) Average current densities elicited by voltage steps from -80 to +10 mV. (E) Average peak resurgent current densities over a range of voltages from -65 to +5 mV.

density, compared to vehicle, from -45 to -35 mV (Fig. 17B, vehicle vs. CBD $p < 0.05$ from

-45 to -25 mV, two-way ANOVA $p < 0.0001$). Therefore, these data suggest that CBD (1

µM) does not significantly reduce maximum peak transient current density, but it does

inhibit average current density (compared to vehicle) from -45 to -25 mV in HEK cells

stably expressing WT hNav1.2 channels.

Average maximum peak resurgent current densities were unaltered by methanol

(Fig. 17C, untreated -23.79 ± 2.52 pA/pF, vehicle (methanol) -19.93 ± 2.37 pA/pF, $p >$

0.9999) but significantly reduced by 1 µM CBD (Fig. 17C, CBD -8.07 ± 1.08 pA/pF; CBD vs.

vehicle (methanol), $p = 0.0137$; CBD vs. untreated, $p = 0.0005$). When the resurgent

current densities were averaged at each tested membrane potential, I observed a

significant reduction of average peak resurgent current densities by methanol (Fig. 17D,

vehicle (methanol) vs. untreated, $p = 0.0533$ at -55 mV, $p = 0.0055 - 0.0274$ at all other

measured voltages from -35 to -65 mV) and a further reduction by CBD (Fig. 17D, CBD

vs. vehicle (methanol), $p = < 0.0001 - 0.0120$ from -20 to -55 mV; CBD vs. untreated, $p =$

$< 0.0001 - 0.0305$ from -20 to -80 mV). Therefore, resurgent current is moderately

reduced by methanol and significantly reduced by 1 µM CBD in HEK cells stably

expressing WT hNav1.2 channels.

The peak persistent current density was not significantly reduced by methanol

(Fig. 17E, untreated -6.55 ± 1.29 pA/pF, vehicle (methanol) -4.54 ± 0.67 pA/pF, ANOVA p

$= 0.0727$) and was slightly reduced by CBD (Fig. 17E, CBD -3.38 ± 0.39 pA/pF, ANOVA $p =$

0.0727). Thus, methanol and 1 µM CBD may moderately inhibit persistent current in

HEK cells stably expressing WT hNav1.2 channels.

GS967 Effects on $I_{Na}T$, $I_{Na}R$, and $I_{Na}P$

Compared to untreated cells, the vehicle (DMSO) had no effect on average maximum peak transient current amplitude (untreated -11.84 ± 1.31 nA, n = 12; vehicle (DMSO) -11.33 ± 1.36 nA, n = 11; ANOVA p = 0.1011) or average maximum peak transient current density (Fig. 18A, untreated -0.62 ± 0.07 nA/pF, vehicle (DMSO) -0.63 ± 0.06 nA/pF; ANOVA p = 0.0685). GS967 (1 μM) slightly reduced average maximum peak transient current amplitude (-8.37 ± 0.47 nA, n = 10, ANOVA p = 0.1011) and average maximum peak transient current density (Fig. 18A, -0.46 ± 0.02 nA/pF) compared to untreated or methanol-treated cells (ANOVA p = 0.0685). However, when the current densities were averaged within groups at each tested membrane potential, GS967 significantly inhibited the transient current density, compared to vehicle, from -40 to +10 mV (Fig. 18B, p = 0.0145 at -40 mV, p < 0.0001 from -35 - +5 mV, p = 0.0003 at +10 mV). Therefore, these data suggest that GS967 (1 μM) does not significantly reduce maximum peak transient current density, but it does inhibit average current density (compared to vehicle) at voltages positive to -45 mV in HEK cells stably expressing WT hNav1.2 channels.

Average maximum peak resurgent current densities were unaltered by DMSO (Fig. 18C, untreated -18.16 ± 2.09 pA/pF, vehicle (DMSO) -19.15 ± 3.29 pA/pF; ANOVA p = 0.1193) and only slightly reduced by 1 μM GS967 (Fig. 18C, GS967 -12.35 ± 1.03 pA/pF; ANOVA p = 0.1193). When the resurgent current densities were averaged at each tested membrane potential, I observed that DMSO did not alter average peak resurgent current densities (Fig. 18D, vehicle (DMSO) vs. untreated, p > 0.5000 at all
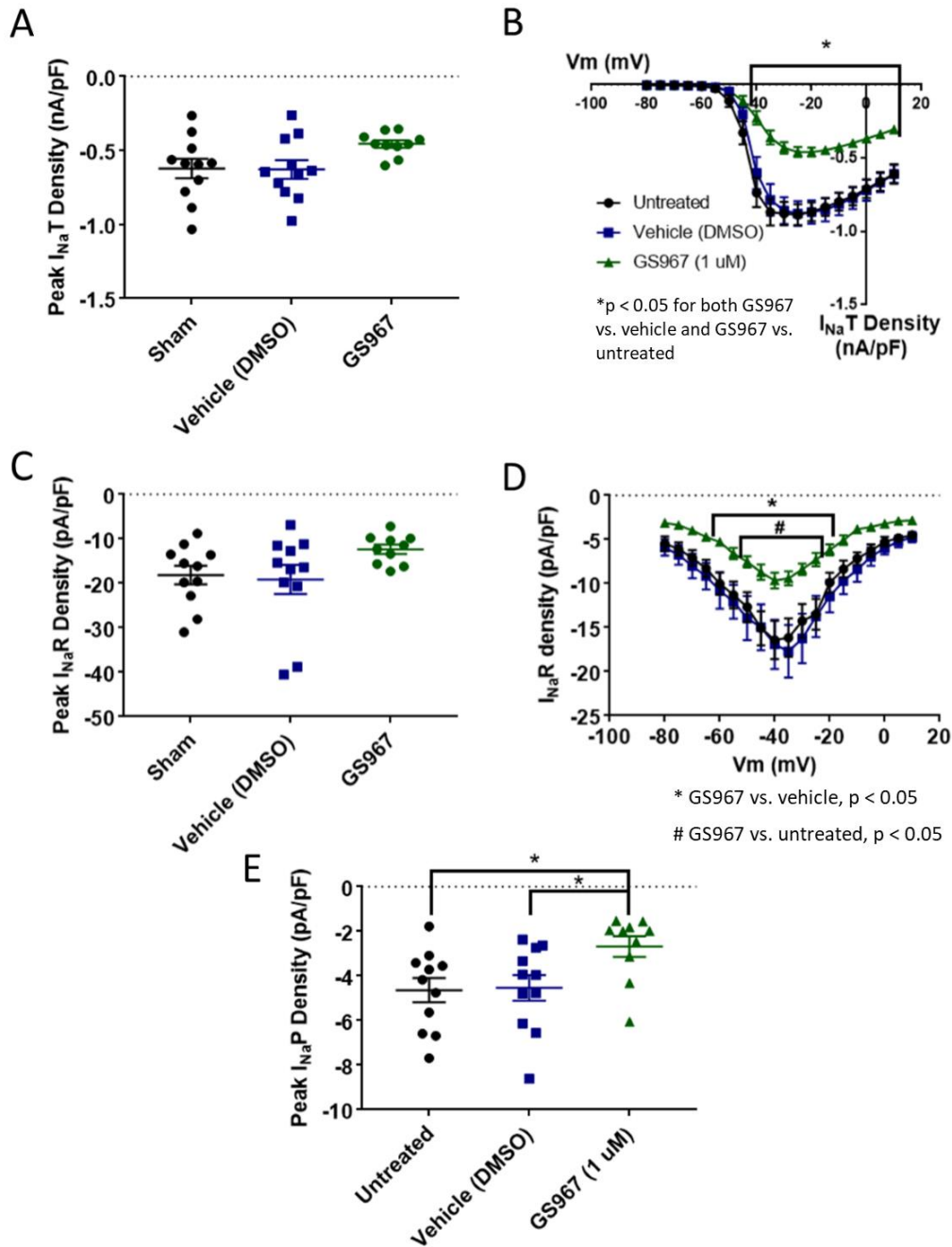
Figure 18. Effects of GS967 on WT hNav1.2 in HEK cell lines stably expressing hNav1.2. Published as Figure 6 in (Mason and Cummins, 2020). The Navβ4 peptide was included in the pipette solution for all experiments with GS967. (A) The maximal peak transient current density of each cell is plotted; average and SEM for each group is indicated by bars. (B) The maximal peak resurgent current density of each cell is plotted; average and SEM for each group is indicated by bars. (C) The maximal peak resurgent current density of each cell is plotted; average and SEM for each group is indicated by bars. (D) Average current densities elicited by voltage steps from -80 to +10 mV. (E) Average peak resurgent current densities over a range of voltages from -65 to +5 mV.

tested voltages). Compared to vehicle (DMSO), GS967 significantly inhibited resurgent current densities from -50 to -25 mV (Fig. 18D, GS967 vs. vehicle (DMSO), p = 0.0003 - 0.0326 from -20 to -55 mV). Therefore, resurgent current is not affected by DMSO and moderately reduced by 1 μM GS967 in HEK cells stably expressing WT hNav1.2 channels.

The peak persistent current density was not significantly reduced by DMSO (Fig. 18E, untreated -4.64 ± 0.54 pA/pF, vehicle (DMSO) -4.53 ± 0.58 pA/pF, p > 0.9999) and was significantly reduced by GS967 (Fig. 18E, GS967 -2.69 ± 0.46 pA/pF, GS967 vs. vehicle (DMSO) p = 0.0425). Thus, while persistent current in HEK cells stably expressing WT hNav1.2 channels is apparently unaffected by DMSO, it is significantly inhibited by 1 μM GS967**.**

Cannabidiol (CBD) Effects on hNav1.2 Gating

In order to better understand how CBD and GS967 inhibit hNav1.2 currents, I examined the effects of these compounds on the voltage dependence of activation and inactivation.

The vehicle for CBD, methanol, did not alter the conductance-voltage relationship (Fig. 19A, Tukey's multiple comparisons, vehicle vs. untreated, p = 0.3931 at -40 mV, p > 0.9000 at all other tested voltages) or the average estimated midpoint of activation (Fig. 19B, untreated -40.14 ± 0.48 mV, vehicle -39.78 ± 1.69 mV, Dunn's multiple comparisons, vehicle vs. untreated, p > 0.9999). CBD elicited a depolarizing shift in the voltage dependence of activation, as evidenced by depolarizing shifts in the conductance-voltage relationship (Fig. 19A, CBD vs. vehicle, p = < 0.0001 – 0.0173 from -40 to -25 mV) and in the average estimated
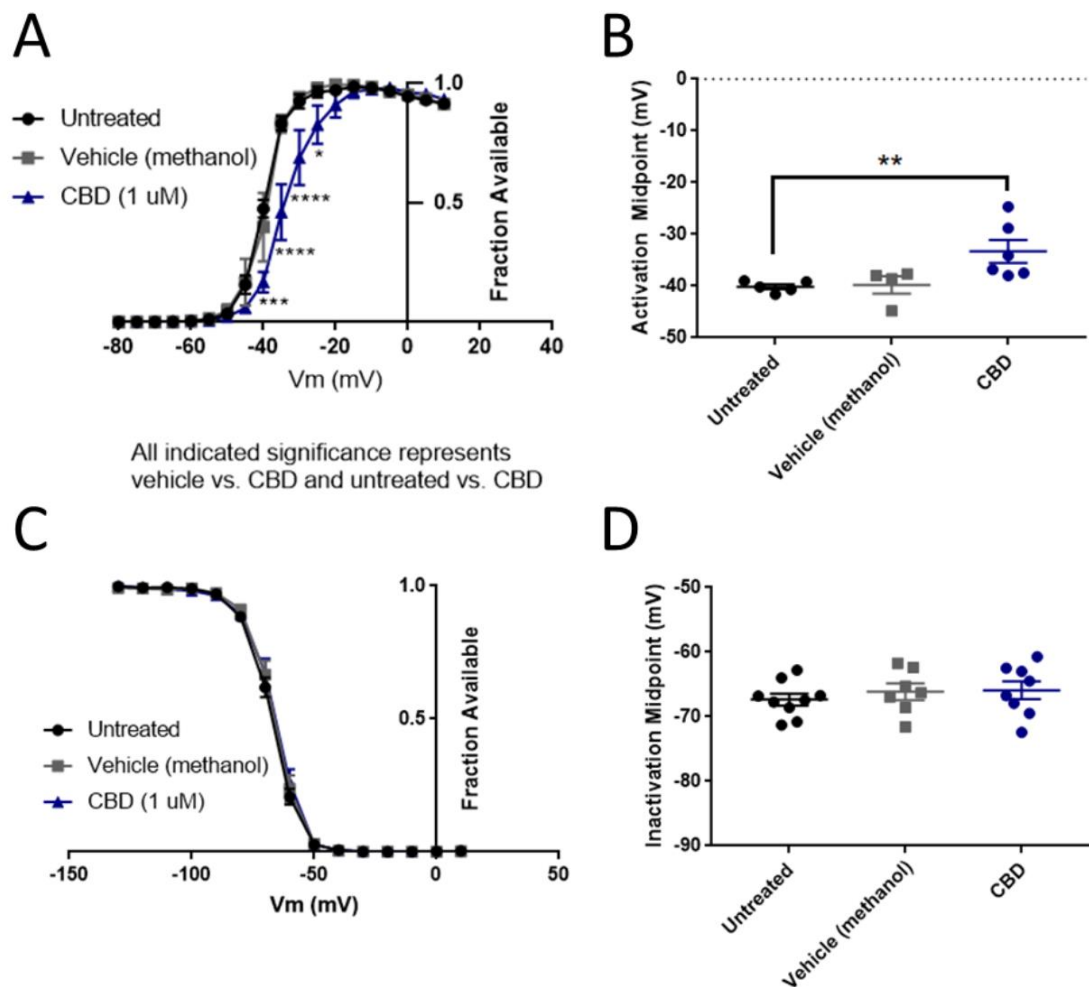
Figure 19. Effects of CBD on WT hNav1.2 gating in HEK cell lines stably expressing hNav1.2. Published as Figure 7 in (Mason and Cummins, 2020). (A) Activation curves. Conductance was calculated as G/Gmax, where G = I/(Vm-Vrev), Vrev = reversal potential, and Gmax = maximum inward conductance across all tested voltages. (B) The estimated activation midpoint for each cell is plotted; average and SEM for each group is indicated by bars. (C) Inactivation curves. Fraction available was calculated as I/Imax for each cell at each voltage step. (D) The estimated inactivation midpoint for each cell is plotted; average and SEM for each group is indicated by bars.

midpoint of activation (Fig. 19B, CBD -33.32 ± 2.21 mV, Dunn's multiple comparisons, CBD vs. vehicle, p = 0.1534). Though the shift in the average estimated midpoint of activation was insignificant when compared to the vehicle group, it was significant when compared to the untreated group (Dunn's multiple comparisons, CBD vs. untreated, p = 0.0069; vehicle vs. untreated, p > 0.9999). Thus, CBD produces a depolarizing shift in

the voltage dependence of activation for WT hNav1.2 channels stably expressed in HEK cells.

Neither the vehicle or CBD produced any shift in the voltage dependence of inactivation, as evidenced by the absence of any shift in the inactivation-voltage relationship (Fig. 19C, two-way ANOVA $p = 0.4304$) or in the average estimated midpoint of inactivation (Fig. 19D, untreated -67.34 ± 0.93 mV, vehicle -66.11 ± 1.30 mV, CBD -65.9 ± 1.39 mV, $p = 0.6159$). Thus, CBD does not alter the voltage dependence of inactivation for WT hNav1.2 channels stably expressed in HEK cells.

GS967 Effects on hNav1.2 Gating

The vehicle for GS967, DMSO, significantly depolarized the conductance-voltage relationship (Fig. 20A, Tukey's multiple comparisons, vehicle (DMSO) vs. untreated, $p < 0.001$ from -45 - -35 mV) but only mildly depolarized the average estimated midpoint of activation (Fig. 20B, untreated -41.15 ± 1.97 mV, vehicle (DMSO) -35.92 ± 1.53 mV, Dunn's multiple comparisons, vehicle (methanol) vs. untreated, $p = 0.0648$). Compared to vehicle (DMSO), GS967 did not shift the voltage dependence of activation, as evidenced by the absence of any shift in the conductance-voltage relationship (20A, GS967 vs. vehicle (DMSO), $p = 0.2332 – 0.8550$ from -50 - -35 mV, $p > 0.9000$ at all other tested voltages) and in the average estimated midpoint of activation (Fig. 20B, GS967 -37.30 ± 1.16 mV, Dunn's multiple comparisons, GS967 vs. vehicle (DMSO), $p > 0.9999$). Thus, while DMSO produces a depolarizing shift in the voltage dependence of activation, GS967 has no effect on the voltage dependence of activation for WT hNav1.2 channels stably expressed in HEK cells.
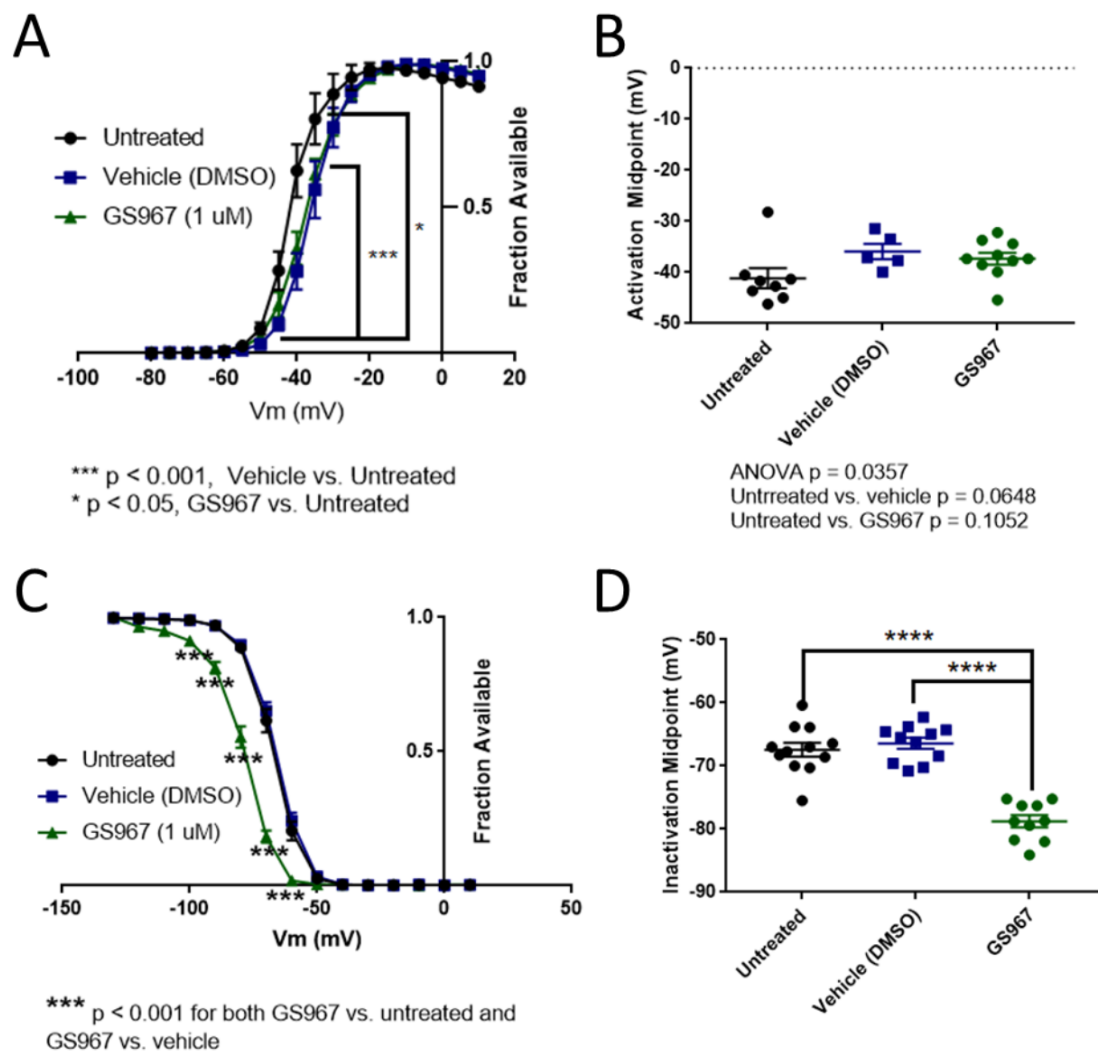
Figure 20. Effects of GS967 on WT hNav1.2 gating in HEK cell lines stably expressing hNav1.2. Published as Figure 8 in (Mason and Cummins, 2020). (A) Activation curves. Conductance was calculated as G/Gmax, where G = I/(Vm-Vrev), Vrev = reversal potential, and Gmax = maximum inward conductance across all tested voltages. (B) The estimated activation midpoint for each cell is plotted; average and SEM for each group is indicated by bars. (C) Inactivation curves. Fraction available was calculated as I/Imax for each cell at each voltage step. (D) The estimated inactivation midpoint for each cell is plotted; average and SEM for each group is indicated by bars.

The vehicle (DMSO) did not shift the voltage dependence of inactivation, compared to untreated cells, as evidenced by the absence of any shift in the inactivation-voltage relationship (Fig. 20C, Tukey's multiple comparisons, vehicle

(DMSO) vs. untreated, p = 0.1492 – 0.8390 from -80 - -60 mV, p > 0.9000 at all other

tested voltages) or in the average estimated midpoint of inactivation (Fig. 20D,

untreated -67.41 ± 1.10 mV, vehicle (DMSO) -66.42 ± 0.87 mV, Dunn's multiple

comparisons, vehicle (DMSO) vs. untreated, p = 0.7543). GS967 produced a

hyperpolarizing shift in the voltage dependence of inactivation, as evidenced by

hyperpolarizing shifts in the inactivation-voltage relationship (Fig. 20C, Tukey's multiple

comparisons, GS967 vs. vehicle (DMSO), p < 0.001 from -100 mV- -60 mV) and in the

average estimated midpoint of inactivation (Fig. 20D, GS967 -78.77 ± 0.97 mV, Dunn's

multiple comparisons, GS967 vs. vehicle (DMSO), p < 0.0001). Thus, GS967 produces a

hyperpolarizing shift in the voltage dependence of inactivation for WT hNav1.2 channels

stably expressed in HEK cells.

IV. DISCUSSION

Mutations in neuronal voltage-gated sodium channel isoforms are increasingly being identified as underlying otherwise idiopathic cases of epilepsy. Though over 250 different mutations in the Nav1.2 gene, *SCN2A*, have been reported as likely causes of epilepsy, biophysical characterization of only 21 of these mutations have been studied *in vitro*. Nine have been shown to have only gain-of-function effects, six have primarily loss-of-function effects, and six have mixed gain- and loss-of-function effects (not including the mutations in this study). However, our study (work published in Mason et al., 2019, available at https://www.eneuro.org/content/6/5/ENEURO.0141-19.2019) is the first to identify enhanced resurgent currents and gating pore currents as effects of *SCN2A* disease mutations.

The L835F mutation has been identified in the *SCN2A* gene of a patient with severe epilepsy and is not found in healthy control genomes; therefore it is suspected to be an epileptogenic mutation. Among the *SCN2A* mutations suspected to cause epilepsy in human patients, R853Q and R1882Q are two of the most commonly reported mutations (Wolff et al., 2017). The R853Q mutation was identified in patients who were diagnosed with West Syndrome or unspecified epileptic encephalopathy. Most or all of these patients had late onsets of seizures (6 mos. – 3 yrs.); and many exhibit dystonia and/or choreoathetosis (Allen et al., 2013; Nakamura et al., 2013; Samanta and Ramakrishnaiah, 2015; Kobayashi et al., 2016; Wolff et al., 2017). In contrast, the R1882Q mutation has been reported in numerous patients diagnosed with

early onset epileptic encephalopathies (6/7 reported onset of 1 day) (Carvill et al., 2013; Howell et al., 2015; Trump et al., 2016; Wolff et al., 2017).

L835F Mutation Effects on hNav1.2 Function and Predicted Effects on Neuronal Excitability

Very little is known about the L835F mutation so far. This leucine residue is in the third transmembrane segment (S3) of domain II (DII), which is believed to be clustered with S1, S2, and S4 in the tertiary structure of the channel. Leucine and phenylalanine are both nonpolar residues, and their structures are closely related. Phenylalanine contains a benzene ring where leucine contains a dimethyl group, making phenylalanine larger. This increase in size, despite the retention of nonpolarity at this position, may affect the residue's interactions within the protein or with lipids in the surrounding membrane. If this substitution produces such an alteration in interactions with nearby residues or molecules, then it may alter the protein conformation. Since the mutation significantly enhances persistent current, it may destabilize the inactivated conformation of the channel or indirectly disrupt interactions between the inactivation particle and the central pore. It is also possible that the L835F mutation acts in tandem with another genetic variant in another gene/protein to create a net effect of neuronal hyperexcitability that underlies this patient's seizures. Several studies have demonstrated that alterations in expression levels of other genes can alter seizure susceptibility and severity in rodents, including mouse models of *SCN1A* and *SCN2A* epilepsy (Jorge et al., 2011; Miller et al., 2014; Hawkins & Kearney, 2016; Lamar et al., 2017, Follwaczny et al., 2017; Calhoun et al., 2017; Hawkins et al., 2019), and one

pharmacogenetics study suggested that a pair of particular single nucleotide

polymorphisms (SNPs, i.e. variants) in the *SCN2A* and *ABAT* (which encodes GABA-T, a

protein that catalyzes GABA) genes is correlated with the efficacy of valproate

treatment in epileptic patients (Li et al., 2016). Therefore, L835 and a variant of another

gene may increase seizure susceptibility individually, and these effects could be additive

or synergistic when both variants are present.

If the non-significant shifts in the voltage dependencies of activation and

inactivation are taken into account as effects of the L835F mutation, the slight

depolarization of the activation midpoint (+7 mV) may overpower the slight

depolarization of the inactivation midpoint (+4 mV) to decrease the window current

(not analyzed in this study) and thus confer a net slight loss of function on the channel.

This slight loss of function would probably be outweighed by the gains of function

represented by the significant increase in persistent current and the slight slowing of

inactivation (evidenced by slightly larger inactivation constants), which both aberrantly

augment the sodium current through the channel. Since enhancement of persistent

currents is strongly associated with neuronal hyperexcitability, and the only significant

difference the L835F mutation confers on the hNav1.2 channel in HEK cells is an

increase in persistent current, this mutation is expected to cause affected neurons to be

hyperexcitable.

Enhancements in persistent currents are associated with increases in resurgent

current and neuronal excitability, though it is unknown whether these effects

accompany the increase in persistent current caused by the L835F mutation. Also, given

that L835F is proximal to the region in which gating pores have been suggested to occur, there is a possibility that the L835F mutation affects the local channel conformation to create a gating pore. The potential effect of this mutation on resurgent current and the possibility that it creates a conducting gating pore have not been investigated. It is likely that this dissertation work has revealed only part of the full spectrum of biophysical effects of the L835F mutation on Nav1.2 channel function. Further evidence suggesting that the L835F mutation causes a net gain of function in Nav1.2 channel function and hyperexcitability in affected neurons is needed to confirm the pathogenicity of this mutation.

R853Q Mutation Effects on hNav1.2 Function and Predicted Effects on Neuronal Excitability

A 2018 study of *SCN2A* mutations utilizing Chinese hamster ovary (CHO) cells transiently transfected with hNav1.2 reported that the R853Q mutation in the human Nav1.2 channel decreases peak transient current density and produces a hyperpolarizing shift in the voltage dependence of inactivation (Berecki et al.); these observations were corroborated in this present study using HEK cells. The data presented in Figure 9 also suggested that the R853Q mutation reduces persistent and resurgent currents. The reductions in Q_{max} in oocytes and in current density in HEK cells resulting from the R853Q mutation, compared to the wild-type channel, suggest that this mutation reduces the surface expression of the channel. All of these are loss-of-function effects, which are predicted to decrease neuronal excitability. Though loss of

Nav1.2 function is common among late-onset *SCN2A* epilepsies, it is unclear how loss of

function in Nav1.2, which is predicted to decrease the excitability of excitatory neurons,

could lead to the aberrant firing of excitatory neurons that underlies seizures. The only

proposed effect of the R853Q mutation that represents an anomalous channel function

and, thus, explains how it may cause neuronal hyperexcitability, is the creation of a

gating pore that conducts cationic current. Neuronal resting membrane potential is

typically around -70 mV, a membrane potential at which the gating pore in R853Q

mutant channels is conducting, according to my results. The inward cationic current,

though small, flows through the channel when it is in its resting conformation and,

therefore, it may chronically depolarize the affected neurons, making them

hyperexcitable. Multiple studies have shown that mutations of the highly conserved

voltage-sensing residues in the second domain of Nav channels result in gating pore

currents (Sokolov et al., 2005, 2007, 2008, 2010; Struyk & Cannon, 2007). Patch clamp

data and molecular dynamic simulations have shown that mutation of the second

voltage-sensing arginine residue in the bacterial channel, which is homologous to the

hNav1.2 residue R853, creates a distinct gating pore that is open in the resting state

channel conformation (Gamal El-Din et al., 2014; Jiang et al., 2018). In rat Nav1.2, the

R853Q mutation, when paired with the R850Q mutation, produced an inward gating

pore current in *Xenopus* oocytes, but the R853Q mutation alone did not produce an

observable gating pore current that was significantly different from that of the wild-type

rat channel (Sokolov et al., 2005). This may indicate a species difference in

susceptibility. The R853Q mutation in hNav1.2 did not produce an observable gating

pore current in CHO cells (Berecki et al., 2018); however, this is likely due to the low

current amplitude and density of R853Q channels in CHO cells. We obtained robust

expression of hNav1.2 channels in *Xenopus* oocytes and observed substantial gating

pore currents with the hNav1.2 R853Q construct. A linear correlation between the

gating pore current amplitude and the gating charge has been observed in gating pore

currents caused by Nav1.4 disease mutations (Struyk & Cannon, 2007; Mi et al., 2014),

and we observed a similar correlation in the gating pore current caused by the R853Q

mutation in Nav1.2 (Fig. 13A). This provides validation that the current we observed

was actually gating pore current. The slope of this correlation observed in our

experiments is -118.0 ± 8.8 nA/nC (n = 11). By comparison, for the gating pore current

observed with Nav1.4 in hypokalemic periodic paralysis mutants, the slopes range from

50-150 nA/nC (Struyk & Cannon, 2007; Mi et al., 2014). This indicates that the severity

of the gating pore leak induced by R853Q in hNav1.2 is comparable to those observed

with Nav1.4 disease mutations, and, therefore, that the gating pore current observed in

our experiments with the R853Q mutation may be involved in the pathogenesis of

epilepsy.

Inward gating pore currents resulting from the mutation of one of the first two

arginines in DIIS4 (in hNav1.2, R850 or R853) are predicted to destabilize and even

chronically depolarize the membrane potential of affected neurons. Gating pore

currents may also disrupt intracellular ion homeostasis, allowing excess sodium ions and

possibly even protons to leak into affected neurons through the gating pore (Struyk &

Cannon, 2007; Sokolov et al., 2007). Though the generation of gating pore current adds

an aberrant function to the hNav1.2 channel, the impact of this anomalous current may depend on the cell background. A depolarizing influence, such as excess sodium entry into the cell, could increase the activity of some neurons by bringing the membrane potential closer to the action potential firing threshold, while paradoxically decreasing excitability in others if the depolarization of the membrane potential reduces sodium channel availability due to the accumulation of inactivated channels. The other effects of the R853Q mutation confer a moderate loss of function on hNav1.2, which is predicted to contribute to decreased neuronal excitability. This prediction was tested in 2018 using a dynamic action potential clamp model. This approach fuses voltage clamp of CHO cells transiently expressing Nav1.2 channels with a computer model of a typical cortical neuron axon initial segment, and it was used to predict that the R853Q mutation would decrease action potential firing activity and thus reduce overall neuronal excitability (Berecki et al., 2018). However, the dynamic clamp model did not consider the possibility that gating pore currents may be induced by the R853Q mutation, and that these currents could alter neuronal activity directly, by reducing the action potential threshold, or indirectly, by chronically impacting ion homeostasis and energy metabolism in neurons. Such alterations could cause variable and/or chronic changes in neuronal properties, and these changes may not be readily apparent using dynamic clamp or traditional electrophysiological analyses in heterologous expression systems. Moreover, seizures in patients with R853Q are refractory to AEDs that block the conventional sodium-conducting pore, consistent with a pathophysiological mechanism based on the gating pore current.

Though only one epilepsy patient with the R853Q mutation has been reported to have been diagnosed with autism (Butler et al., 2017), most patients that have been reported to have the same mutation reportedly suffered severe intellectual disability and/or developmental delays (Allen et al., 2013; Nakamura et al., 2013; Samanta and Ramakrishnaiah, 2015; Kobayashi et al., 2016; Li et al., 2016; Butler et al., 2017; Wolff et al., 2017; Lindy et al., 2018). Since *SCN2A* mutations that appear to have exclusively loss-of-function effects are typically associated with autism, which is also a developmental disorder, the association of the R853Q mutation with predominately loss-of-function effects on channel function supports (and may explain) its association with phenotypes of severe developmental and intellectual disorders. Since the overall effect of the R853Q mutation on neuronal excitability is unclear, its mechanistic role in epileptogenesis is undetermined. If the mutation causes neuronal hyperexcitability, it could be reasoned that the gating pore current confers an overall gain-of-function effect on the channel via inducing gating pore current. If it decreases neuronal hyperexcitability, another explanation for the seizure phenotype, such as compensatory upregulation of Nav1.6 in affected neurons that leads to neuronal hyperexcitability, must be considered.

Though the mechanism by which the R853Q mutation causes the observed clinical phenotype is unclear, its high incidence in otherwise idiopathic epilepsy cases and the fact that mutations in the homologous residue in three other Nav isoforms (Nav1.1, 1.4, & 1.5) have been shown to be associated with disorders of excitability make it clear that it is a pathogenic mutation. In addition to R853Q, ten other

neutralizing mutations of seven different voltage-sensing residues in Nav1.2 have been

implicated in over 30 cases of epilepsy. Three mutations in domains I and III of hNav1.2

have been studied *in vitro* (R223Q, R1312T, & R1319Q), though none of these studies

included analysis of gating pore currents. Of these three, one (R1312T, in DIII) also

exhibits a loss-of-function hyperpolarizing shift in fast inactivation, compared to wild-

type, but R1312T also exhibited multiple gain-of-function effects that were not seen in

my experiments with the R853Q mutant (Lossin et al., 2012). The other two (R223Q,

R1319Q) were shown to have the opposite effect, exhibiting a depolarizing shift in the

voltage dependence of fast inactivation (Scalmani et al., 2006; Misra et al., 2008). The

R1319Q mutation, like R853Q, has been shown to reduce the current density of Nav1.2;

and the R1319Q mutation was also shown to reduce the surface expression of the

channel (Misra et al., 2008), which, based on the data from this dissertation work, is also

likely one effect of the R853Q mutation. Clinically, the R853Q phenotype most

resembles that of R1312T, causing severe seizures that are often refractory to

antiepileptic medications, having a late onset (typically >6 mos.), and being

accompanied by severe intellectual disability (Wolff et al., 2017; Kobayashi et al., 2016;

Allen et al., 2013; Nakamura et al., 2013; Samanta and Ramakrishnaiah, 2015; Shi et al.,

2009).

Only one other voltage-sensing residue in domain II of Nav1.2, R856, has been

reported to have mutations implicated in epilepsy (Howell et al., 2015; Moller et al.,

2016; Wolff et al., 2017). The R856L mutation has been identified in one patient who

was diagnosed with epilepsy of infancy with migrating focal seizures (Howell et al.,

2015), and the R856Q mutation was identified in two patients diagnosed with Ohtahara

Syndrome (Moller et al., 2016; Wolff et al., 2017). Neither mutation has been studied in

the laboratory. In contrast to patients with the R853Q mutation, the seizure onsets for

R856L and R856Q patients was reported to be early (1-2 days) in two of the cases,

representing both mutations (Howell et al., 2015; Wolff et al., 2017). At least one child

with the R856Q mutation was refractory to antiepileptic medicines and died at the age

of 3 months (Moller et al., 2016; Wolff et al., 2017). Since R853Q and R856Q are

mutations of adjacent voltage-sensing residues in the functional Nav1.2 protein, the

proximity of these two residues and the severe, refractory epileptic phenotypes caused

by both suggests that these mutations may have similar effects on the structure, and

thus also the function of the channel. I predict that several, if not all, of these other S4

mutations in hNav1.2 may also induce gating pore currents.

R1882Q Mutation Effects on hNav1.2 Function and Predicted Effects on Neuronal Excitability

Four different mutations of the R1882 residue in Nav1.2 have been reported as

being putatively pathogenic in epilepsy cases (R1882L, R1882P, R1882G, & R1882Q)

(Baasch et al., 2014; Schwarz et al., 2016; Howell et al., 2015; Trump et al., 2016; Carvill

et al., 2013; Parrini et al., 2017; Wolff et al., 2017). The biophysical effects of the

R1882L and R1882P mutations have not been studied. The R1882G mutation, which,

like R1882Q, neutralizes the positive residue, has been shown to cause gain-of-function

effects on Nav1.2 channels in tsA201 cells, though the mutational effects on resurgent currents was not investigated (Schwarz et al., 2016).

The 2018 study utilizing CHO cells revealed that the R1882Q mutation causes a depolarizing shift in the voltage dependence of fast inactivation, enhances persistent currents, and slows fast inactivation, compared to the wild-type channel (Berecki et. al). The results of the present study corroborate those findings. Additionally, I show that the R1882Q mutation substantially enhances resurgent currents in HEK cells, whereas the CHO cell study did not address the possibility of changes in resurgent current due to this mutation. In CHO cells the R1882Q mutation was also reported to increase peak current density and hyperpolarize the voltage dependence of activation (Berecki et al., 2018), but I did not observe those effects in my experiments. All of the observed changes enhance Nav1.2 channel function, which is predicted to increase neuronal excitability. The dynamic action potential clamp experiments predicted that the R1882Q mutation would chronically depolarize neurons and increase their action potential firing activity (Berecki et al., 2018). Importantly, this model system did not incorporate resurgent current mechanisms, which are predicted to further enhance the pro-excitatory impact of the R1882Q mutation.

Resurgent currents have been identified as drivers of both repetitive action potential activity and spontaneous action potential generation (Raman and Bean, 1997; Bant and Raman, 2010; Khaliq et al., 2003; Barbosa et al., 2015; Xiao et al., 2019). Resurgent currents are also enhanced by pro-excitatory disease mutations in other voltage-gated sodium channel isoforms which are associated with pain, myotonia

congenital, long-QT syndrome, and *SCN8A* epilepsies (Jarecki et al., 2010; Patel et al.,

2016; Xiao et al., 2019). Although ours is the first study to investigate the impact of

SCN2A mutations on resurgent currents, recordings from DRG neurons demonstrated

that Nav1.2 channels can produce resurgent currents in a neuronal background (Rush et

al., 2005). Altogether, this strongly suggests that the enhancement of resurgent

currents by the R1882Q mutation is part of its pathogenic mechanism.

The primary effect of the *SCN2A* R1882Q mutation is impairment of inactivation,

which contributes to both increased persistent and resurgent currents (Grieco and

Raman, 2004; Theile et al., 2011). It has been shown that the C terminal domain of

Nav1.2 (Mantegazza et al., 2001; Nguyen and Goldin, 2010; Lee and Goldin, 2008), as

well as Nav1.3 (Nguyen and Goldin 2010), Nav1.5 (Cormier et al., 2002; Glaaser et al.,

2006), Nav1.6 (Lee and Goldin, 2008; Wagnon et al., 2016), and Nav1.8 (1.5 & 1.8;

Motoike et al., 2004; Choi et al., 2004), is involved in modulating fast inactivation. In a

study utilizing ND7/23 cells, it was shown that the R1872Q mutation in mouse Nav1.6,

which is homologous to the hNav1.2 R1882Q mutation, slows inactivation (as evidenced

by increased inactivation time constants), hyperpolarizes the voltage dependence of

activation, and depolarizes the voltage dependence of inactivation, compared to wild-

type (Wagnon et al., 2016). Since Nav1.2 and Nav1.6 share a high degree of homology

in structure and function (amino acid sequences have 75% identity, 85% similarity)

homologous mutations in the two isoforms are predicted to have similar functional

results. My results demonstrate that, like the Nav1.6 R1872Q mutation, the R1882Q

mutation increased inactivation time constants, indicating a slowing of fast inactivation,

and depolarized the voltage dependence of inactivation. In my experiments, the

R1882Q mutation also increased persistent currents at physiologically-relevant

membrane potentials (amplitude increased significantly from -50 to -20 mV, % of

transient current increased significantly from -45 to -25 mV). This effect was seen when

R1872 in Nav1.6 was mutated to leucine (L), but not when it was mutated to glutamine

(Q) or tryptophan (W). Additionally, the hNav1.2 R1882Q mutation enhanced resurgent

currents, which were not investigated in the study of the mouse Nav1.6 R1872Q

mutation. There is substantial evidence suggesting that the C-terminal domain of

voltage-gated sodium channels can modulate fast inactivation and persistent currents

by interacting with the domain III/IV linker that contains the inactivation particle

(Clairfeuille et al., 2019; Wagnon et al., 2016; Nguyen and Goldin, 2010; Lee and Goldin,

2008; Motoike et al., 2004; Mantegazza et al., 2001).   The neutralizing R1882Q

mutation may directly or indirectly alter this interaction, thus impairing inactivation and

enhancing persistent currents.

Effects of the Navβ4 Peptide and cDNA Expression Modality on Measured Parameters

Since the original experimental setup included a WT group that was subjected to

all the same conditions as the mutant groups, I am very confident in these results.

However, in order to investigate whether the mutational effects I observed in the

transiently transfected HEK cells were genuine and not due to the presence of the

Navβ4 peptide or the cDNA expression modality, I repeated the experiments comparing

WT, R853Q, and R1882Q mutations in three conditions: transiently transfected cells in

the absence of the Navβ4 peptide, cell lines stably expressing hNav1.2 in the absence of

the peptide, and cell lines stably expressing hNav1.2 in the presence of the peptide (WT

vs. R1882Q only in this last experiment); and I compared the observed mutational

effects across the four experimental conditions, which are summarized in Tables 4-5.

Unfortunately, the four sets of experiments (transiently transfected cells with the

peptide, transiently transfected cells without the peptide, cell lines stably expressing

hNav1.2 with the peptide, and cell lines stably expressing hNav1.2 without the peptide)

were performed in different time periods, so the four experimental datasets are non-

contemporaneous. This caveat needs to be considered when comparing the results

from the various experimental paradigms.

Table 4. Effects of the R853Q mutation on currents and gating parameters across experimental conditions.

	R853Q Transient		R853Q Stably Expressing	
	w/peptide (n = 41 WT, 16 R853Q)	w/o peptide (n = 18 WT, 9 R853Q)	w/peptide (n = 0 WT, 0 R853Q)	w/o peptide (n = 23 WT, 27 R853Q)
INaT Amplitude, Density	Decreased*, Decreased*	Decreased*, No change/ Decreased		No change/Decreased, Decreased*
Activation Midpoint	No change	No change		No change
Inactivation Mid-point	Hyperpolarized*	No change/ Hyperpolarized		Hyperpolarized*
INaP Amplitude	Decreased*	No change/Decreased		Decreased*
INaP as % of INaT	No change/Decreased	No change/Increased		No change/Decreased
INaR Amplitude	Decreased*			
INaR as % of INaT	No change/Decreased			

*Significant difference ($p < 0.05$), mutant vs. WT, within same experimental conditions

Table 5. Effects of the R1882Q mutation on currents and gating parameters across experimental conditions.

	R1882Q Transient		Stably Expressing R1882Q	
	w/peptide (n = 48 WT, 27 R1882Q)	w/o peptide (n = 18 WT, 6 R1882Q)	w/peptide (n = 13 WT, 14 R1882Q)	w/o peptide (n = 23 WT, 13 R1882Q)
INaT Amplitude, Density	No change, No change	No change/Increased, No change/Increased	No change, No change	No change/Increased, No change/Increased
Activation Mid-point	No change	No change	No change	No change
Inactivation Mid-point	Depolarized*	Depolarized*	Depolarized*	Depolarized*
INaP Amplitude	Increased*	No change/Increased	Increased*	Increased*
INaP as % of INaT	Increased*	Increased*	Increased*	Increased*
INaR Amplitude	No change/Increased		No change	
INaR as % of INaT	Increased*		No change	

*Significant difference ($p < 0.05$), mutant vs. WT, within same experimental conditions

Transient Transfections without the Navβ4 Peptide

In both the presence and absence of the Navβ4 peptide, the R853Q mutation produced a significant decrease in the average maximum peak transient current amplitude, compared to that of the WT channel. Though the average estimated activation midpoint was slightly depolarized by the mutation in the absence of the peptide, no significant change was observed in this parameter in either condition, and the slight depolarizing shift is consistent with the effects of the full-length Navβ4 subunit (Aman et al., 2009). The average maximum inactivation midpoint was depolarized in both conditions, though only significantly in the presence of the peptide. While both the maximum peak persistent current amplitude and the maximum peak

99

persistent current expressed as percent of transient current were decreased in the

presence of the peptide, the persistent current expressed as a percentage was non-

significantly increased by the R853Q mutation in the absence of the peptide. The only

significant change seen in the persistent current measurements between WT and R853Q

mutant channels was a significant decrease in the average maximum persistent current

amplitude in the presence of the peptide. Thus, the mutation seems to decrease

persistent currents in the presence of the peptide but have no effect on them in the

absence thereof, in HEK cells transiently expressing hNav1.2 channels. This discrepancy

and the differences in significance seen in the effects of the R853Q mutation on

maximum peak transient current density and average estimated midpoint of

inactivation are likely due to the differences in sample sizes for the two conditions. The

sample sizes were much larger in the presence of the Navβ4 peptide (n = 41 WT, 16

R853Q) than in its absence (n = 18 WT, 9 R853Q). If the latter experiment had larger

sample sizes, I would have expected the significances of the observed mutational effects

to more closely resemble those in the former experiment. I am more confident in the

results of the former experiment than the results of the latter; and the mutational

effects observed in the absence of the peptide echo those observed in its presence.

Given this analysis of the R853Q mutation in both the presence and absence of Navβ4

peptide, I am confident that the R853Q mutation decreases transient current, has no

significant effect on activation, and hyperpolarizes the voltage dependence of

inactivation in HEK cells transiently expressing the hNav1.2 channel.

The effects of the R1882Q mutation observed in the absence of the Navβ4 peptide were very similar to the effects observed in its presence. There was no significant change in the average maximum peak transient current amplitude or density in either condition, nor was there any change in the voltage dependence of activation. In both conditions, the voltage dependence of inactivation was significantly depolarized and the persistent current expressed as a percentage of transient current was significantly increased. The maximum peak persistent current amplitude was increased in both conditions, though the increase was only significant in the presence of the Navβ4 peptide. As stated above, the sample sizes were much larger in the presence of the Navβ4 peptide (n = 41 WT, 27 R1882Q) than in its absence (n = 18 WT, 6 R1882Q). If the latter experiment had larger sample sizes, I would have expected the increase in the maximum peak persistent current amplitude in the absence of the peptide to be significant, compared to the corresponding WT control group. Given this analysis of the R1882Q mutation in both the presence and absence of the Navβ4 peptide, I am confident that the R1882Q mutation has no significant effect on transient current or the voltage dependence of activation, significantly depolarizes the voltage dependence of inactivation, and increases persistent currents in HEK cells transiently expressing the hNav1.2 channel.

Considering my analyses of both the R853Q and R1882Q mutations in both the presence and absence of the Navβ4 peptide, I do not believe that the Navβ4 peptide had any significant effects on any of the biophysical effects observed in HEK cells transiently expressing hNav1.2 cDNA. However, when the data from the WT groups in

the presence and absence of the peptide are compared (see Table 6), the peptide seems to produce hyperpolarizing shifts in the voltage dependencies of activation (~6.5 mV shift) and inactivation (~8 mV shift). This suggests that, in recordings of HEK cells transiently expressing hNav1.2 cDNA, the Navβ4 peptide may produce hyperpolarizing shifts of similar magnitude in the voltage dependencies of activation and inactivation. This, however, did not impact the overall results, since each experiment had its own WT control group, to which the mutant groups in each experiment were compared.

Table 6. Summary of WT current magnitudes and gating parameters across experimental conditions.

	Transient + Navβ4 (n = 41)	Stably Express-ing + Navβ4 (n = 13)	Transients w/o peptide (n = 18)	Stably Express-ing w/o peptide (n = 23)
Peak Transient Current Amplitude	-8.75 ± 0.76 nA	-16.69 ± 1.47 nA	-10.40 ± 1.30 nA	-11.02 ± 0.77 nA
Peak Transient Current Density	-0.5515 ± 0.05 nA/pF	-0.947 ± 0.14 nA/pF	-0.6205 ± 0.09 nA/pF	-0.6504 ± 0.05 nA/pF
Activation Midpoint	-26.50 ± 1.48 mV	-32.58 ± 1.32 mV	-20.03 ± 1.70 mV	-23.52 ± 0.92 mV
Inactivation Midpoint	-65.01 ± 1.27 mV	-63.17 ± 1.33 mV	-56.83 ± 1.55 mV	-56.31 ± 0.87 mV
Peak Persistent Cur-rent Amplitude	-69.87 ± 5.81 pA	-141.9 ± 21.01 pA	-74.8 ± 13.0 pA	-88.81 ± 10.83 pA
Persistent Current as % Peak INaT	0.96 ± 0.11 %	0.95 ± 0.17%	0.738 ± 0.10 %	0.96 ± 0.19 %
Peak Resurgent Cur-rent Amplitude	-205.7 ± 17.39 pA	-382.7 ± 43.6 pA		
Resurgent Current as % Peak INaT	2.86 ± 0.24 %	2.414 ± 0.32 %		

Transient Transfections vs. Cell Lines Stably Expressing hNav1.2

In my analyses of the R853Q and R1882Q mutations in HEK cells stably

expressing hNav1.2 cDNA, I found very few discrepancies in the observed mutational

effects, compared to the effects I observed in transiently transfected cells.

Since the R853Q mutation was not studied in the presence of the Navβ4 peptide

in the cell line stably expressing the mutant channel, the only comparison of results

between transiently and stably expressing cells that can be made for this mutation are

the results of the experiments in the absence of the peptide. For the most part, the

mutational effects seen in these two experiments were very similar. Though each

observed effect, which included decreased transient currents, depolarization of the

voltage dependence of inactivation, and a decrease in the maximum peak persistent

current amplitude, was only significant in one of the two datasets, the corresponding

non-significant changes were in the same directions as the significant ones. No

significant change in the voltage dependence of activation or in the maximum peak

persistent current expressed as a percentage of peak transient current was seen in cell

lines stably expressing hNav1.2 or transiently transfected cells. Therefore, the

magnitude of the reduction in persistent currents by the R853Q mutation depends on

the experimental conditions. Several of the effects of the R853Q mutation on hNav1.2

in HEK cells were consistent, at least in direction, across experimental conditions, which

strengthened my confidence that they were truly functional effects of the mutation.

These effects include a hyperpolarizing shift in the voltage dependence of inactivation,

decreases in peak transient and persistent currents, and no effect on the voltage dependence of activation.

In the absence of the Navβ4 peptide, the R1882Q mutation caused very similar effects in transiently transfected cells and cell lines stably expressing hNav1.2. In both groups, there were non-significant increases in peak transient currents, no change in the voltage dependence of activation, a significant depolarizing shift in the voltage dependence of inactivation, and a significant increase in the maximum peak persistent current expressed as a percentage of peak transient current. The maximum peak persistent current amplitude was increased in both groups, though the increase was only significant in the results from the cell lines stably expressing the channels.

In the presence of the Navβ4 peptide, the R1882Q mutation caused very similar effects in transiently transfected cells and cell lines stably expressing hNav1.2; and the effects seen in these two experiments were very similar to the two experiments that did not utilize the peptide. In all four experiments examining the R1882Q mutation, compared to the respective WT control groups, there was no change in the voltage dependence of activation, a significant depolarizing shift in the voltage dependence of inactivation, and a significant increase in the maximum persistent current expressed as a percentage of peak transient current. The R1882Q mutation increased the maximum peak persistent current amplitude in all four experiments, of which three reached statistical significance. The maximum peak transient current amplitudes and densities were not significantly altered by the R1882Q mutation in any of the experiments, though these parameters were slightly increased, compared to WT, in the two

experiments that did not utilize the Navβ4 peptide. Since there was a large degree of

consistency in the functional effects of the R1882Q mutation on hNav1.2 in HEK cells

across all four experimental conditions, I am confident that this mutation depolarizes

the voltage dependence of inactivation, enhances peak persistent currents, and does

not alter peak transient currents or the voltage dependence of activation.

The cDNA expression modality did seem to influence the effects of the R1882Q

mutation on resurgent current in HEK cells. In the presence of the Navβ4 peptide,

compared to the respective WT control groups, the R1882Q mutation increased

resurgent currents in the transiently transfected cells, but not in the cell lines stably

expressing hNav1.2. In fact, the average maximum peak resurgent current amplitude

and the average maximum resurgent current expressed as percentage of transient

current were slightly lower in the R1882Q group than in the WT group, in the

experiment utilizing cell lines stably expressing hNav1.2.   This discrepancy in the effect

on resurgent currents in transiently transfected cells versus cell lines stably expressing

hNav1.2 suggests that the Nav1.2 channels are differentially modulated in transient and

cell lines stably expressing hNav1.2. For example, the cell lines stably expressing

hNav1.2 may compensate for the initial increase in resurgent current by altering channel

modifications such as phosphorylation levels. An alteration in channel modification may

speed or stabilize inactivation, or it might decrease trafficking and membrane

expression levels of the channel. An alteration of trafficking and membrane expression

seems unlikely, since the transient peak current density is not altered by the cDNA

expression modality. However, a compensatory enhancement of inactivation may

develop over a matter of days or weeks in cells stably expressing R1882Q mutant channels.

Our analyses of both the R853Q and R1882Q mutations in both transiently transfected cells and cell lines stably expressing the channels suggest that the modality of cDNA expression in HEK cells may significantly alter the measurements of peak persistent and resurgent currents, but that it does not affect the measurements of peak transient currents, the voltage dependence of activation, or the voltage dependence of inactivation.

No consistent differences were observed when the data from the WT groups in the cell lines stably expressing hNav1.2 were compared to that of the WT groups in transiently transfected cells, (see Table 6). When the data from cells stably expressing the WT channel were compared to that of the cells transiently expressing the WT channel in the presence of the Navβ4 peptide, I observed increases in the average maximum peak transient current amplitude and density, as well as in the average maximum peak persistent and resurgent current amplitudes. However, the average maximum peak persistent and resurgent currents expressed as percentages of maximum peak transient current were not significantly different between these two WT groups. This can be attributed to the fact that the average maximum peak transient, persistent, and resurgent currents were all augmented to similar degrees in the cell line stably expressing WT hNav1.2 channels, compared to the transiently transfected cells. While the voltage dependence of activation was distinctly hyperpolarized in the cell line stably expressing the channels, compared to the transiently transfected cells, the

voltage dependence of inactivation was unaltered. When the data from cells stably

expressing the WT channel was compared to that of the cells transiently expressing the

WT channel in the absence of the Navβ4 peptide, the only difference observed was a

slight hyperpolarization of the voltage dependence of activation in the cells stably

expressing WT channels, compared to transiently transfected cells. The

hyperpolarization of the voltage dependence of activation that was seen in the cells

stably expressing WT channels in the presence of the peptide and, to a lesser degree, in

its absence suggests that the voltage dependence of HEK cells stably expressing hNav1.2

cDNA may be hyperpolarized compared to transiently transfected cells. This

hyperpolarization decreases channel availability and may represent an adaptation of

HEK cells to the new extraneous channels.   This, however, did not impact the overall

results, since each experiment had its own WT control group, to which the mutant

groups in each experiment were compared.

Overall Effects of the L835F, R853Q, and R1882Q Epilepsy Mutations on hNav1.2 Channel Function

The overall effects of the three mutations in my experiments with HEK cells are

noted in bold in Table 7. Cross-experimental comparisons revealed that the effects of

the R853Q and R1882Q mutations were fairly consistent across experimental

conditions.   Several effects of each mutation were consistent across my experiments,

including highly consistent effects on the transient current measurements, voltage

dependence of activation, and persistent current measurements, as well as a consistent

lack of effect on the voltage dependence of activation. Therefore, I am very confident in

the results reported here for the L835F, R853Q, and R1882Q mutations.

Table 7. Overall effects of the L835F, R853Q, and R1882Q mutations on hNav1.2 channel function.

	L835F	R853Q	R1882Q
INaT Amplitude, Density	No change†, No change†	**Decreased, Decreased**	**Increased (ns), Increased (ns)**
Activation Midpoint	**Depolarized (ns)†**	No change	No change
Inactivation Midpoint	No change†	**Hyperpolarized**	**Depolarized**
INaP Amplitude	**Increased†**	**Decreased**	**Increased**
INaP as % of INaT	**Increased†**	No change	**Increased**
INaR Amplitude	N/A	**Decreased†**	**Increased (ns) ††**
INaR as % of INaT	N/A	**Decreased**	**Increased††**

†Only measured in transiently transfected cells
†† Only increased in transiently transfected cells; unchanged in stable cell line

Bold = notably changed compared to WT

Pharmacology

The primary goal of this study was to characterize the functional effects of three

missense mutations on the hNav1.2 channel, in order to develop a better understanding

of the mechanisms by which ion channel mutations lead to seizure disorders. The

various profiles of biophysical functional changes caused by the epileptogenic *SCN2A*

mutations that have been studied *in vitro* suggests that distinct missense mutations in

hNav1.2 have different biophysical mechanisms of seizure generation. For example,

R853Q and R1882Q both lead to severe epilepsy, though with distinct clinical

phenotypes (Allen et al., 2013; Nakamura et al., 2013; Samanta and Ramakrishnaiah,

2015; Kobayashi et al., 2016; Carvill et al., 2013; Howell et al., 2015; Trump et al., 2016;

Wolff et al., 2017); and, in this study, these mutations have opposite effects on hNav1.2

persistent current, resurgent current, and voltage dependence of inactivation. Given

that distinct missense mutations in the same ion channel generate seizures by unique

molecular mechanisms, individual mutations may require targeted

pharmacotherapeutic strategies in order to normalize the channel activity and prevent

epileptogenesis (seizure generation). For example, epileptic patients with a mutation

that increases persistent current as the primary pathological effect (e.g. A263V, Parrini

et al., 2017) would benefit from a pharmacological compound that selectively or

preferentially inhibits persistent current; while the same compound would likely be

ineffective in patients with mutations generating seizures through a loss of channel

expression (e.g. R102X, Kamiya et al., 2004). An ideal pharmacotherapeutic strategy for

any epileptic patient with a pathogenic *SCN2A* mutation may involve selectively, or at

least preferentially, targeting the specific pathological biophysical effects of each

mutation, which may include the enhancement of aberrant currents such as persistent

and resurgent currents, or the generation of a gating pore. Such a strategy would

maintain or restore healthy channel conductance and gating, as is seen in wild-type

hNav1.2 channels, so as not to produce excessive sedation or other adverse effects in

patients. My data (work published in Mason and Cummins, 2020, available at

https://www.mdpi.com/1422-0067/21/7/2454) suggests that CBD and GS967

preferentially inhibit, respectively, resurgent and persistent current over transient

current; and therefore that these compounds may be more effective than current AEDs

with less severe side effects, especially in patients with *SCN2A* mutations that enhance resurgent and/or persistent currents.

Though CBD reduced transient current density in this study, CBD inhibited the transient current density to a lesser degree than the resurgent current. The inhibition of resurgent current density by CBD was significantly different from that of the vehicle and untreated control groups over a wider range of voltages than its inhibition of transient current density. The selectivity of CBD for resurgent current is also suggested by the significant inhibition of maximum peak resurgent current density and the lack of significant inhibition of maximum peak transient current density. The vehicle for CBD, methanol, mildly reduced hNav1.2 resurgent current densities at negative voltages, but the inhibitory effect of CBD was significant even compared to the methanol effect. There was also a trend toward inhibition of persistent current by both methanol and CBD, though this effect was not significant according to the limited analysis that I performed. In this study, CBD produced a significant depolarizing shift in the voltage dependence of activation (see fig. 19A), which contributed to the inhibition of current densities by limiting channel availability. As seen with WT hNav1.6, 1 μM CBD significantly reduced the maximum resurgent current (measured both as resurgent current density and as a percentage of transient current amplitude; latter data not shown) in HEK cells stably expressing hNav1.2, while not significantly reducing the maximum peak transient current density. The same study that demonstrated the ability of CBD to block resurgent currents over transient currents in WT hNav1.6 also demonstrated its ability to preferentially block aberrant resurgent and persistent

currents generated by epileptogenic *SCN8A* (hNav1.6) mutations (Patel et al., 2016).

Given the similarities in structure and function between Nav1.2 and Nav1.6, their

predominant expression in excitatory (vs. inhibitory) neurons, and the similarities

between their responses to CBD, I predict that CBD will demonstrate preferential

inhibition of aberrant resurgent and persistent currents caused by epileptogenic

hNav1.2 (*SCN2A*) mutations. Given the ability of CBD to preferentially inhibit resurgent

currents over transient currents in hNav1.2 and hNav1.6 and its efficacy even in

refractory cases of epilepsy, I predict that this compound will prove to be a more

effective AED than standard treatments such as phenytoin for patients with Nav

mutation-associated epilepsies.

GS967 reduced transient and resurgent currents to similar degrees. The

inhibition of resurgent current density by GS967 was significantly different from vehicle

over a narrower range of voltages than its inhibition of transient current density (see fig.

18B, D). Neither the maximum peak transient current density nor the maximum peak

resurgent current density were significantly reduced by this compound (see fig. 18A, C).

The significant inhibition of transient and resurgent current densities in the current

density-voltage relationships can be attributed to the depolarizing shift in the voltage

dependence of activation elicited by DMSO and the hyperpolarizing shift in the voltage

dependence of inactivation elicited by GS967, which both reduce channel availability.

The hyperpolarizing shift in inactivation also suggests that GS967 could be a state-

dependent Nav inhibitor, like phenytoin. My limited analysis of the effect of GS967 on

persistent current suggested that GS967 may inhibit persistent current to a larger

degree than transient current in HEK cells stably expressing WT hNav1.2 (see fig. 18E).

The effects of 1 µM GS967 on WT hNav1.2 seen in this study are congruent with

previous reports that GS967 preferentially inhibits persistent current over transient

current and hyperpolarizes the voltage dependence of inactivation in pyramidal neurons

from the brains of mouse models of *SCN8A* epilepsy and in ND7/23 cells expressing the

corresponding mutation (Baker et al., 2018; Bunton-Stasyshyn et al., 2019; Wengert et

al., 2019). Also, as in this study, WT Nav1.6 resurgent current was not significantly

inhibited by GS967 in pyramidal subiculum neurons from one of these mouse models,

though the compound did inhibit resurgent and persistent currents that were aberrantly

enhanced by the epilepsy mutation (Wengert et al., 2019). GS967 has been shown to

prolong the survival of mice expressing two different *SCN8A* epilepsy mutations (Baker

et al., 2018; Bunton-Stasyshyn et al., 2019) and protect against both spontaneous and

evoked seizures in genetic models of *SCN1A*, *SCN2A*, and *SCN8A* epilepsies (Anderson et

al., 2014, 2017; Baker et al., 2018). Further studies need to be performed in order to

confirm the ability of GS967 to preferentially block persistent over transient hNav1.2

currents and investigate whether or not it preferentially blocks persistent and resurgent

currents aberrantly enhanced by *SCN2A* epilepsy mutations; and no phase 2 clinical

trials have been performed to evaluate its efficacy as an antiepileptic drug in humans.

Given the ability of GS967 to preferentially inhibit persistent over transient and

resurgent currents in WT Nav channels, its propensity to preferentially block aberrant

persistent and resurgent currents associated with Nav epilepsy mutations, and its

efficacy as an AED in preclinical models of epilepsy, I predict that this compound will

prove to be a more effective AED than standard treatments such as phenytoin for

patients with Nav mutation-associated epilepsies.

As of early 2020, there have not been any reported studies examining the effects

of AEDs on gating pore current, but the refractoriness of most reported R853Q epilepsy

cases suggests that the conventional AEDs do not block the primary pathogenic effect(s)

of the mutation. My collaborators and I propose that the gating pore current created by

the R853Q mutation is its primary pathogenic mechanism, and that this current must be

selectively targeted in order to prevent seizures in patients with this mutation. One

pharmacotherapeutic strategy that could be pursued in order to selectively target gating

pore current through a given domain is the development of a gating modifier molecule

that interacts with the voltage sensor in that domain. Gating modifiers alter the gating

kinetics of ion channels, and most that have been shown to impact Nav channel function

are toxins. The crab spider toxin, Hm-3, has been reported to inhibit gating pore

currents generated by a Nav1.4 disease mutation in the voltage sensor of domain I by

interacting with the voltage sensor in that domain (Männikkö et al., 2018). Hm-3 did

not inhibit gating pore current caused by disease mutations in the voltage sensors in

domains II or III, suggesting that it selectively targets the voltage sensor and gating pore

in domain I. It also strongly inhibited transient currents in WT channels, so it remains to

be determined whether or not this toxin preferentially inhibits gating pore current over

transient current in WT or mutant Nav1.4, or in any other Nav isoform (Männikkö et al.,

2018). Hm-3 has been shown to inhibit transient current in most Nav channel isoforms,

though it is selective, in this respect, for Nav1.4 and Nav1.5 over Nav1.1, Nav1.2,

Nav1.3, Nav1.6, and Nav1.8 (Berkut et al., 2015). The authors of the 2018 study

suggested that Hm-3 binds to the voltage sensor of domain I in Nav1.4 with a higher

affinity when the channel is in the closed conformation, either directly occluding the

gating pore or causing a shift in the local channel conformation that occludes the gating

pore. Toxins or other molecules that have similar mechanisms of action through

interactions at other voltage sensing segments could be sought in order to inhibit gating

pore currents generated by disease mutations in domains II-IV. These molecules and

Hm-3 could be used as templates for the development of drugs that selectively inhibit

gating pore current through each domain without notably inhibiting the transient

current.   One caveat of this method to consider is that, if a molecule interacts with the

voltage sensor of the affected domain in such a way that shifts the sensor slightly so

that the gating pore is occluded indirectly, this could bias the channel toward or away

from activation. This could result in an aberrant increase or decrease, respectively, in

neuronal excitability, which could cause unintended CNS effects such as exacerbation of

seizures or sedation. Nevertheless, novel AEDs that selectively inhibit gating pore

current over transient current could prove to be effective in preventing seizures in

patients with refractory epilepsy caused by mutations that result in gating pore

currents.

Applications

Our data demonstrated that neutralizing a voltage-sensing residue in hNav1.2

(R853Q) creates a gating pore that does not exist in the WT channel. This is the first

demonstration of this phenomenon as an effect of a disease mutation in a neuronal Nav channel. Many of the over two dozen S4 charge neutralizing mutations in Nav1.1, Nav1.2, and Nav1.6 that have been identified in patients with epilepsy may also induce gating pore currents that contribute to the disease phenotype. Due to their physical distinction from the central pore, where traditional sodium channel blockers have been shown to bind, gating pore currents are unlikely to be targeted by standard clinical therapies. Thus, novel approaches, such as blocking the gating pore with a gating modifier molecule, may be needed to ameliorate the impact of the gating pore currents produced by some neuronal sodium channel disease mutations.

Our data also demonstrated that enhancement of resurgent currents is an effect of at least one epileptogenic *SCN2A* mutation that is likely involved in the pathogenesis of the resulting epilepsy. Therefore, as suggested with Nav1.6 epilepsy mutations (Patel et al., 2016), I believe that targeting resurgent Nav currents over transient Nav currents is a valuable strategy for the treatment of epilepsy. The results of my study of CBD suggest that this compound targets resurgent current over transient current in hNav1.2, as it does in hNav1.6, (both of which are neuronal Nav channels predominantly expressed in excitatory/pyramidal neurons) and thus that this preferential inhibition contributes to its proven efficacy as an AED.

Persistent currents are known to be enhanced by some epileptogenic *SCN2A* mutations, and that enhancement is believed to be involved in the pathogenesis of the resulting epilepsies. The results of my study with GS967, along with previous studies, suggest that this compound preferentially inhibits persistent neuronal Nav currents over

transient neuronal Nav currents. Therefore, as suggested in the context of Nav1.6

epilepsies (Baker et al., 2018; Wengert et al., 2019), I believe that targeting persistent

Nav currents over transient Nav currents is a valuable strategy for the treatment of

epilepsy, and that GS967 will thus prove to be an efficacious AED in human patients.

Ultimately, I expect that this research will contribute to a knowledge base and

resources that will lead to more effective treatments for patients with epileptogenic

SCN2A mutations. The next step in that process will be screening conventional

antiepileptic drugs and novel, putatively antiepileptic compounds in cells expressing

mutant hNav1.2 channels, with the aim of discovering the compound that best

normalizes the channel activity (to resemble that of wild-type) for each mutation. The

therapeutic value of such compounds could be confirmed in neurons expressing the

mutant channels, and the correlation of patient-reported efficacy of conventional

antiepileptic drugs with the effects of the same drugs on mutant channels *in vitro* could

be studied. If the correlation is strong, then the *in vitro* studies could provide

suggestions of compounds that will likely be efficacious in patients with particular

epileptogenic mutations.

V. FUTURE DIRECTIONS

In Vitro Studies

This study characterized the biophysical effects of three epileptogenic *SCN2A*

mutations on hNav1.2 channels, but these channels were transiently expressed in

HEK293 cells. Though they are human cells with a full set of human DNA, HEK293 cells

are not neurons. Their endogenous expression of voltage-gated sodium and potassium

channels, both of which are strongly endogenously expressed in neurons, is weak (He

and Soderlund, 2010).   Primarily for this reason, HEK293 cells are not excitable and

cannot conduct action potentials. This weak endogenous voltage-gated ion channel

expression makes HEK293 cells a great cell type in which to study the effects of various

mutations and treatments on the function of an isolated voltage-gated sodium channel

isoform. However, this method does not consider the potential effects of cell type-

specific protein expression or membrane compositions on channel function. Though

HEK293 cells share some genetic characteristics of neuronal stem cells (Shaw et al.,

2002), the differences in proteome and protein expression levels may result in

differences in the functionality of the voltage-gated sodium channels in HEK cells and

neurons. For example, neurons in many brain regions express FGF14b (Wang et al.,

2002), which has been shown to inhibit transient currents in Nav1.1, Nav1.2, Nav1.5,

and Nav1.6 (Lou et al., 2005; Laezza et al., 2009) and to generate resurgent currents in

cerebellar Purkinje neurons (Yan et al., 2014; White et al., 2019). FGF14b is not known

to be expressed in HEK293 cells, and thus, FGF14b may modulate transient and

resurgent currents in neurons in ways that are absent in HEK293 cells expressing the

same Nav channel isoforms. Additionally, the membrane compositions of HEK293 cells and neurons may differ substantially, so the Nav channels in the membranes of the two cell types likely differ in their molecular interactions with surrounding membrane components and in the resulting modulations that those interactions may have on Nav channel function.

Since HEK293 cells are not excitable, this method does not allow for the direct study of the effects of mutations or treatments on neuronal (or other cellular) excitability. Therefore, further studies of these and other epileptogenic *SCN2A* mutations in neurons are needed in order to confirm that these mutations alter Nav channel function and excitability in neurons. Voltage-clamp studies of *SCN2A* epilepsy mutations should include the analysis of mutational effects on all of the parameters included in this study, as well as on membrane trafficking in neurons. Though some studies have revealed defects in membrane expression levels of Nav1.2 channels bearing epilepsy mutations in HEK cells, it is unclear whether or not these trafficking defects also occur in neurons endogenously expressing *SCN2A* epilepsy mutations. Membrane expression assays, such as immunocytochemistry, could reveal trafficking defects associated with particular mutations, which could contribute to the pathogenesis of the disease.

For neuronal studies, there are multiple potential experimental strategies. The source and type of neurons, method of mutation expression, and culture setup of the neurons are all variables that could affect the experimental results.

The neurons could be derived from induced pluripotent stem cells (iPSCs), or they could be primary cultures from rodents or humans. Human primary neurons could come from a collaborating neurologist or biobank and would likely be derived from resections of diseased brain tissues. The mutation of interest could be introduced into the neurons via one of several different methods. A point mutation conferring resistance to TTX could be introduced into the cDNA for the WT and mutant forms of the channel, and these channels could be transiently transfected into the neurons, so that TTX could be used in the bath solution to inhibit all endogenous TTX-sensitive (TTX-S) Nav currents and limit the Nav currents to TTX-resistant (TTX-R) channels in the neurons. All of the Nav channel isoforms expressed in the brain (Nav1.1, Nav1.2, Nav1.3, and Nav1.6) are TTX-S, so saturating brain neurons with TTX would limit voltage-gated sodium currents to the exogenous TTX-R channels that are transfected in, which may result in decreased excitability of the neurons, if whole-cell currents and resulting depolarization fall short of the endogenous whole-cell currents and depolarization. Another approach could be to knock down endogenous Nav1.2 channel expression with shRNA and transiently transfect the channel bearing the epilepsy mutation, then studying the neurons in the absence of TTX. For studies generating and/or utilizing genetic animal models of epilepsy, in which the animal heterozygously expresses the mutation of interest, wild-type littermates could be used as controls; and the WT or mutant channel of interest would be endogenously expressed in primary neurons. If the study allows for the generation of induced pluripotent stem cells, fibroblasts from patients and unaffected siblings or other close relatives without the mutation could be

used to generate iPSCs that are then differentiated into model neurons. If cells from

epileptic patient(s) with the mutation of interest are not available, CRISPR-Cas9 could be

utilized to induce the point mutation in healthy iPSCs, which could then be

differentiated into model neurons. Pluripotent stem cells induced from human

fibroblasts have demonstrated great potential as research tools since around 2010, and

multiple techniques have been described for the effective differentiation of these stem

cells into fully functional neurons (Zhang et al. 2013, Mariani et al. 2012, Espuny-

Camacho et al. 2013). The predictive value of drug screens utilizing hiPSC-derived

neurons has not been strongly established as of early 2020, but it has been supported

by demonstrating that hiPSC-derived motor neurons modeling ALS mimicked human

patients' failure to respond to two trial drug compounds.

The neurons could be cultured at a low density, in order to study isolated cells,

or at a high density, in order to study neurons in a network. Studying isolated cells is

informative regarding mutation and drug effects on individual neuronal excitability and

activity, but this experimental approach fails to properly recapitulate the complexity of a

neuron's environment and activity *in vivo*. Thus, studying neurons in a network can also

provide valuable translational insights. In the patients' brains, the affected neurons are

highly integrated into a neuronal network, likely receiving input from multiple

presynaptic neurons and releasing neurotransmitters to influence multiple postsynaptic

neurons. This enables synchronous firing of many interconnected neurons, which is

believed to cause the large-amplitude bursts of activity seen on EEGs of epileptic

patients during seizures. Additionally, since Nav1.2 is implicated in backpropagation,

studying the effects of *SCN2A* mutations on neurons in a network allows for the investigation of the effects of the mutations on synaptic plasticity.   Microelectrode array (MEA) culture dishes, which have a grid of electrodes built in and exposed on the bottom, can be used to study the synchronous bursting activity of both dissociated neurons and intact brain slices (Dossi et al., 2014; Gullo et al., 2014; Tidball and Parent, 2016). This approach could be useful in confirming the pathogenicity of epilepsy-associated Nav mutations, as well as for screening AEDs against specific epileptogenic Nav mutations. Therefore, this could prove to be a valuable tool in the development of personalized medicine for epilepsy patients. Cerebral organoids are showing promise as *in vitro* models of brain development and disorders, and these may constitute another highly translational model in which to study the pathogenesis, including the temporal development, of genetic epilepsies (see Antill-O'Brien, Bourke, and O'Connell, 2019 for review).

Though the study of the effects of Nav epilepsy mutations in cultured neurons derived from patient iPSC cells holds high translational value, it may still fail to properly model the complexity of the human disease. There are many neuronal subtypes in the brain, each expressing a slightly different milieu of genes, and it is unclear which of these subtypes express *SCN2A*. Therefore, the cell-specific background of the affected neurons in the patients, such as which Nav α and β subunits they express or what genetic modifiers may be present, is unknown. Also, neurons in culture may not respond to the mutations in the same ways, or to the same extent, as do the affected neurons in the patients' brains. For example, there could be compensation that occurs

in patients' brains that relies on a gene that is expressed in the affected neuronal subtype but not in the cultured neuronal population. However, as studies continue to characterize the neuronal subtypes in the human brain, scientists will be better able to recreate these neuronal subtypes, including the affected neurons, more accurately in culture.

The pharmacological experiments in this dissertation work included only single doses of two antiepileptic compounds, CBD and GS967, tested on HEK cells stably expressing WT hNav1.2 channels. Additional studies of the effects of these drugs on transient, resurgent, and persistent currents in neurons could be performed in HEK cells or neurons to investigate whether they preferentially inhibit currents that are aberrantly enhanced by epilepsy mutations in neuronal Nav channels. Dose-response studies could be performed to validate the selectivity of CBD and GS967 for, respectively, resurgent and persistent currents; these studies would be expected to reveal a greater potency of the drug for the inhibition of resurgent or persistent current than for the inhibition of transient current. Further studies should be performed to examine the effects of a panel of AEDs and potentially antiepileptic compounds on both WT hNav1.2 channels and hNav1.2 channels expressing epilepsy-associated mutations, expressed in isolation or co-expressed with WT channels in HEK293 cells, in order to examine their abilities to block aberrant resurgent and persistent currents over transient current and restore functionality of mutant channels to resemble that of WT. The compounds should also be studied in neurons to determine their effects on neuronal Nav currents and excitability, in both the presence and absence of epilepsy Nav mutations. In both HEK

cell and neuron studies, the compounds should be tested at varying concentrations, in order to generate concentration-response curves. These studies would aim to find one or more compounds that selectively block aberrant currents generated by epilepsy mutations while not notably blocking healthy WT currents, thus blocking aberrant hyperexcitability in affected neurons. I expect that such compounds would demonstrate greater potency and efficacy than conventional AEDs, and that CBD and GS967/Prax330 will be the first drugs in this novel subclass of AEDs.

In Vivo Studies

Though *in vitro* studies seem to confirm the pathogenicity of many *SCN2A* epilepsy mutations, further studies are needed to show that these mutations actually cause epilepsy phenotype (e.g. spontaneous seizures) *in vivo*.

Rodent models of epilepsy have been used to test the antiepileptic potential of novel drug compounds for over 70 years, but until the 21st century, these models typically required experimental induction of epilepsy (e.g. by electroshock or PTZ, status epilepticus (SE) induced by kainite or pilocarpine). Early genetic rodent models of epilepsy resulted from random mutagenesis or spontaneous mutations, but the mutations were not necessarily in genes homologous to those implicated in human cases of epilepsy. The responses of these early epilepsy model rodents to AEDs has generally been highly predictive of the human patient response, but these models only model the predominant phenotypes of epilepsy and not the etiology. Though some of the induced epilepsy models reproduce the phenotype of refractory seizures, it is highly

unlikely that the induction method produces the same biophysical effects and

complexity as do the mutations that often underlie refractory seizures in the patients.

In order to confidently identify antiepileptic compounds that will effectively and

specifically block the pathogenic molecular mechanism of epilepsy mutations in human

patients, animal models bearing the responsible mutation and corresponding epilepsy

phenotype are needed. These genetic models of epilepsy could be used to study the

disease itself, investigate novel antiepileptic therapies, and screen compounds to tailor

the pharmaceutical treatment to the molecular etiology of the patient's epilepsy.

Progress in the development of genetic rodent models of *SCN2A* epilepsy is slow and

challenging, although the costs of advanced genetic approaches to the development of

such models, such as CRISPR/Cas9 gene editing, are decreasing. Dravet Syndrome, the

predominant form of *SCN1A* epilepsy, can be modeled fairly simply by the knockdown or

knockout of one allele of *SCN1A*, which mimics the loss of function in that gene and the

resulting Nav1.1 protein due to the human patients' mutations. There are two mouse

models of epilepsy that heterozygously express pathogenic human *SCN8A* mutations

(Wagnon et al., 2015; Bunton-Stasyshyn et al., 2019), but so far there are no such

rodent models bearing human *SCN2A* mutations. The Q54 mouse line, which bears an

SCN2A transgene with the GAL879-881QQQ mutation in the cytoplasmic S4-S5 linker of

domain II, was established as an *SCN2A* model of epilepsy in 2001 (Kearney et al.), but

this particular triplet of point mutations has not been reported in any human cases of

epilepsy. Efforts are ongoing to develop mice heterozygously expressing epilepsy-

associated *SCN2A* mutations. One lab has reported producing a mouse strain

heterozygous for the R1882Q mutation, which display spontaneous seizures as early as

postnatal day 1 and do not survive past postnatal day 30 without treatment (Petrou et

al., 2018), but as of early 2020, these claims have not been substantiated by publication.

Another lab claims to have produced a mouse strain heterozygous for the R853Q

mutation, but this claim is also unsubstantiated and these animals do not display any

spontaneous seizures or increased susceptibility to induced seizures, whereas the

human patients heterozygous for this mutation experience severe spontaneous

seizures. The challenges in generating a mouse model bearing an epileptogenic *SCN2A*

mutation and a corresponding phenotype of spontaneous seizures or increased

susceptibility to seizures are not well understood, but they may include species

differences in gene expression in the affected neurons, which could result in differences

in Nav channel modulation.

Another promising model organism for the study of epilepsy is the zebrafish

(*Danio rerio*). Though they are not as closely related to humans as mice and rats in

terms of genetics or anatomy, they are vertebrates, and zebrafish expressing mutations

in multiple genes implicated in human cases of epilepsy do show increased susceptibility

to seizures compared to wild-type fish (Schoonheim et al., 2010; Zhang et al., 2015;

Grone et al., 2016; Pena et al., 2017; Zabinyakov et al., 2017). Their reproduction results

in a large number of progeny that develop more quickly than their rodent counterparts,

which makes the zebrafish favorable as a model organism in which to conduct high-

throughput drug screens. Housing and care of the zebrafish is cost- and space-efficient,

and there is no known risk of developing allergies to them from working with them in

the lab. Since they develop independently in transparent eggs from the moment of

fertilization, their entire development can be easily observed and studied, without

requiring the sacrifice of any adults, as is required in the study of the prenatal rodent

brain. The larvae themselves are also mostly transparent until about 3 weeks post-

fertilization, which enables *in vivo* imaging and electrophysiology studies. By about 3

days post-fertilization, excitatory glutamatergic (Higashijima et. al. 2004), inhibitory

GABAergic (Higashijima et. al. 2004, Mueller et. al. 2006), and monoaminergic (Kaslin

and Panula 2001, McLean and Fetcho 2004) neurons are present in the brain, confirming

at least a moderate degree of neuron subtype homology between zebrafish and

humans.

The zebrafish homologue of human Nav1.2 (*SCN2A*) is the *Scn1lab* gene. It is

also homologous to human *Scn1a* and *Scn3a*, and, like its human homologues, it is

expressed predominantly in the central nervous system (Novak 2006). In zebrafish, it

can be found throughout the brain and hindbrain and in ventral regions of the spinal

cord by 48 hours post-fertilization (Novak 2006). The *Scn1lab* and *SCN2A* gene products

are 79% identical. While this is a relatively high identity (*Scn1lab* and *SCN1A* are 76%

identical), the pharmacology of *Scn1lab* and *SCN2A* sodium channels could differ in

important aspects such as cell type distribution and AED binding affinities. This could

diminish the predictive accuracy/value of the zebrafish model, but parallel *in vitro*

assays using human channel construct bearing the mutation of interest could be

performed to confirm that the drug responses in those models correspond to the drug

responses of the model fish. Chemical mutagenesis and morpholino knockdown of

Scn1lab have been used to generate zebrafish models of Dravet Syndrome (Schoonheim et al., 2010; Zhang et al., 2015), which have been used to screen non-AED FDA-approved drugs for antiepileptic therapeutic potential and identify a few that may be efficacious in Dravet Syndrome patients (Griffin et al., 2018; Sourbron et al., 2019). This suggests that, if zebrafish with gain-of-function *Scn1lab* mutations can be generated and shown to have an epileptic phenotype, they may be a useful platform in which to screen epilepsy drugs for efficacy.

Efforts to create point mutations in zebrafish homologous to those found in genetic human epilepsies using CRISPR/Cas9 have yielded very low success rates thus far, and we were unable to generate zebrafish bearing point mutations in *Scn1lab* with that technique in my collaboration with the Marrs lab (IUPUI School of Science, Dept. of Biology). We were, however, successful in generating a transgenic zebrafish that expressed the WT human *SCN2A* gene, under a zebrafish neuron-specific promoter (Satou et al., 2013), alongside both endogenous *Scn1lab* alleles. The expression of an extraneous neuronal Nav gene has proven useful in a model of cardiac arrhythmia associated with a Nav1.5 mutation (Huttner et al., 2013). Our transgenic zebrafish model is still in development as of early 2020, but we hope to use CRISPR/Cas9 to create epilepsy point mutations in the transgene and thus produce genetic zebrafish models of epilepsy that can be used to screen for antiepileptic compounds that may protect against seizures in patients with epilepsy caused by *SCN2A* channel mutations. We expect that the phenotypic effects of epileptogenic mutations in the transgenic human Nav channel gene will include abnormal swimming behavior (e.g. alterations in average

swimming velocity, whirlpool-like swimming, or bursts of erratic activity) and bursts of

abnormal electrophysiolgical activity in the brain. We expect that the phenotypic

effects will be either spontaneous in mutant fish and absent in WT fish or more easily

evoked in mutant fish than WT fish. If this transgene model of epilepsy is unsuccessful,

we may return to the CRISPR-Cas9 mutagenesis strategy using an optimized protocol,

such as the one published by Prykhozhij et al. in 2017. Once the effects of the Nav1.2

channel mutations in zebrafish have been characterized, these fish could be used to

screen for antiepileptic pharmacological compounds that reduce or eliminate those

effects.

Since generating mutant zebrafish could be a much faster process than

generating mutant mice, we hope to establish a high-throughput screening system in

which we can screen potentially antiepileptic compounds using zebrafish modeling ion

channelopathies that cause treatment-resistant epilepsies in humans. Zebrafish

screening assays would aim to identify compounds that inhibit the rapid swimming and

convulsive behavior of the mutant zebrafish, and electrophysiological analyses would

need to be performed to confirm that they also inhibit the epileptiform electrical

discharges in the brain. Such a compound would be further investigated, using other

model systems, to further substantiate its potential therapeutic efficacy against clinical

seizures caused by the particular mutation being studied. We believe that this approach

could be used to identify compounds that are effective in preventing seizures in patients

with Nav1.2 mutation-driven epilepsy that is refractory to the conventional antiepileptic

treatments.

VI. SUMMARY AND CONCLUSIONS

Missense mutations in *SCN2A* and other genes are increasingly being identified as causative in otherwise idiopathic cases of epilepsy, many of which are refractory to traditional antiepileptic drugs (AEDs, e.g. phenytoin, carbamazepine, levetiracetam, etc.). Our understanding of how these mutations alter the channel function and neuronal excitability is limited, so this study aimed to characterize the biophysical effects of three *SCN2A* mutations that are associated with refractory epilepsy and expand our understanding of the potential pathogenic biophysical effects of these mutations. I also sought to investigate the abilities of two novel antiepileptic compounds, CBD and GS967, to preferentially inhibit persistent and/or resurgent currents over transient current. The results of this dissertation work suggest that individual *SCN2A* epilepsy mutations alter hNav1.2 channel function differently, and that changes in resurgent current and the creation of a gating pore current should be considered as potential pathogenic effects of these mutations. In cases when the mutation effects, such as the induction of a gating pore, are not targeted by traditional AEDs, patients will likely require novel AEDs that target the biophysical defect in order to effectively suppress their seizures.   Moreover, AEDs that preferentially inhibit aberrant Nav currents resulting from epilepsy mutation will likely prove to be efficacious at doses that minimally disturb the normal activity of the channels, allowing patients to be seizure-free without significant impairment of normal brain activity. My results suggest that CBD and GS967 preferentially inhibit resurgent and persistent Nav currents, respectively, over transient Nav currents, and, thus, that these compounds may be more

potent and efficacious than traditional AEDs in the treatment of refractory *SCN2A*-

associated epilepsy.

Overall, this thesis addressed gaps in our understanding of the potentially

pathogenic biophysical effects of epileptogenic *SCN2A* mutations and in our

understanding of the mechanisms of action of two novel antiepileptic compounds. The

results may guide future studies of epileptogenic Nav channel mutations and screens of

antiepileptic compounds to include resurgent and gating pore currents as potential

biophysical effects of the mutations and as potential therapeutic targets. Tailoring the

treatment to block the particular pathogenic effects of the patient's epilepsy mutation

will allow for more targeted and effective suppression of both manageable and

refractory seizures.

VII. REFERENCES

Afshari, F. S., Ptak, K., Khaliq, Z. M., Grieco, T. M., Slater, N. T., McCrimmon, D. R., & Raman, I. M. (2004). Resurgent Na currents in four classes of neurons of the cerebellum. J Neurophysiol, 92(5), 2831-2843. doi:10.1152/jn.00261.2004

Allen, A. S., Berkovic, S. F., Cossette, P., Delanty, N., Dlugos, D., Eichler, E. E., . . . Winawer, M. R. (2013). De novo mutations in epileptic encephalopathies. Nature, 501(7466), 217-221. doi:10.1038/nature12439

Aman, T. K., Grieco-Calub, T. M., Chen, C., Rusconi, R., Slat, E. A., Isom, L. L., & Raman, I. M. (2009). Regulation of persistent Na current by interactions between beta subunits of voltage-gated Na channels. J Neurosci, 29(7), 2027-2042. doi:10.1523/jneurosci.4531-08.2009

Anderson, L. L., Hawkins, N. A., Thompson, C. H., Kearney, J. A., & George, A. L., Jr. (2017). Unexpected Efficacy of a Novel Sodium Channel Modulator in Dravet Syndrome. Sci Rep, 7(1), 1682. doi:10.1038/s41598-017-01851-9

Anderson, L. L., Thompson, C. H., Hawkins, N. A., Nath, R. D., Petersohn, A. A., Rajamani, S., . . . George, A. L., Jr. (2014). Antiepileptic activity of preferential inhibitors of persistent sodium current. Epilepsia, 55(8), 1274-1283. doi:10.1111/epi.12657

Antill-O'Brien, N., Bourke, J., & O'Connell, C. D. (2019). Layer-By-Layer: The Case for 3D Bioprinting Neurons to Create Patient-Specific Epilepsy Models. Materials (Basel), 12(19). doi:10.3390/ma12193218

Aronica, E., Yankaya, B., Troost, D., van Vliet, E. A., Lopes da Silva, F. H., & Gorter, J. A. (2001). Induction of neonatal sodium channel II and III alpha-isoform mRNAs in

neurons and microglia after status epilepticus in the rat hippocampus. Eur J

Neurosci, 13(6), 1261-1266. doi:10.1046/j.0953-816x.2001.01502.x

Baasch, A. L., Huning, I., Gilissen, C., Klepper, J., Veltman, J. A., Gillessen-Kaesbach, G., . . . Lohmann, K. (2014). Exome sequencing identifies a de novo SCN2A mutation in a patient with intractable seizures, severe intellectual disability, optic atrophy, muscular hypotonia, and brain abnormalities. Epilepsia, 55(4), e25-29. doi:10.1111/epi.12554

Baker, E. M., Thompson, C. H., Hawkins, N. A., Wagnon, J. L., Wengert, E. R., Patel, M. K., . . . Kearney, J. A. (2018). The novel sodium channel modulator GS-458967 (GS967) is an effective treatment in a mouse model of SCN8A encephalopathy. Epilepsia, 59(6), 1166-1176. doi:10.1111/epi.14196

Bant, J. S., & Raman, I. M. (2010). Control of transient, resurgent, and persistent current by open-channel block by Na channel beta4 in cultured cerebellar granule neurons. Proc Natl Acad Sci U S A, 107(27), 12357-12362. doi:10.1073/pnas.1005633107

Barbosa, C., Tan, Z. Y., Wang, R., Xie, W., Strong, J. A., Patel, R. R., . . . Cummins, T. R. (2015). Navbeta4 regulates fast resurgent sodium currents and excitability in sensory neurons. Mol Pain, 11, 60. doi:10.1186/s12990-015-0063-9

Barker, B. S., Nigam, A., Ottolini, M., Gaykema, R. P., Hargus, N. J., & Patel, M. K. (2017). Pro-excitatory alterations in sodium channel activity facilitate subiculum neuron hyperexcitability in temporal lobe epilepsy. Neurobiol Dis, 108, 183-194. doi:10.1016/j.nbd.2017.08.018

Beleza, P. (2009). Refractory epilepsy: a clinically oriented review. Eur Neurol, 62(2), 65-71. doi:10.1159/000222775

Beneski, D. A., & Catterall, W. A. (1980). Covalent labeling of protein components of the sodium channel with a photoactivable derivative of scorpion toxin. Proc Natl Acad Sci U S A, 77(1), 639-643. doi:10.1073/pnas.77.1.639

Ben-Shalom, R., Keeshen, C. M., Berrios, K. N., An, J. Y., Sanders, S. J., & Bender, K. J. (2017). Opposing Effects on NaV1.2 Function Underlie Differences Between SCN2A Variants Observed in Individuals With Autism Spectrum Disorder or Infantile Seizures. Biol Psychiatry, 82(3), 224-232. doi:10.1016/j.biopsych.2017.01.009

Berecki, G., Howell, K. B., Deerasooriya, Y. H., Cilio, M. R., Oliva, M. K., Kaplan, D., . . . Petrou, S. (2018). Dynamic action potential clamp predicts functional separation in mild familial and severe de novo forms of SCN2A epilepsy. Proc Natl Acad Sci U S A, 115(24), E5516-e5525. doi:10.1073/pnas.1800077115

Berkovic, S. F., Heron, S. E., Giordano, L., Marini, C., Guerrini, R., Kaplan, R. E., . . . Scheffer, I. E. (2004). Benign familial neonatal-infantile seizures: characterization of a new sodium channelopathy. Ann Neurol, 55(4), 550-557. doi:10.1002/ana.20029

Berkut, A. A., Peigneur, S., Myshkin, M. Y., Paramonov, A. S., Lyukmanova, E. N., Arseniev, A. S., . . . Vassilevski, A. A. (2015). Structure of membrane-active toxin from crab spider Heriaeus melloteei suggests parallel evolution of sodium

channel gating modifiers in Araneomorphae and Mygalomorphae. J Biol Chem, 290(1), 492-504. doi:10.1074/jbc.M114.595678

Bialer, M., Johannessen, S. I., Levy, R. H., Perucca, E., Tomson, T., & White, H. S. (2013). Progress report on new antiepileptic drugs: a summary of the Eleventh Eilat Conference (EILAT XI). Epilepsy Res, 103(1), 2-30. doi:10.1016/j.eplepsyres.2012.10.001

Broomfield, EB, JE Cavazos, & JI Sirven, editors. An Introduction to Epilepsy [Internet]. West Hartford (CT): American Epilepsy Society; 2006. Chapter 1, Basic Mechanisms Underlying Seizures and Epilepsy. Available from: http://www.ncbi.nlm.nih.gov/books/NBK2510/. Accessed February, 2020

Brunklaus, A., Ellis, R., Reavey, E., Semsarian, C., & Zuberi, S. M. (2014). Genotype phenotype associations across the voltage-gated sodium channel family. J Med Genet, 51(10), 650-658. doi:10.1136/jmedgenet-2014-102608

Buffington, S. A., & Rasband, M. N. (2013). Na+ channel-dependent recruitment of Navbeta4 to axon initial segments and nodes of Ranvier. J Neurosci, 33(14), 6191-6202. doi:10.1523/jneurosci.4051-12.2013

Bunton-Stasyshyn, R. K. A., Wagnon, J. L., Wengert, E. R., Barker, B. S., Faulkner, A., Wagley, P. K., . . . Meisler, M. H. (2019). Prominent role of forebrain excitatory neurons in SCN8A encephalopathy. Brain, 142(2), 362-375. doi:10.1093/brain/awy324

Butler, K. M., da Silva, C., Alexander, J. J., Hegde, M., & Escayg, A. (2017). Diagnostic

Yield From 339 Epilepsy Patients Screened on a Clinical Gene Panel. Pediatr

Neurol, 77, 61-66. doi:10.1016/j.pediatrneurol.2017.09.003

Caldwell, J. H., Schaller, K. L., Lasher, R. S., Peles, E., & Levinson, S. R. (2000). Sodium

channel Na(v)1.6 is localized at nodes of ranvier, dendrites, and synapses. Proc

Natl Acad Sci U S A, 97(10), 5616-5620. doi:10.1073/pnas.090034797

Calhoun, J. D., Hawkins, N. A., Zachwieja, N. J., & Kearney, J. A. (2017). Cacna1g is a

genetic modifier of epilepsy in a mouse model of Dravet syndrome. Epilepsia,

58(8), e111-e115. doi:10.1111/epi.13811

Carvill, G. L., Heavin, S. B., Yendle, S. C., McMahon, J. M., O'Roak, B. J., Cook, J., . . .

Mefford, H. C. (2013). Targeted resequencing in epileptic encephalopathies

identifies de novo mutations in CHD2 and SYNGAP1. Nat Genet, 45(7), 825-830.

doi:10.1038/ng.2646

Castelli, L., Biella, G., Toselli, M., & Magistretti, J. (2007). Resurgent Na+ current in

pyramidal neurones of rat perirhinal cortex: axonal location of channels and

contribution to depolarizing drive during repetitive firing. J Physiol, 582(Pt 3),

1179-1193. doi:10.1113/jphysiol.2007.135350

Catterall, W. A., Goldin, A. L., & Waxman, S. G. (2005). International Union of

Pharmacology. XLVII. Nomenclature and structure-function relationships of

voltage-gated sodium channels. Pharmacol Rev, 57(4), 397-409.

doi:10.1124/pr.57.4.4

Chen, C., Calhoun, J. D., Zhang, Y., Lopez-Santiago, L., Zhou, N., Davis, T. H., . . . Isom, L.

L. (2012). Identification of the cysteine residue responsible for disulfide linkage

of Na+ channel alpha and beta2 subunits. J Biol Chem, 287(46), 39061-39069.

doi:10.1074/jbc.M112.397646

Chen, Y., Yu, F. H., Sharp, E. M., Beacham, D., Scheuer, T., & Catterall, W. A. (2008).

Functional properties and differential neuromodulation of Na(v)1.6 channels.

Mol Cell Neurosci, 38(4), 607-615. doi:10.1016/j.mcn.2008.05.009

Choi, J. S., Tyrrell, L., Waxman, S. G., & Dib-Hajj, S. D. (2004). Functional role of the C-

terminus of voltage-gated sodium channel Na(v)1.8. FEBS Lett, 572(1-3), 256-

260. doi:10.1016/j.febslet.2004.07.047

Clairfeuille, T., Cloake, A., Infield, D. T., Llongueras, J. P., Arthur, C. P., Li, Z. R., . . .

Payandeh, J. (2019). Structural basis of alpha-scorpion toxin action on Nav

channels. Science. doi:10.1126/science.aav8573

Cormier, J. W., Rivolta, I., Tateyama, M., Yang, A. S., & Kass, R. S. (2002). Secondary

structure of the human cardiac Na+ channel C terminus: evidence for a role of

helical structures in modulation of channel inactivation. J Biol Chem, 277(11),

9233-9241. doi:10.1074/jbc.M110204200

Cummins, T. R., Xia, Y., & Haddad, G. G. (1994). Functional properties of rat and human

neocortical voltage-sensitive sodium currents. J Neurophysiol, 71(3), 1052-1064.

doi:10.1152/jn.1994.71.3.1052

Davis, T. H., Chen, C., & Isom, L. L. (2004). Sodium channel beta1 subunits promote
neurite outgrowth in cerebellar granule neurons. J Biol Chem, 279(49), 51424-
51432. doi:10.1074/jbc.M410830200

De Rubeis, S., He, X., Goldberg, A. P., Poultney, C. S., Samocha, K., Cicek, A. E., . . .
Buxbaum, J. D. (2014). Synaptic, transcriptional and chromatin genes disrupted
in autism. Nature, 515(7526), 209-215. doi:10.1038/nature13772

Devinsky, O., Cross, J. H., Laux, L., Marsh, E., Miller, I., Nabbout, R., . . . Wright, S. (2017).
Trial of Cannabidiol for Drug-Resistant Seizures in the Dravet Syndrome. New
England Journal of Medicine, 376(21), 2011-2020. doi:10.1056/NEJMoa1611618

Devinsky, O., Marsh, E., Friedman, D., Thiele, E., Laux, L., Sullivan, J., . . . Cilio, M. R.
(2016). Cannabidiol in patients with treatment-resistant epilepsy: an open-label
interventional trial. The Lancet Neurology, 15(3), 270-278.
doi:https://doi.org/10.1016/S1474-4422(15)00379-8

Devinsky, O., Patel, A. D., Cross, J. H., Villanueva, V., Wirrell, E. C., Privitera, M., . . .
Zuberi, S. M. (2018). Effect of Cannabidiol on Drop Seizures in the Lennox-
Gastaut Syndrome. N Engl J Med, 378(20), 1888-1897.
doi:10.1056/NEJMoa1714631

Dossi, E., Blauwblomme, T., Nabbout, R., Huberfeld, G., & Rouach, N. (2014). Multi-
electrode array recordings of human epileptic postoperative cortical tissue. J Vis
Exp(92), e51870. doi:10.3791/51870

Drugs.com (2020) Briviact Approval History. Updated February 2020. Available from
https://www.drugs.com/history/briviact.html. Accessed February, 2020

Drugs.com (2019) Epidiolex (cannabidiol) FDA approval history. Updated January 2019.

Available from https://www.drugs.com/history/epidiolex.html. Accessed

February, 2020

DuBridge, R. B., Tang, P., Hsia, H. C., Leong, P. M., Miller, J. H., & Calos, M. P. (1987).

Analysis of mutation in human cells by using an Epstein-Barr virus shuttle

system. Mol Cell Biol, 7(1), 379-387.

During, M. J., & Spencer, D. D. (1993). Extracellular hippocampal glutamate and

spontaneous seizure in the conscious human brain. Lancet, 341(8861), 1607-

1610. doi:10.1016/0140-6736(93)90754-5

Espuny-Camacho, I., Michelsen, K. A., Gall, D., Linaro, D., Hasche, A., Bonnefont, J., . . .

Vanderhaeghen, P. (2013). Pyramidal neurons derived from human pluripotent

stem cells integrate efficiently into mouse brain circuits in vivo. Neuron, 77(3),

440-456. doi:10.1016/j.neuron.2012.12.011

Feyissa, A. (2019). Brivaracetam in the treatment of epilepsy: a review of clinical trial

data. Neuropsychiatr Dis Treat, Volume 15, 2587-2600.

doi:10.2147/NDT.S143548

Follwaczny, P., Schieweck, R., Riedemann, T., Demleitner, A., Straub, T., Klemm, A. H., . .

. Kiebler, M. A. (2017). Pumilio2-deficient mice show a predisposition for

epilepsy. Dis Model Mech, 10(11), 1333-1342. doi:10.1242/dmm.029678

French, J. A. (2007). Refractory epilepsy: clinical overview. Epilepsia, 48 Suppl 1, 3-7.

doi:10.1111/j.1528-1167.2007.00992.x

Gamal El-Din, T. M., Scheuer, T., & Catterall, W. A. (2014). Tracking S4 movement by gating pore currents in the bacterial sodium channel NaChBac. J Gen Physiol, 144(2), 147-157. doi:10.1085/jgp.201411210

Ghovanloo, M. R., Shuart, N. G., Mezeyova, J., Dean, R. A., Ruben, P. C., & Goodchild, S. J. (2018). Inhibitory effects of cannabidiol on voltage-dependent sodium currents. J Biol Chem. doi:10.1074/jbc.RA118.004929

Glaaser, I. W., Bankston, J. R., Liu, H., Tateyama, M., & Kass, R. S. (2006). A carboxyl-terminal hydrophobic interface is critical to sodium channel function. Relevance to inherited disorders. J Biol Chem, 281(33), 24015-24023. doi:10.1074/jbc.M605473200

Goldin, A. (2001). Resurgence of sodium research. Annual review of physiology, 63, 871-894. doi:10.1146/annurev.physiol.63.1.871

Gong, B., Rhodes, K. J., Bekele-Arcuri, Z., & Trimmer, J. S. (1999). Type I and type II Na+ channel α-subunit polypeptides exhibit distinct spatial and temporal patterning, and association with auxiliary subunits in rat brain. Journal of Comparative Neurology, 412(2), 342-352. doi:doi:10.1002/(SICI)1096-9861(19990920)412:2<342::AID-CNE11>3.0.CO;2-2

Gosselin-Badaroudine, P., Keller, D. I., Huang, H., Pouliot, V., Chatelier, A., Osswald, S., . . . Chahine, M. (2012). A proton leak current through the cardiac sodium channel is linked to mixed arrhythmia and the dilated cardiomyopathy phenotype. PLoS One, 7(5), e38331. doi:10.1371/journal.pone.0038331

Grieco, T. M., Malhotra, J. D., Chen, C., Isom, L. L., & Raman, I. M. (2005). Open-channel

block by the cytoplasmic tail of sodium channel beta4 as a mechanism for

resurgent sodium current. Neuron, 45(2), 233-244.

doi:10.1016/j.neuron.2004.12.035

Grieco, T. M., & Raman, I. M. (2004). Production of resurgent current in NaV1.6-null

Purkinje neurons by slowing sodium channel inactivation with beta-

pompilidotoxin. J Neurosci, 24(1), 35-42. doi:10.1523/jneurosci.3807-03.2004

Griffin, A., Hamling, K. R., Hong, S., Anvar, M., Lee, L. P., & Baraban, S. C. (2018).

Preclinical Animal Models for Dravet Syndrome: Seizure Phenotypes,

Comorbidities and Drug Screening. Front Pharmacol, 9(573).

doi:10.3389/fphar.2018.00573

Grone, B. P., Marchese, M., Hamling, K. R., Kumar, M. G., Krasniak, C. S., Sicca, F., . . .

Baraban, S. C. (2016). Epilepsy, Behavioral Abnormalities, and Physiological

Comorbidities in Syntaxin-Binding Protein 1 (STXBP1) Mutant Zebrafish. PLoS

One, 11(3), e0151148. doi:10.1371/journal.pone.0151148

Gullo, F., Manfredi, I., Lecchi, M., Casari, G., Wanke, E., & Becchetti, A. (2014). Multi-

electrode array study of neuronal cultures expressing nicotinic beta2-V287L

subunits, linked to autosomal dominant nocturnal frontal lobe epilepsy. An in

vitro model of spontaneous epilepsy. Front Neural Circuits, 8, 87.

doi:10.3389/fncir.2014.00087

Hargus, N. J., Merrick, E. C., Nigam, A., Kalmar, C. L., Baheti, A. R., Bertram, E. H., 3rd, &

Patel, M. K. (2011). Temporal lobe epilepsy induces intrinsic alterations in Na

channel gating in layer II medial entorhinal cortex neurons. Neurobiol Dis, 41(2), 361-376. doi:10.1016/j.nbd.2010.10.004

Hargus, N. J., Nigam, A., Bertram, E. H., 3rd, & Patel, M. K. (2013). Evidence for a role of Nav1.6 in facilitating increases in neuronal hyperexcitability during epileptogenesis. J Neurophysiol, 110(5), 1144-1157. doi:10.1152/jn.00383.2013

Hartshorne, R. P., & Catterall, W. A. (1981). Purification of the saxitoxin receptor of the sodium channel from rat brain. Proc Natl Acad Sci U S A, 78(7), 4620-4624. doi:10.1073/pnas.78.7.4620

Hartshorne, R. P., Messner, D. J., Coppersmith, J. C., & Catterall, W. A. (1982). The saxitoxin receptor of the sodium channel from rat brain. Evidence for two nonidentical beta subunits. J Biol Chem, 257(23), 13888-13891.

Hawkins, N. A., Calhoun, J. D., Huffman, A. M., & Kearney, J. A. (2019). Gene expression profiling in a mouse model of Dravet syndrome. Exp Neurol, 311, 247-256. doi:10.1016/j.expneurol.2018.10.010

Hawkins, N. A., & Kearney, J. A. (2016). Hlf is a genetic modifier of epilepsy caused by voltage-gated sodium channel mutations. Epilepsy Res, 119, 20-23. doi:10.1016/j.eplepsyres.2015.11.016

He, B., & Soderlund, D. M. (2010). Human embryonic kidney (HEK293) cells express endogenous voltage-gated sodium currents and Na v 1.7 sodium channels. Neurosci Lett, 469(2), 268-272. doi:10.1016/j.neulet.2009.12.012

Henderson, R., & Wang, J. H. (1972). Solubilization of a specific tetrodotoxin-binding

   component from garfish olfactory nerve membrane. Biochemistry, 11(24), 4565-

   4569. doi:10.1021/bi00774a022

Heron, S. E., Crossland, K. M., Andermann, E., Phillips, H. A., Hall, A. J., Bleasel, A., . . .

   Scheffer, I. E. (2002). Sodium-channel defects in benign familial neonatal-

   infantile seizures. Lancet, 360(9336), 851-852. doi:10.1016/s0140-

   6736(02)09968-3

Higashijima, S., Schaefer, M., & Fetcho, J. R. (2004). Neurotransmitter properties of

   spinal interneurons in embryonic and larval zebrafish. J Comp Neurol, 480(1), 19-

   37. doi:10.1002/cne.20279

Hill, A. J., Jones, N. A., Smith, I., Hill, C. L., Williams, C. M., Stephens, G. J., & Whalley, B.

   J. (2014). Voltage-gated sodium (NaV) channel blockade by plant cannabinoids

   does not confer anticonvulsant effects per se. Neurosci Lett, 566, 269-274.

   doi:10.1016/j.neulet.2014.03.013

Hodgkin, A. L., & Huxley, A. F. (1952). A quantitative description of membrane current

   and its application to conduction and excitation in nerve. J Physiol, 117(4), 500-

   544. doi:10.1113/jphysiol.1952.sp004764

Hodgkin, A. L., & Katz, B. (1949). The effect of sodium ions on the electrical activity of

   the giant axon of the squid. J Physiol, 108, 37-77.

Howell, K. B., McMahon, J. M., Carvill, G. L., Tambunan, D., Mackay, M. T., Rodriguez-

   Casero, V., . . . Scheffer, I. E. (2015). SCN2A encephalopathy: A major cause of

epilepsy of infancy with migrating focal seizures. Neurology, 85(11), 958-966.

doi:10.1212/wnl.0000000000001926

Hu, W., Tian, C., Li, T., Yang, M., Hou, H., & Shu, Y. (2009). Distinct contributions of

Na(v)1.6 and Na(v)1.2 in action potential initiation and backpropagation. Nat

Neurosci, 12(8), 996-1002. doi:10.1038/nn.2359

Huttner, I., Trivedi, G., Jacoby, A., Mann, S., Vandenberg, J., & Fatkin, D. (2013). A

Transgenic Zebrafish Model of a Human Cardiac Sodium Channel Mutation

Exhibits Bradycardia, Conduction-System Abnormalities and Early Death. J Mol

Cell Cardiol, 61. doi:10.1016/j.yjmcc.2013.06.005

Iossifov, I., O'Roak, B. J., Sanders, S. J., Ronemus, M., Krumm, N., Levy, D., . . . Wigler, M.

(2014). The contribution of de novo coding mutations to autism spectrum

disorder. Nature, 515(7526), 216-221. doi:10.1038/nature13908

Ito, M., Shirasaka, Y., Hirose, S., Sugawara, T., & Yamakawa, K. (2004). Seizure

phenotypes of a family with missense mutations in SCN2A. Pediatr Neurol, 31(2),

150-152. doi:10.1016/j.pediatrneurol.2004.02.013

Jarecki, B. W., Piekarz, A. D., Jackson, J. O., 2nd, & Cummins, T. R. (2010). Human

voltage-gated sodium channel mutations that cause inherited neuronal and

muscle channelopathies increase resurgent sodium currents. J Clin Invest,

120(1), 369-378. doi:10.1172/jci40801

Jiang, D., Gamal El-Din, T. M., Ing, C., Lu, P., Pomes, R., Zheng, N., & Catterall, W. A.

(2018). Structural basis for gating pore current in periodic paralysis. Nature,

557(7706), 590-594. doi:10.1038/s41586-018-0120-4

Johannesen, K. M., Miranda, M. J., Lerche, H., & Moller, R. S. (2016). Letter to the editor:

confirming neonatal seizure and late onset ataxia in SCN2A Ala263Val. J Neurol,

263(7), 1459-1460. doi:10.1007/s00415-016-8149-5

Jones, N. A., Hill, A. J., Smith, I., Bevan, S. A., Williams, C. M., Whalley, B. J., & Stephens,

G. J. (2010). Cannabidiol displays antiepileptiform and antiseizure properties in

vitro and in vivo. J Pharmacol Exp Ther, 332(2), 569-577.

doi:10.1124/jpet.109.159145

Jorge, B. S., Campbell, C. M., Miller, A. R., Rutter, E. D., Gurnett, C. A., Vanoye, C. G., . . .

Kearney, J. A. (2011). Voltage-gated potassium channel KCNV2 (Kv8.2)

contributes to epilepsy susceptibility. Proc Natl Acad Sci U S A, 108(13), 5443-

5448. doi:10.1073/pnas.1017539108

Kaczmarek, L. K. (2019). Loss of Na$_V$1.2-Dependent Backpropagating Action

Potentials in Dendrites Contributes to Autism and Intellectual Disability. Neuron,

103(4), 551-553. doi:10.1016/j.neuron.2019.07.032

Kamiya, K., Kaneda, M., Sugawara, T., Mazaki, E., Okamura, N., Montal, M., . . .

Yamakawa, K. (2004). A nonsense mutation of the sodium channel gene SCN2A

in a patient with intractable epilepsy and mental decline. J Neurosci, 24(11),

2690-2698. doi:10.1523/jneurosci.3089-03.2004

Kaplan, M. R., Cho, M. H., Ullian, E. M., Isom, L. L., Levinson, S. R., & Barres, B. A. (2001).

Differential control of clustering of the sodium channels Na(v)1.2 and Na(v)1.6 at

developing CNS nodes of Ranvier. Neuron, 30(1), 105-119. doi:10.1016/s0896-

6273(01)00266-5

Kaslin, J., & Panula, P. (2001). Comparative anatomy of the histaminergic and other

aminergic systems in zebrafish (Danio rerio). J Comp Neurol, 440(4), 342-377.

doi:10.1002/cne.1390

Kasteleijn-Nolst Trenite, D. G. A., DiVentura, B. D., Pollard, J. R., Krauss, G. L., Mizne, S.,

& French, J. A. (2019). Suppression of the photoparoxysmal response in

photosensitive epilepsy with cenobamate (YKP3089). Neurology, 93(6), e559-

e567. doi:10.1212/wnl.0000000000007894

Kearney, J. A., Plummer, N. W., Smith, M. R., Kapur, J., Cummins, T. R., Waxman, S. G., . .

. Meisler, M. H. (2001). A gain-of-function mutation in the sodium channel gene

Scn2a results in seizures and behavioral abnormalities. Neuroscience, 102(2),

307-317. doi:10.1016/s0306-4522(00)00479-6

Ketelaars, S. O., Gorter, J. A., van Vliet, E. A., Lopes da Silva, F. H., & Wadman, W. J.

(2001). Sodium currents in isolated rat CA1 pyramidal and dentate granule

neurones in the post-status epilepticus model of epilepsy. Neuroscience, 105(1),

109-120. doi:10.1016/s0306-4522(01)00176-2

Keynes, R. D., & Lewis, P. R. (1951). The sodium and potassium content of cephalopod

nerve fibres. J Physiol, 114, 151-182.

Khaliq, Z. M., Gouwens, N. W., & Raman, I. M. (2003). The contribution of resurgent

sodium current to high-frequency firing in Purkinje neurons: an experimental

and modeling study. J Neurosci, 23(12), 4899-4912.

Kim, J. H., Kushmerick, C., & von Gersdorff, H. (2010). Presynaptic resurgent Na+

currents sculpt the action potential waveform and increase firing reliability at a

CNS nerve terminal. J Neurosci, 30(46), 15479-15490.

doi:10.1523/jneurosci.3982-10.2010

Kobayashi, Y., Tohyama, J., Kato, M., Akasaka, N., Magara, S., Kawashima, H., . . .

Matsumoto, N. (2016). High prevalence of genetic alterations in early-onset

epileptic encephalopathies associated with infantile movement disorders. Brain

Dev, 38(3), 285-292. doi:10.1016/j.braindev.2015.09.011

Koltun, D. O., Parkhill, E. Q., Elzein, E., Kobayashi, T., Notte, G. T., Kalla, R., . . . Zablocki, J.

A. (2016). Discovery of triazolopyridine GS-458967, a late sodium current

inhibitor (Late INai) of the cardiac NaV 1.5 channel with improved efficacy and

potency relative to ranolazine. Bioorganic & Medicinal Chemistry Letters, 26(13),

3202-3206. doi:https://doi.org/10.1016/j.bmcl.2016.03.101

Krauss, G. L., Klein, P., Brandt, C., Lee, S. K., Milanov, I., Milovanovic, M., . . . Kamin, M.

(2020). Safety and efficacy of adjunctive cenobamate (YKP3089) in patients with

uncontrolled focal seizures: a multicentre, double-blind, randomised, placebo-

controlled, dose-response trial. Lancet Neurol, 19(1), 38-48. doi:10.1016/s1474-

4422(19)30399-0

Kuczewski, N., Porcher, C., Ferrand, N., Fiorentino, H., Pellegrino, C., Kolarow, R., . . .

Gaiarsa, J. L. (2008). Backpropagating action potentials trigger dendritic release

of BDNF during spontaneous network activity. J Neurosci, 28(27), 7013-7023.

doi:10.1523/jneurosci.1673-08.2008

Kuczewski, N., Porcher, C., Lessmann, V., Medina, I., & Gaiarsa, J. L. (2008). Back-propagating action potential: A key contributor in activity-dependent dendritic release of BDNF. Commun Integr Biol, 1(2), 153-155. doi:10.4161/cib.1.2.7058

Laezza, F., Lampert, A., Kozel, M. A., Gerber, B. R., Rush, A. M., Nerbonne, J. M., . . . Ornitz, D. M. (2009). FGF14 N-terminal splice variants differentially modulate Nav1.2 and Nav1.6-encoded sodium channels. Molecular and cellular neurosciences, 42(2), 90-101. doi:10.1016/j.mcn.2009.05.007

Lamar, T., Vanoye, C. G., Calhoun, J., Wong, J. C., Dutton, S. B. B., Jorge, B. S., . . . Kearney, J. A. (2017). SCN3A deficiency associated with increased seizure susceptibility. Neurobiol Dis, 102, 38-48. doi:10.1016/j.nbd.2017.02.006

Lauxmann, S., Boutry-Kryza, N., Rivier, C., Mueller, S., Hedrich, U. B., Maljevic, S., . . . Lesca, G. (2013). An SCN2A mutation in a family with infantile seizures from Madagascar reveals an increased subthreshold Na(+) current. Epilepsia, 54(9), e117-121. doi:10.1111/epi.12241

Laxer, K. D., Trinka, E., Hirsch, L. J., Cendes, F., Langfitt, J., Delanty, N., . . . Benbadis, S. R. (2014). The consequences of refractory epilepsy and its treatment. Epilepsy & Behavior, 37, 59-70. doi:https://doi.org/10.1016/j.yebeh.2014.05.031

Lee, A., & Goldin, A. L. (2008). Role of the amino and carboxy termini in isoform-specific sodium channel variation. J Physiol, 586(16), 3917-3926. doi:10.1113/jphysiol.2008.156299

Levinson, S. R., & Ellory, J. C. (1973). Molecular size of the tetrodotoxin binding site

estimated by irradiation inactivation. Nat New Biol, 245(143), 122-123.

doi:10.1038/newbio245122a0

Lewis, A. H., & Raman, I. M. (2011). Cross-species conservation of open-channel block by

Na channel beta4 peptides reveals structural features required for resurgent Na

current. J Neurosci, 31(32), 11527-11536. doi:10.1523/jneurosci.1428-11.2011

Lewis, A. H., & Raman, I. M. (2014). Resurgent current of voltage-gated Na(+) channels. J

Physiol, 592(22), 4825-4838. doi:10.1113/jphysiol.2014.277582

Li, X., Zhang, J., Wu, X., Yan, H., Zhang, Y., He, R. H., . . . Liu, J. (2016). Polymorphisms of

ABAT, SCN2A and ALDH5A1 may affect valproic acid responses in the treatment

of epilepsy in Chinese. Pharmacogenomics, 17(18), 2007-2014. doi:10.2217/pgs-

2016-0093

Liao, Y., Anttonen, A. K., Liukkonen, E., Gaily, E., Maljevic, S., Schubert, S., . . . Lehesjoki,

A. E. (2010). SCN2A mutation associated with neonatal epilepsy, late-onset

episodic ataxia, myoclonus, and pain. Neurology, 75(16), 1454-1458.

doi:10.1212/WNL.0b013e3181f8812e

Liao, Y., Deprez, L., Maljevic, S., Pitsch, J., Claes, L., Hristova, D., . . . Lerche, H. (2010).

Molecular correlates of age-dependent seizures in an inherited neonatal-

infantile epilepsy. Brain, 133(Pt 5), 1403-1414. doi:10.1093/brain/awq057

Lindy, A. S., Stosser, M. B., Butler, E., Downtain-Pickersgill, C., Shanmugham, A.,

Retterer, K., . . . McKnight, D. A. (2018). Diagnostic outcomes for genetic testing

of 70 genes in 8565 patients with epilepsy and neurodevelopmental disorders.

   Epilepsia, 59(5), 1062-1071. doi:10.1111/epi.14074

Löscher, W., Klitgaard, H., Twyman, R. E., & Schmidt, D. (2013). New avenues for anti-

   epileptic drug discovery and development. Nat Rev Drug Discov, 12(10), 757-776.

   doi:10.1038/nrd4126

Lossin, C., Shi, X., Rogawski, M. A., & Hirose, S. (2012). Compromised function in the

   Na(v)1.2 Dravet syndrome mutation R1312T. Neurobiol Dis, 47(3), 378-384.

   doi:10.1016/j.nbd.2012.05.017

Lou, J.-Y., Laezza, F., Gerber, B. R., Xiao, M., Yamada, K. A., Hartmann, H., . . . Ornitz, D.

   M. (2005). Fibroblast growth factor 14 is an intracellular modulator of voltage-

   gated sodium channels. J Physiol, 569(Pt 1), 179-193.

   doi:10.1113/jphysiol.2005.097220

Männikkö, R., Shenkarev, Z. O., Thor, M. G., Berkut, A. A., Myshkin, M. Y., Paramonov, A.

   S., . . . Vassilevski, A. A. (2018). Spider toxin inhibits gating pore currents

   underlying periodic paralysis. Proceedings of the National Academy of Sciences,

   115(17), 4495-4500. doi:10.1073/pnas.1720185115

Mantegazza, M., Curia, G., Biagini, G., Ragsdale, D. S., & Avoli, M. (2010). Voltage-gated

   sodium channels as therapeutic targets in epilepsy and other neurological

   disorders. Lancet Neurol, 9(4), 413-424. doi:10.1016/s1474-4422(10)70059-4

Mantegazza, M., Yu, F. H., Catterall, W. A., & Scheuer, T. (2001). Role of the C-terminal

   domain in inactivation of brain and cardiac sodium channels. Proc Natl Acad Sci

   U S A, 98(26), 15348-15353. doi:10.1073/pnas.211563298

Mao, K., You, C., Lei, D., & Zhang, H. (2015). High dosage of cannabidiol (CBD) alleviates

 pentylenetetrazole-induced epilepsy in rats by exerting an anticonvulsive effect.

 Int J Clin Exp Med, 8(6), 8820-8827.

Mariani, J., Simonini, M. V., Palejev, D., Tomasini, L., Coppola, G., Szekely, A. M., . . .

 Vaccarino, F. M. (2012). Modeling human cortical dMevelopment in vitro using

 induced pluripotent stem cells. Proc Natl Acad Sci U S A, 109(31), 12770-12775.

 doi:10.1073/pnas.1202944109

Mason ER, Wu F, Patel RR, Xiao Y, Cannon SC, and Cummins, TR. (2019). Resurgent and

 Gating Pore Currents Induced by de novo SCN2A Epilepsy Mutations. *eNeuro*

 6(5). doi: 10.1523/eneuro.0141-19.2019

Mason ER, and Cummins, TR. (2020). Differential inhibition of human Nav1.2 resurgent

 and persistent sodium currents by cannabidiol and GS967. *International Journal*

 of Molecular Sciences. doi: 10.3390/ijms21072454

McLean, D. L., & Fetcho, J. R. (2004). Ontogeny and innervation patterns of

 dopaminergic, noradrenergic, and serotonergic neurons in larval zebrafish. J

 Comp Neurol, 480(1), 38-56. doi:10.1002/cne.20280

Mercer, J. N., Chan, C. S., Tkatch, T., Held, J., & Surmeier, D. J. (2007). Nav1.6 Sodium

 Channels Are Critical to Pacemaking and Fast Spiking in Globus Pallidus Neurons.

 The Journal of Neuroscience, 27(49), 13552-13566. doi:10.1523/jneurosci.3430-

 07.2007

Mercimek-Mahmutoglu, S., Patel, J., Cordeiro, D., Hewson, S., Callen, D., Donner, E. J., . . . Snead, O. C., 3rd. (2015). Diagnostic yield of genetic testing in epileptic encephalopathy in childhood. Epilepsia, 56(5), 707-716. doi:10.1111/epi.12954

Mi, W., Rybalchenko, V., & Cannon, S. C. (2014). Disrupted coupling of gating charge displacement to Na+ current activation for DIIS4 mutations in hypokalemic periodic paralysis. J Gen Physiol, 144(2), 137-145. doi:10.1085/jgp.201411199

Miller, A. R., Hawkins, N. A., McCollom, C. E., & Kearney, J. A. (2014). Mapping genetic modifiers of survival in a mouse model of Dravet syndrome. Genes Brain Behav, 13(2), 163-172. doi:10.1111/gbb.12099

Misra, S. N., Kahlig, K. M., & George, A. L., Jr. (2008). Impaired NaV1.2 function and reduced cell surface expression in benign familial neonatal-infantile seizures. Epilepsia, 49(9), 1535-1545. doi:10.1111/j.1528-1167.2008.01619.x

Miyazaki, H., Oyama, F., Wong, H. K., Kaneko, K., Sakurai, T., Tamaoka, A., & Nukina, N. (2007). BACE1 modulates filopodia-like protrusions induced by sodium channel beta4 subunit. Biochem Biophys Res Commun, 361(1), 43-48. doi:10.1016/j.bbrc.2007.06.170

Moller, R. S., Larsen, L. H., Johannesen, K. M., Talvik, I., Talvik, T., Vaher, U., . . . Dahl, H. A. (2016). Gene Panel Testing in Epileptic Encephalopathies and Familial Epilepsies. Mol Syndromol, 7(4), 210-219. doi:10.1159/000448369

Moreau, A., Gosselin-Badaroudine, P., Delemotte, L., Klein, M. L., & Chahine, M. (2015). Gating pore currents are defects in common with two Nav1.5 mutations in

patients with mixed arrhythmias and dilated cardiomyopathy. J Gen Physiol, 145(2), 93-106. doi:10.1085/jgp.201411304

Moshe, S. L., Perucca, E., Ryvlin, P., & Tomson, T. (2015). Epilepsy: new advances. Lancet, 385(9971), 884-898. doi:10.1016/s0140-6736(14)60456-6

Motoike, H. K., Liu, H., Glaaser, I. W., Yang, A. S., Tateyama, M., & Kass, R. S. (2004). The Na+ channel inactivation gate is a molecular complex: a novel role of the COOH-terminal domain. J Gen Physiol, 123(2), 155-165. doi:10.1085/jgp.200308929

Mueller, T., Vernier, P., & Wullimann, M. F. (2006). A phylotypic stage in vertebrate brain development: GABA cell patterns in zebrafish compared with mouse. J Comp Neurol, 494(4), 620-634. doi:10.1002/cne.20824

Nakamura, K., Kato, M., Osaka, H., Yamashita, S., Nakagawa, E., Haginoya, K., . . . Saitsu, H. (2013). Clinical spectrum of SCN2A mutations expanding to Ohtahara syndrome. Neurology, 81(11), 992-998. doi:10.1212/WNL.0b013e3182a43e57

Nakamura, M., Cho, J. H., Shin, H., & Jang, I. S. (2019). Effects of cenobamate (YKP3089), a newly developed anti-epileptic drug, on voltage-gated sodium channels in rat hippocampal CA3 neurons. Eur J Pharmacol, 855, 175-182. doi:10.1016/j.ejphar.2019.05.007

Nguyen, H. M., & Goldin, A. L. (2010). Sodium Channel Carboxyl-terminal Residue Regulates Fast Inactivation. J Biol Chem, 285(12), 9077-9089. doi:10.1074/jbc.M109.054940

Nicita, F., De Liso, P., Danti, F. R., Papetti, L., Ursitti, F., Castronovo, A., . . . Spalice, A. (2012). The genetics of monogenic idiopathic epilepsies and epileptic encephalopathies. Seizure, 21(1), 3-11. doi:10.1016/j.seizure.2011.08.007

Niespodziany, I., Andre, V. M., Leclere, N., Hanon, E., Ghisdal, P., & Wolff, C. (2015). Brivaracetam differentially affects voltage-gated sodium currents without impairing sustained repetitive firing in neurons. CNS Neurosci Ther, 21(3), 241-251. doi:10.1111/cns.12347

Noda, M., Ikeda, T., Kayano, T., Suzuki, H., Takeshima, H., Kurasaki, M., . . . Numa, S. (1986)a. Existence of distinct sodium channel messenger RNAs in rat brain. Nature, 320(6058), 188-192. doi:10.1038/320188a0

Noda, M., Ikeda, T., Suzuki, H., Takeshima, H., Takahashi, T., Kuno, M., & Numa, S. (1986)b. Expression of functional sodium channels from cloned cDNA. Nature, 322(6082), 826-828. doi:10.1038/322826a0

Noda, M., Shimizu, S., Tanabe, T., Takai, T., Kayano, T., Ikeda, T., . . . et al. (1984). Primary structure of Electrophorus electricus sodium channel deduced from cDNA sequence. Nature, 312(5990), 121-127. doi:10.1038/312121a0

Noebels, J. L. (2019). Predicting the impact of sodium channel mutations in human brain disease. Epilepsia, 60 Suppl 3(Suppl 3), S8-S16. doi:10.1111/epi.14724

Novak, A. E., Taylor, A. D., Pineda, R. H., Lasda, E. L., Wright, M. A., & Ribera, A. B. (2006). Embryonic and larval expression of zebrafish voltage-gated sodium channel α-subunit genes. Developmental Dynamics, 235(7), 1962-1973. doi:10.1002/dvdy.20811

Ogiwara, I., Ito, K., Sawaishi, Y., Osaka, H., Mazaki, E., Inoue, I., . . . Yamakawa, K. (2009).

De novo mutations of voltage-gated sodium channel alphaII gene SCN2A in

intractable epilepsies. Neurology, 73(13), 1046-1053.

doi:10.1212/WNL.0b013e3181b9cebc

Ottolini, M., Barker, B. S., Gaykema, R. P., Meisler, M. H., & Patel, M. K. (2017). Aberrant

Sodium Channel Currents and Hyperexcitability of Medial Entorhinal Cortex

Neurons in a Mouse Model of SCN8A Encephalopathy. J Neurosci, 37(32), 7643-

7655. doi:10.1523/jneurosci.2709-16.2017

Parrini, E., Marini, C., Mei, D., Galuppi, A., Cellini, E., Pucatti, D., . . . Guerrini, R. (2017).

Diagnostic Targeted Resequencing in 349 Patients with Drug-Resistant Pediatric

Epilepsies Identifies Causative Mutations in 30 Different Genes. Hum Mutat,

38(2), 216-225. doi:10.1002/humu.23149

Patel, R. R., Barbosa, C., Brustovetsky, T., Brustovetsky, N., & Cummins, T. R. (2016).

Aberrant epilepsy-associated mutant Nav1.6 sodium channel activity can be

targeted with cannabidiol. Brain, 139(Pt 8), 2164-2181.

doi:10.1093/brain/aww129

Patel, R. R., Barbosa, C., Xiao, Y., & Cummins, T. R. (2015). Human Nav1.6 Channels

Generate Larger Resurgent Currents than Human Nav1.1 Channels, but the

Navbeta4 Peptide Does Not Protect Either Isoform from Use-Dependent

Reduction. PLoS One, 10(7), e0133485. doi:10.1371/journal.pone.0133485

Patton, D. E., Isom, L. L., Catterall, W. A., & Goldin, A. L. (1994). The adult rat brain beta 1 subunit modifies activation and inactivation gating of multiple sodium channel alpha subunits. J Biol Chem, 269(26), 17649-17655.

Pena, I. A., Roussel, Y., Daniel, K., Mongeon, K., Johnstone, D., Weinschutz Mendes, H., . . . MacKenzie, A. (2017). Pyridoxine-Dependent Epilepsy in Zebrafish Caused by Aldh7a1 Deficiency. Genetics, 207(4), 1501-1518. doi:10.1534/genetics.117.300137

Petrou, S., Li, M., Jancovsk, N., Jafar-nahad, P., Burbano, L., Nemiroff, A., Dalby, K., Maljevic, S., Reid, C., and Rigo, F. "Antisense oligonucleotide therapy for SCN2A gain-of-function epilepsies." Annual Meeting of the American Epilepsy Society, New Orleans, LA, 30 Nov – 4 Dec 2018.

Press, C. A., Knupp, K. G., & Chapman, K. E. (2015). Parental reporting of response to oral cannabis extracts for treatment of refractory epilepsy. Epilepsy & Behavior, 45, 49-52. doi:https://doi.org/10.1016/j.yebeh.2015.02.043

Raman, I. M., & Bean, B. P. (1997). Resurgent sodium current and action potential formation in dissociated cerebellar Purkinje neurons. J Neurosci, 17(12), 4517-4526.

Rogawski, M. A., & Loscher, W. (2004). The neurobiology of antiepileptic drugs. Nat Rev Neurosci, 5(7), 553-564. doi:10.1038/nrn1430

Rothenberg, M. A. (1950). Studies on permeability in relation to nerve function, ionic movements across exonal membranes. Biochim Biophys Acta, 4(1-3), 96-114. doi:10.1016/0006-3002(50)90012-6

Royeck, M., Kelly, T., Opitz, T., Otte, D. M., Rennhack, A., Woitecki, A., . . . Beck, H. (2015). Downregulation of Spermine Augments Dendritic Persistent Sodium Currents and Synaptic Integration after Status Epilepticus. J Neurosci, 35(46), 15240-15253. doi:10.1523/jneurosci.0493-15.2015

Rusconi, R., Scalmani, P., Cassulini, R. R., Giunti, G., Gambardella, A., Franceschetti, S., . . . Mantegazza, M. (2007). Modulatory proteins can rescue a trafficking defective epileptogenic Nav1.1 Na+ channel mutant. J Neurosci, 27(41), 11037-11046. doi:10.1523/jneurosci.3515-07.2007

Rush, A. M., Dib-Hajj, S. D., & Waxman, S. G. (2005). Electrophysiological properties of two axonal sodium channels, Nav1.2 and Nav1.6, expressed in mouse spinal sensory neurones. J Physiol, 564(Pt 3), 803-815. doi:10.1113/jphysiol.2005.083089

Samanta, D., & Ramakrishnaiah, R. (2015). De novo R853Q mutation of SCN2A gene and West syndrome. Acta Neurol Belg. doi:10.1007/s13760-015-0454-8

Sato, C., Sato, M., Iwasaki, A., Doi, T., & Engel, A. (1998). The sodium channel has four domains surrounding a central pore. J Struct Biol, 121(3), 314-325. doi:10.1006/jsbi.1998.3990

Satou, C., Kimura, Y., Hirata, H., Suster, M. L., Kawakami, K., & Higashijima, S. (2013). Transgenic tools to characterize neuronal properties of discrete populations of zebrafish neurons. Development, 140(18), 3927-3931. doi:10.1242/dev.099531

Savage, T. E., Sourbron, J., Bruno, P. L., Skirvin, L. A., Wolper, E. S., Anagnos, C. J., & Thiele, E. A. (2019). Efficacy of cannabidiol in subjects with refractory epilepsy

relative to concomitant use of clobazam. Epilepsy Res, 160, 106263.

doi:10.1016/j.eplepsyres.2019.106263

Sawaishi, Y., Yano, T., Enoki, M., & Takada, G. (2002). Lidocaine-dependent early

infantile status epilepticus with highly suppressed EEG. Epilepsia, 43(2), 201-204.

Scalmani, P., Rusconi, R., Armatura, E., Zara, F., Avanzini, G., Franceschetti, S., &

Mantegazza, M. (2006). Effects in neocortical neurons of mutations of the

Na(v)1.2 Na+ channel causing benign familial neonatal-infantile seizures. J

Neurosci, 26(40), 10100-10109. doi:10.1523/jneurosci.2476-06.2006

Schoonheim, P. J., Arrenberg, A. B., Del Bene, F., & Baier, H. (2010). Optogenetic

Localization and Genetic Perturbation of Saccade-Generating Neurons in

Zebrafish. The Journal of Neuroscience, 30(20), 7111-7120.

doi:10.1523/jneurosci.5193-09.2010

Schwarz, N., Hahn, A., Bast, T., Muller, S., Loffler, H., Maljevic, S., . . . Hedrich, U. B.

(2016). Mutations in the sodium channel gene SCN2A cause neonatal epilepsy

with late-onset episodic ataxia. J Neurol, 263(2), 334-343. doi:10.1007/s00415-

015-7984-0

Shao, H., Yang, Y., Qi, A. P., Hong, P., Zhu, G. X., Cao, X. Y., . . . Zhu, Z. R. (2017).

Gastrodin Reduces the Severity of Status Epilepticus in the Rat Pilocarpine Model

of Temporal Lobe Epilepsy by Inhibiting Nav1.6 Sodium Currents. Neurochem

Res, 42(2), 360-374. doi:10.1007/s11064-016-2079-6

Sharma R, Song WS, Nakamura M, et al. Effects of cenobamate on GABA-A receptor

modulation. *AES 2018 Annual Meeting Abstract Database*. Abstract 3.306.

https://www.aesnet.org/meetings_events/annual_meeting_abstracts/view/500
273. Accessed January 16, 2020

Shi, X., Yasumoto, S., Kurahashi, H., Nakagawa, E., Fukasawa, T., Uchiya, S., & Hirose, S.
(2012). Clinical spectrum of SCN2A mutations. Brain Dev, 34(7), 541-545.
doi:10.1016/j.braindev.2011.09.016

Shi, X., Yasumoto, S., Nakagawa, E., Fukasawa, T., Uchiya, S., & Hirose, S. (2009).
Missense mutation of the sodium channel gene SCN2A causes Dravet syndrome.
Brain Dev, 31(10), 758-762. doi:10.1016/j.braindev.2009.08.009

Shin, W., Kweon, H., Kang, R., Kim, D., Kim, K., Kang, M., . . . Kim, E. (2019). Scn2a
Haploinsufficiency in Mice Suppresses Hippocampal Neuronal Excitability,
Excitatory Synaptic Drive, and Long-Term Potentiation, and Spatial Learning and
Memory. Frontiers in Molecular Neuroscience, 12(145).
doi:10.3389/fnmol.2019.00145

Sigworth, F. J. (1980). The variance of sodium current fluctuations at the node of
Ranvier. J Physiol, 307, 97-129. doi:10.1113/jphysiol.1980.sp013426

Singh, D., Lau, M., Ayers, T., Singh, Y., Akingbola, O., Barbiero, L., & Nelson, S. (2016). De
Novo Heterogeneous Mutations in SCN2A and GRIN2A Genes and Seizures With
Ictal Vocalizations. Clin Pediatr (Phila), 55(9), 867-870.
doi:10.1177/0009922815601060

Sirven, JI MD, TA Pedley, & JL Wilterdink (2016) Evaluation and management of drug-
resistant epilepsy. Available at: http://www.uptodate.com/contents/evaluation-
and-management-of-drug-resistant-epilepsy. Accessed February, 2020

Smith, R. S., Kenny, C. J., Ganesh, V., Jang, A., Borges-Monroy, R., Partlow, J. N., . . .

      Lehtinen, M. K. (2018). Sodium Channel SCN3A (NaV1.3) Regulation of Human

      Cerebral Cortical Folding and Oral Motor Development. Neuron, 99(5), 905-

      913.e907. doi:10.1016/j.neuron.2018.07.052

Sokolov, S., Scheuer, T., & Catterall, W. A. (2005). Ion permeation through a voltage-

      sensitive gating pore in brain sodium channels having voltage sensor mutations.

      Neuron, 47(2), 183-189. doi:10.1016/j.neuron.2005.06.012

Sokolov, S., Scheuer, T., & Catterall, W. A. (2007). Gating pore current in an inherited ion

      channelopathy. Nature, 446(7131), 76-78. doi:10.1038/nature05598

Sokolov, S., Scheuer, T., & Catterall, W. A. (2008). Depolarization-activated gating pore

      current conducted by mutant sodium channels in potassium-sensitive

      normokalemic periodic paralysis. Proc Natl Acad Sci U S A, 105(50), 19980-19985.

      doi:10.1073/pnas.0810562105

Sokolov, S., Scheuer, T., & Catterall, W. A. (2010). Ion permeation and block of the

      gating pore in the voltage sensor of NaV1.4 channels with hypokalemic periodic

      paralysis mutations. J Gen Physiol, 136(2), 225-236. doi:10.1085/jgp.201010414

Sourbron, J., Partoens, M., Scheldeman, C., Zhang, Y., Lagae, L., & de Witte, P. (2019).

      Drug repurposing for Dravet syndrome in scn1Lab−/− mutant zebrafish.

      Epilepsia, 60(2), e8-e13. doi:10.1111/epi.14647

Spratt, P. W. E., Ben-Shalom, R., Keeshen, C. M., Burke, K. J., Clarkson, R. L., Sanders, S.

      J., & Bender, K. J. (2019). The Autism-Associated Gene Scn2a Contributes to

Dendritic Excitability and Synaptic Function in the Prefrontal Cortex. Neuron,

103(4), 673-685.e675. doi:https://doi.org/10.1016/j.neuron.2019.05.037

Srinivasan, J., Schachner, M., & Catterall, W. A. (1998). Interaction of voltage-gated

sodium channels with the extracellular matrix molecules tenascin-C and

tenascin-R. Proc Natl Acad Sci U S A, 95(26), 15753-15757.

doi:10.1073/pnas.95.26.15753

Struyk, A. F., & Cannon, S. C. (2007). A Na+ channel mutation linked to hypokalemic

periodic paralysis exposes a proton-selective gating pore. J Gen Physiol, 130(1),

11-20. doi:10.1085/jgp.200709755

Stühmer, W., Conti, F., Suzuki, H., Wang, X., Noda, M., Yahagi, N., . . . Numa, S. (1989).

Structural parts involved in activation and inactivation of the sodium channel.

Nature, 339(6226), 597-603. doi:10.1038/339597a0

Sugawara, T., Tsurubuchi, Y., Agarwala, K. L., Ito, M., Fukuma, G., Mazaki-Miyazaki, E., . .

. Yamakawa, K. (2001). A missense mutation of the Na+ channel alpha II subunit

gene Na(v)1.2 in a patient with febrile and afebrile seizures causes channel

dysfunction. Proc Natl Acad Sci U S A, 98(11), 6384-6389.

doi:10.1073/pnas.111065098

Szaflarski, J. P., Bebin, E. M., Comi, A. M., Patel, A. D., Joshi, C., Checketts, D., . . . group,

C. E. s. (2018). Long-term safety and treatment effects of cannabidiol in children

and adults with treatment-resistant epilepsies: Expanded access program results.

Epilepsia, 59(8), 1540-1548. doi:10.1111/epi.14477

Szaflarski, J. P., Bebin, E. M., Cutter, G., DeWolfe, J., Dure, L. S., Gaston, T. E., . . . Ver

Hoef, L. W. (2018). Cannabidiol improves frequency and severity of seizures and

reduces adverse events in an open-label add-on prospective study. Epilepsy &

Behavior, 87, 131-136. doi:https://doi.org/10.1016/j.yebeh.2018.07.020

Tanaka, B. S., Zhao, P., Dib-Hajj, F. B., Morisset, V., Tate, S., Waxman, S. G., & Dib-Hajj, S.

D. (2016). A gain-of-function mutation in Nav1.6 in a case of trigeminal neuralgia.

Mol Med, 22, 338-348. doi:10.2119/molmed.2016.00131

Theile, J. W., Jarecki, B. W., Piekarz, A. D., & Cummins, T. R. (2011). Nav1.7 mutations

associated with paroxysmal extreme pain disorder, but not erythromelalgia,

enhance Navbeta4 peptide-mediated resurgent sodium currents. J Physiol,

589(Pt 3), 597-608. doi:10.1113/jphysiol.2010.200915

Thiele, E. A., Marsh, E. D., French, J. A., Mazurkiewicz-Beldzinska, M., Benbadis, S. R.,

Joshi, C., . . . Sommerville, K. (2018). Cannabidiol in patients with seizures

associated with Lennox-Gastaut syndrome (GWPCARE4): a randomised, double-

blind, placebo-controlled phase 3 trial. Lancet, 391(10125), 1085-1096.

doi:10.1016/s0140-6736(18)30136-3

Tian, C., Wang, K., Ke, W., Guo, H., & Shu, Y. (2014). Molecular identity of axonal sodium

channels in human cortical pyramidal cells. Front Cell Neurosci, 8, 297.

doi:10.3389/fncel.2014.00297

Tidball, A. M., & Parent, J. M. (2016). Concise Review: Exciting Cells: Modeling Genetic

Epilepsies with Patient-Derived Induced Pluripotent Stem Cells. Stem Cells, 34(1),

27-33. doi:10.1002/stem.2203

Touma, M., Joshi, M., Connolly, M. C., Grant, P. E., Hansen, A. R., Khwaja, O., . . .

      Agrawal, P. B. (2013). Whole genome sequencing identifies SCN2A mutation in

      monozygotic twins with Ohtahara syndrome and unique neuropathologic

      findings. Epilepsia, 54(5), e81-85. doi:10.1111/epi.12137

Trimmer, J. S., & Rhodes, K. J. (2004). Localization of voltage-gated ion channels in

      mammalian brain. Annu Rev Physiol, 66, 477-519.

      doi:10.1146/annurev.physiol.66.032102.113328

Trump, N., McTague, A., Brittain, H., Papandreou, A., Meyer, E., Ngoh, A., . . . Scott, R. H.

      (2016). Improving diagnosis and broadening the phenotypes in early-onset

      seizure and severe developmental delay disorders through gene panel analysis. J

      Med Genet, 53(5), 310-317. doi:10.1136/jmedgenet-2015-103263

U.S. Food and Drug Administration. Available online: https://www.fda.gov/news-

      events/press-announcements/fda-approves-first-drug-comprised-active-

      ingredient-derived-marijuana-treat-rare-severe-forms (accessed Feb 2020).

van Drongelen, W., Koch, H., Elsen, F. P., Lee, H. C., Mrejeru, A., Doren, E., . . . Ramirez, J.

      M. (2006). Role of persistent sodium current in bursting activity of mouse

      neocortical networks in vitro. J Neurophysiol, 96(5), 2564-2577.

      doi:10.1152/jn.00446.2006

Vreugdenhil, M., Hoogland, G., van Veelen, C. W., & Wadman, W. J. (2004). Persistent

      sodium current in subicular neurons isolated from patients with temporal lobe

      epilepsy. Eur J Neurosci, 19(10), 2769-2778. doi:10.1111/j.1460-

      9568.2004.03400.x

Wagnon, J. L., Barker, B. S., Hounshell, J. A., Haaxma, C. A., Shealy, A., Moss, T., . . .

    Meisler, M. H. (2016). Pathogenic mechanism of recurrent mutations of SCN8A in

    epileptic encephalopathy. Annals of Clinical and Translational Neurology, 3(2),

    114-123. doi:doi:10.1002/acn3.276

Wagnon, J. L., Korn, M. J., Parent, R., Tarpey, T. A., Jones, J. M., Hammer, M. F., . . .

    Meisler, M. H. (2015). Convulsive seizures and SUDEP in a mouse model of

    SCN8A epileptic encephalopathy. Hum Mol Genet, 24(2), 506-515.

    doi:10.1093/hmg/ddu470

Wallace, R. H., Wang, D. W., Singh, R., Scheffer, I. E., George, A. L., Jr., Phillips, H. A., . . .

    Mulley, J. C. (1998). Febrile seizures and generalized epilepsy associated with a

    mutation in the Na+-channel beta1 subunit gene SCN1B. Nat Genet, 19(4), 366-

    370. doi:10.1038/1252

Wang, G. K., Edrich, T., & Wang, S. Y. (2006). Time-dependent block and resurgent tail

    currents induced by mouse beta4(154-167) peptide in cardiac Na+ channels. J

    Gen Physiol, 127(3), 277-289. doi:10.1085/jgp.200509399

Wang, Q., Bardgett, M. E., Wong, M., Wozniak, D. F., Lou, J., McNeil, B. D., . . . Ornitz, D.

    M. (2002). Ataxia and paroxysmal dyskinesia in mice lacking axonally transported

    FGF14. Neuron, 35(1), 25-38. doi:10.1016/s0896-6273(02)00744-4

Wang, X., Zhang, X. G., Zhou, T. T., Li, N., Jang, C. Y., Xiao, Z. C., . . . Li, S. (2016). Elevated

    Neuronal Excitability Due to Modulation of the Voltage-Gated Sodium Channel

    Nav1.6 by Abeta1-42. Front Neurosci, 10, 94. doi:10.3389/fnins.2016.00094

Wengert, E. R., Saga, A. U., Panchal, P. S., Barker, B. S., & Patel, M. K. (2019). Prax330

    reduces persistent and resurgent sodium channel currents and neuronal

    hyperexcitability of subiculum neurons in a mouse model of SCN8A epileptic

    encephalopathy. Neuropharmacology, 107699.

    doi:10.1016/j.neuropharm.2019.107699

Westenbroek, R. E., Merrick, D. K., & Catterall, W. A. (1989). Differential subcellular

    localization of the RI and RII Na+ channel subtypes in central neurons. Neuron,

    3(6), 695-704. doi:https://doi.org/10.1016/0896-6273(89)90238-9

Westenbroek, R. E., Noebels, J. L., & Catterall, W. A. (1992). Elevated expression of type

    II Na+ channels in hypomyelinated axons of shiverer mouse brain. J Neurosci,

    12(6), 2259-2267.

Whitaker, W. R., Faull, R. L., Waldvogel, H. J., Plumpton, C. J., Emson, P. C., & Clare, J. J.

    (2001). Comparative distribution of voltage-gated sodium channel proteins in

    human brain. Brain Res Mol Brain Res, 88(1-2), 37-53.

White, H. V., Brown, S. T., Bozza, T. C., & Raman, I. M. (2019). Effects of FGF14 and

    NaVβ4 deletion on transient and resurgent Na current in cerebellar Purkinje

    neurons. Journal of General Physiology, 151(11), 1300-1318.

    doi:10.1085/jgp.201912390

Wolff, M., Johannesen, K. M., Hedrich, U. B. S., Masnada, S., Rubboli, G., Gardella, E., . . .

    Moller, R. S. (2017). Genetic and phenotypic heterogeneity suggest therapeutic

    implications in SCN2A-related disorders. Brain, 140(5), 1316-1336.

    doi:10.1093/brain/awx054

Wong, V. C., Fung, C. W., & Kwong, A. K. (2015). SCN2A mutation in a Chinese boy with infantile spasm - response to Modified Atkins Diet. Brain Dev, 37(7), 729-732. doi:10.1016/j.braindev.2014.10.008

Wu, F., Mi, W., Burns, D. K., Fu, Y., Gray, H. F., Struyk, A. F., & Cannon, S. C. (2011). A sodium channel knockin mutant (NaV1.4-R669H) mouse model of hypokalemic periodic paralysis. J Clin Invest, 121(10), 4082-4094. doi:10.1172/jci57398

Xiao, Y., Barbosa, C., Pei, Z., Xie, W., Strong, J. A., Zhang, J. M., & Cummins, T. R. (2019). Increased resurgent sodium currents in Nav1.8 contribute to nociceptive sensory neuron hyperexcitability associated with peripheral neuropathies. J Neurosci. doi:10.1523/jneurosci.0468-18.2018

Xiao, Y., Blumenthal, K., & Cummins, T. R. (2014). Gating-Pore Currents Demonstrate Selective and Specific Modulation of Individual Sodium Channel Voltage-Sensors by Biological Toxins. Mol Pharmacol, 86(2), 159-167. doi:10.1124/mol.114.092338

Xiao, Z. C., Ragsdale, D. S., Malhotra, J. D., Mattei, L. N., Braun, P. E., Schachner, M., & Isom, L. L. (1999). Tenascin-R is a functional modulator of sodium channel beta subunits. J Biol Chem, 274(37), 26511-26517. doi:10.1074/jbc.274.37.26511

Xu, R., Thomas, E. A., Jenkins, M., Gazina, E. V., Chiu, C., Heron, S. E., . . . Petrou, S. (2007). A childhood epilepsy mutation reveals a role for developmentally regulated splicing of a sodium channel. Mol Cell Neurosci, 35(2), 292-301. doi:10.1016/j.mcn.2007.03.003

Yan, H., Pablo, J. L., Wang, C., & Pitt, G. S. (2014). FGF14 modulates resurgent sodium

   current in mouse cerebellar Purkinje neurons. Elife, 3, e04193.

   doi:10.7554/eLife.04193

Yu, F. H., Mantegazza, M., Westenbroek, R. E., Robbins, C. A., Kalume, F., Burton, K. A., .

   . . Catterall, W. A. (2006). Reduced sodium current in GABAergic interneurons in

   a mouse model of severe myoclonic epilepsy in infancy. Nat Neurosci, 9(9), 1142-

   1149. doi:10.1038/nn1754

Yu, F. H., Westenbroek, R. E., Silos-Santiago, I., McCormick, K. A., Lawson, D., Ge, P., . . .

   Curtis, R. (2003). Sodium channel beta4, a new disulfide-linked auxiliary subunit

   with similarity to beta2. J Neurosci, 23(20), 7577-7585. doi:10.1523/jneurosci.23-

   20-07577.2003

Yue, C., Remy, S., Su, H., Beck, H., & Yaari, Y. (2005). Proximal persistent Na+ channels

   drive spike afterdepolarizations and associated bursting in adult CA1 pyramidal

   cells. J Neurosci, 25(42), 9704-9720. doi:10.1523/jneurosci.1621-05.2005

Zabinyakov, N., Bullivant, G., Cao, F., Fernandez Ojeda, M., Jia, Z. P., Wen, X. Y., . . .

   Mercimek-Andrews, S. (2017). Characterization of the first knock-out aldh7a1

   zebrafish model for pyridoxine-dependent epilepsy using CRISPR-Cas9

   technology. PLoS One, 12(10), e0186645. doi:10.1371/journal.pone.0186645

Zara, F., Specchio, N., Striano, P., Robbiano, A., Gennaro, E., Paravidino, R., . . . Minetti,

   C. (2013). Genetic testing in benign familial epilepsies of the first year of life:

   clinical and diagnostic significance. Epilepsia, 54(3), 425-436.

   doi:10.1111/epi.12089

Zhang, Y., Kecskés, A., Copmans, D., Langlois, M., D. Crawford, A., Ceulemans, B., . . . V.

Esguerra, C. (2015). Pharmacological Characterization of an Antisense

Knockdown Zebrafish Model of Dravet Syndrome: Inhibition of Epileptic Seizures

by the Serotonin Agonist Fenfluramine (Vol. 10).

Zhang, Y., Pak, C., Han, Y., Ahlenius, H., Zhang, Z., Chanda, S., . . . Sudhof, T. C. (2013).

Rapid single-step induction of functional neurons from human pluripotent stem

cells. Neuron, 78(5), 785-798. doi:10.1016/j.neuron.2013.05.029

Zona, C., Pieri, M., Carunchio, I., Curcio, L., Klitgaard, H., & Margineanu, D. G. (2010).

Brivaracetam (ucb 34714) inhibits Na(+) current in rat cortical neurons in culture.

Epilepsy Res, 88(1), 46-54. doi:10.1016/j.eplepsyres.2009.09.024

CURRICULUM VITAE

Emily R. Mason

Education

Ph.D. in Pharmacology   2020
INDIANA UNIVERSITY | Indianapolis, IN

B.S. in Biochemistry and Molecular Biology, Honors, magna cum laude   2014
BELMONT UNIVERSITY | School of Arts and Sciences | Nashville, TN

Publications

Mason ER, Wu F, Patel RR, Xiao Y, Cannon SC, and Cummins, TR. (2019). Resurgent and
Gating Pore Currents Induced by de novo SCN2A Epilepsy Mutations. *eNeuro*
6(5). doi: 10.1523/eneuro.0141-19.2019

Manuscripts in Preparation

Mason, ER and Cummins, TR. Differential inhibition of human Nav1.2 resurgent and
persistent sodium currents by cannabidiol and GS967.

Abstracts

Electrophysiological Characterization of two Nav1.2 Mutations Implicated in Epilepsy;
Society for Neuroscience conference; San Diego, CA; Nov. 2016
Resurgent and Gating Pore Currents Induced by De Novo SCN2A Epilepsy Mutations;
Annual Meeting of the Greater Indiana Society for Neuroscience; Indianapolis,
IN; March 22, 2019

Honors and Awards

Paradise Travel Award | Indiana University School of Medicine   2016